European Commission

Research on Innovative Corrosion Resistant Gradient Tubes for Biomass Power Generation Installations

(GRAMAT)

EUR 30134 EN

Research and Innovation

Gradient Tubes for Biomass Power Generation Installations (GRAMAT)

European Commission
Directorate-General for Research and Innovation
Directorate D – Clean Planet
Unit D.3 — Low Emission Future Industries
Contact Hervé Martin
E-mail rtd-steel-coal@ec.europa.eu
RTD-PUBLICATIONS@ec.europa.eu

European Commission
B-1049 Brussels

Manuscript completed in 2019.

Luxembourg: Publications Office of the European Union, 2020

PDF ISBN 978-92-76-17316-8 ISSN 1831-9424 doi:10.2777/742196 KI-NA-30-134-EN-N

EUROPEAN COMMISSION

Research Fund for Coal and Steel

Research on Innovative Corrosion Resistant Gradient Tubes for Biomass Power Generation Installations

(GRAMAT)

Anna HAMBALKOVA (Coordinator)
Peter BRZIAK, Mariana BALAZOVA
Vyskumny Ustav Zvaracsky – Priemyselny Institut SR (VUZ – PI SR)
Racianska 71, SK-832 59, Bratislava, SLOVAKIA

Thomas VIETORIS, Martin JUNKER
Benteler Tube Management GMBH (Benteler)
Residenzstrasse 1, DE-33104, Paderborn, GERMANY

Michal ZEMKO, Ladislav MALECEK
COMTES FHT AS (COM)
Prumyslova 995, CZ-334 41, Dobrany, CZECH REPUBLIC

Edgardo CODA, Jouni MAHANEN
Amec Foster Wheeler Energia Oy (AFW)
Metsaneidonkuja 8, FI-02131, ESPOO, FINLAND

Sanni YLI-OLLI
Teknologian Tutkimuskeskus VTT (VTT)
Tekniikantie 4 A, FI-02044 VTT, ESPOO, FINLAND

Martin DOMOVEC
Podbrezova AS (Podbrezova)
Kolkaren 35, SK-976 81, Podbrezova, SLOVAKIA

Martin BALCAR
ZDAS AS (ZDAS)
Strojirenska 6, CZ-591 71 ZDAR NAD Sazavou, CZECH REPUBLIC

Grant Agreement RFSR-CT-2013-00005

1/07/2013 – 30/06/2017

Final Report

2017 Directorate-General for Research and Innovation EUR 30134 EN

Table of content

Scientific and technical description of the results

This section covers the research approach, a description of the experimental work performed on a task per task basis, highlighting the main results achieved.

The section contains the following as requested by the technical reporting guidelines:

1) Objectives of the project

2) Comparison of initially planned activities and work accomplished

3) Description of activities and discussion, conclusions

The content is divided per work packages and is listed on a task per task basis: each Work package description contains description of activities and discussion followed by conclusions, indicating the achievements made.

The conclusions are described per work packages following the description of activities in the previous chapter.

4) Exploitation and impact of the research results

PROJECT OBJECTIVES

Project main aim is to acquire knowledge necessary to develop new cost-effective manufacturing technology of boiler tubes with through thickness gradient chemical composition. Our solution is devoted to application of tubes made from ingots with through thickness gradient chemical composition, tailored to carry both creep loading (low alloyed body) and high temperature corrosion – erosion (high alloyed shell). Desired chemical heterogeneity of ingot was supposed to be obtained by using unique casting approach based on deep understanding of steel and nickel-based alloys metallurgy, their thermal characteristics and high temperature physical properties.

To accomplish this, basic knowledge about gradient material behaviour during casting (metallurgy), rolling (forming) and final properties (operation) were investigated and collected.

Description of activities and discussion, conclusions

Work package 1: Metallurgy

TASK 1.1 MATERIAL SELECTION FOR GRADIENT TUBES

Optimal material compositions for both core and shell of gradient tube have been selected with help of a literature survey, expert "know-how" and advanced materials modelling. Amec Foster Wheeler has selected the most promising combination of outer and inner material of gradient tube - see table below. The selection was based on the real demand for biomass boilers. In addition, AM AFW provided very helpful internal quality standards the GRAMAT tubes should fulfil without any excuse.

Tab. 1 Selection of material combination for gradient tubes

Part	Priority 1	Priority 2	Priority 3a	Priority 3b	Priority 3c
Shell	**347H** (310H)	**347HFG** (HR3C)	**Alloy 59**	Alloy 59	In625
Body	**13CrMo4-5** (10CrMo9-10)	**T91** (T92)	**T91** (T92)	347HFG	13CrMo4-5 (16Mo3 or P235)

All subsequent experimental works have been performed with selection PRIORITY **1** (347H Shell + 10CrMo9-10 body).

TASK 1.2 NUMERICAL SIMULATION OF CASTING

The numerical simulation of various casting processes has been performed in order to ensure (i) better understanding of the processes during gradient material casting, (ii) optimisation of gradient material casting process. Experiences from laboratory casting and physical simulation have served as first inputs for numerical simulation of industrial casting, in latter phases validated by results of industrial trials and subsequently modified to provide an optimised casting setup.

Following key areas have been planned and addressed successfully:

- **Process parameters optimization**

Preheating of the mould, delay before pouring, filling and solidification of molten metal was calculated. Variant simulations have been defined to analyse possible influences of technology deviance like a funnel orientation, mould initial temperature etc.
Influence of filling on position of austenitic shell re melting was analysed. It was found the fluid flow is very different in square and oval shells respectively. Falling liquid metal diverts from casting axis and thus fluid flow is different on each side of the casting. This leads to different temperature fields on cast outer surfaces, see **Fig. 1**.

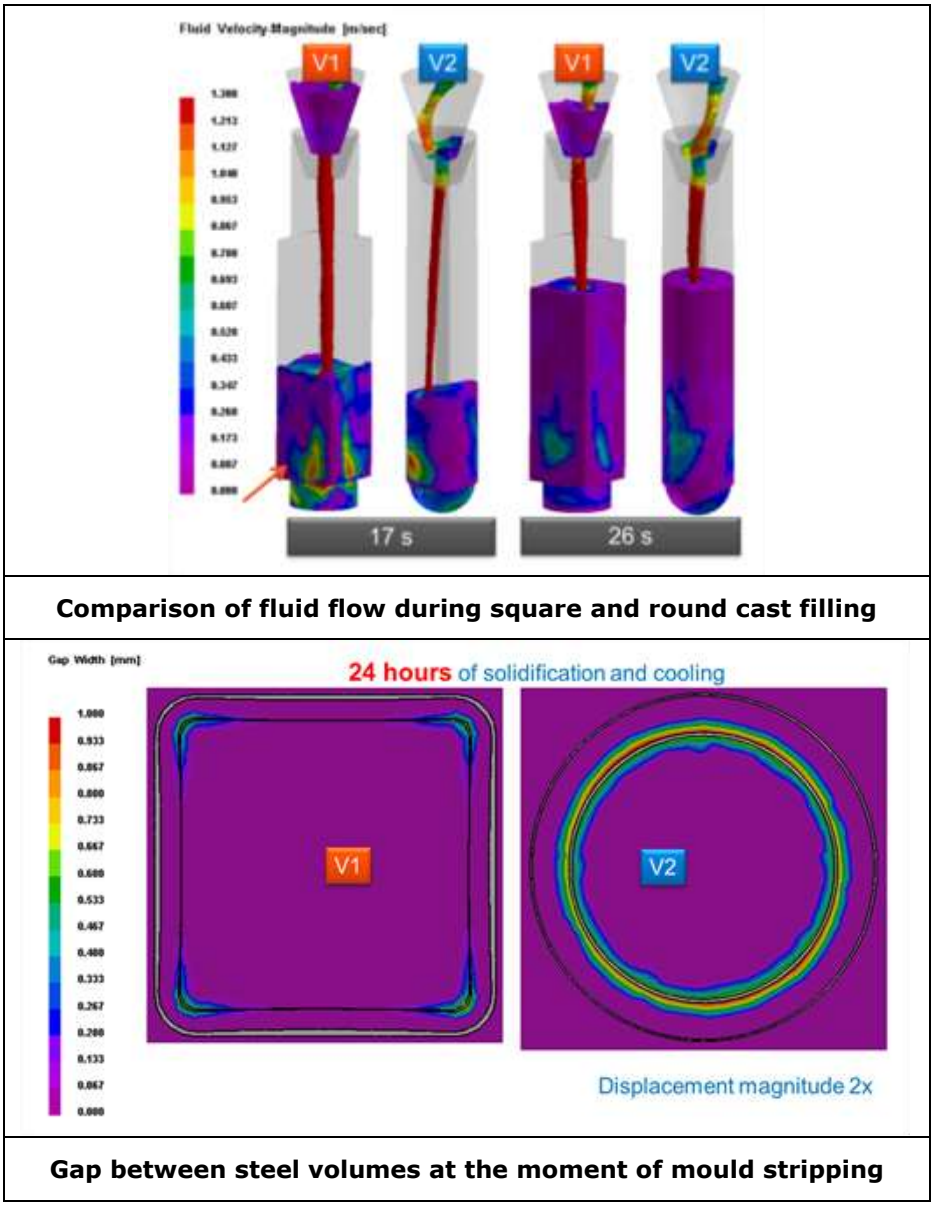

Fig. 1 Comparison of fluid flow during square and round cast filling. Gap between steel volumes at the moment of mould stripping

First casting stress simulation have shown that the sides of the cast are pushed against the walls of austenitic steel profile. That happens at high temperatures when joining of material is possible and there might be even the risk of re-melting of austenitic steel. Lack of material joining at corners of cast was explained by fast heat reground and volume contraction connected with gap formation. The austenitic tube max. thickness of about 12 mm was postulated. Numerical simulation proved the practical difficulties when square shell is used.

With respect to previous results coming from industrial casting (second industrial trial), physical and numerical simulation a new technological set-up has been proposed. Experiments were used to map conditions which lead to diffusion joint, lack of fusion or undesirable extent of re-melting. That helped to find proper simulation parameters which have been successfully applied.

Preheating

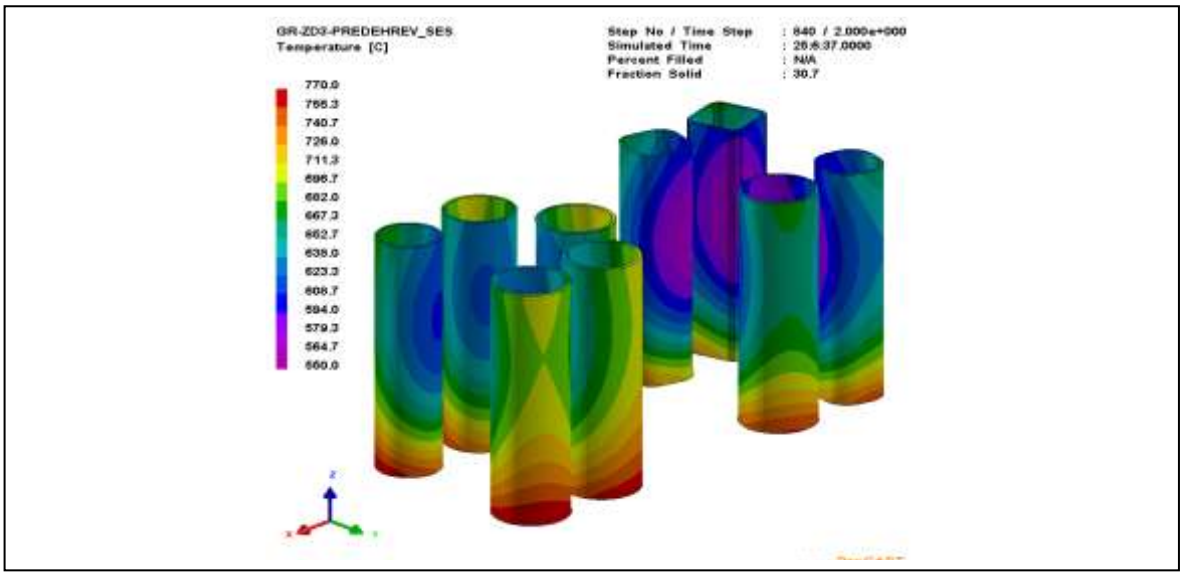

Fig. 2 Thermal fields after preheating, 347 H.

To reach the 700°C preheating of the 347H shell, up to 25 hours of preheating in ZDAS premises was necessary, an even after that the temperature field was not even. However, the technical ability of the foundry has been reached. It is because of proximity with steel desk they are lying on. The high calculated temperatures at shell bottom can be the reason of tube remelting which occurred during the experiments – see **Fig. 2**. To avoid this, several measures have been adopted (thermal insulation for example).

Solidification

Process of preheating is followed by mould temperature homogenization on air and then by melt pouring, solidification and cooling. Several combinations of preheating and poring temperature were used for calculation of most efficient casting parameters. The poring temperatures 1570°C to 1615°C and preheating temperatures 650°C and 700°C were put in calculations. It was proved that from the thermal point of view squared profiles are less suitable for gradient joint creation than round profiles. Examples of thermal fields in ingots after poring are seen in **Fig. 3**.

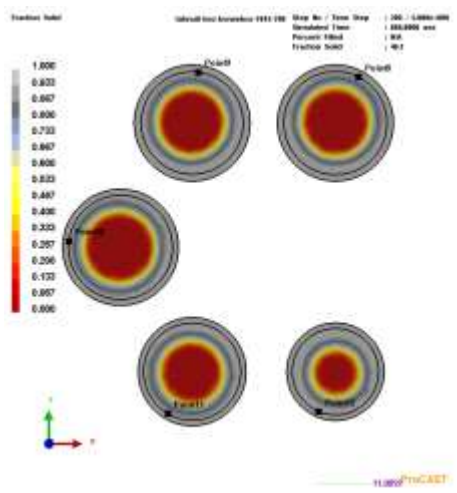	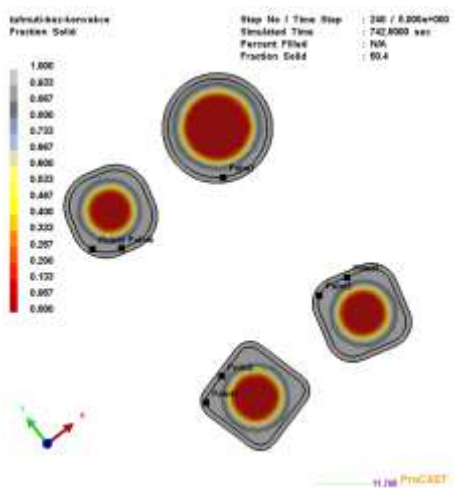
Casting plate 1 with rounded profiles; preheating temperature 700 °C; pouring temperature 1615 °C At some locations temperatures are even higher than 1,300 °C. In such there is a small chance of local remelting. This usually appears at bottom side of the ingot.	Casting plate 2 with squared profiles; preheating temperature 700 °C; pouring temperature 1615 °C. Higher preheating and pouring temperature help to reach temperatures which are needed to get gradient joint. Still the square section of ingot is not favourable because of higher temperature differences across the ingot.

Fig. 3 Temperature fields in ingots

In summary, preheating temperature of 700 °C and pouring temperature of 1615 °C were confirmed as optimal temperatures for most of the tested sizes of ingots.

When radius R80 was used, situation was better but not satisfying.

- **Gating/Feeding system - Mould optimization**

Several mould concepts have been prepared for industrial testing. A metal die with the new design of ingot heel was included as the lowest part of the mould.
Fig. 4 shows the geometry variations which were used to validate the simulation settings.

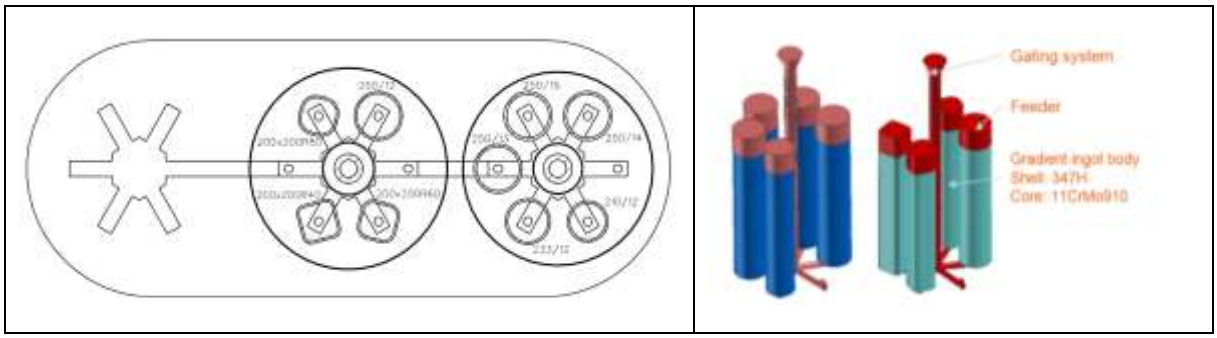

Fig. 4 Positions of austenitic steel profiles together with gating and feeding system

- **Defect elimination and structure and mechanical properties prediction**

Stress calculation was set off to find location of possible hot cracks, deformation of ingot and creation of gap between steels 347H and 11CrMo910. For all types of ingots there was indication of hot tearing. This problem should not threaten production since hot tearing is sited at place which is not used in process of tube elongation.

TASK 1.3 LABORATORY TRIALS OF CASTING

Two types of laboratory casting trials have been performed:

- **Small scale trials**

Small scale trials have provided specimens for microstructure survey, physical simulation and casting parameters optimisation.

- **Large scale trials**

Large scale trials have provided full-scale gradient laboratory casts for preliminary rolling trials in Podbrezova and some temperature measurements for numerical simulation of casting.
Square cross-section tube (200x 200 x 600mm, thickness = 12mm) from high alloyed material was sand moulded and heated up to temperature 800° C by gas burner. Funnel casting was used. Casting temperature was 1560°C. The appearance of laboratory large scale trial is seen in **Fig. 5**.
It was found very soon that casting to the square shell always brings about fatal problems related to the heat flux and increased shrinkage on corners. NDT showed 60% to 70% diffusion joint. In addition, it was found that austenitic steel shell is overheated or even re-melted during the casting.

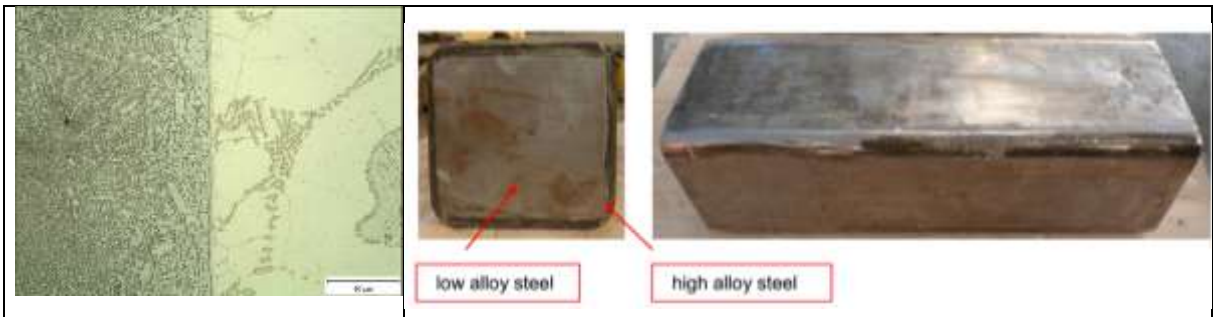

Interface – laboratory trial	**Appearance of square ingot – laboratory trial**

Fig. 5 a) Interface austenitic shell (left) – ferritic core (right) - laboratory trial. b) Appearance of square ingot – laboratory trial

Laboratory trials have been accompanied by basic screening of utility properties (NDT, mechanical testing, metallography). The lack of fusion was repeatedly reported at ingot corners.

TASK 1.4 PHYSICAL SIMULATION OF CASTING

Samples taken of the cast specimens have been studied by physical simulation in order to reveal the technical limits of the casting process (casting temperatures, solidification/cooling rates). Sets of experiments have been carried-out to investigate fusion processes in low-to-high alloy area, in particular the influence of time/stress/cooling rate on the diffusion of principal elements and on further sequence of carbide precipitation; these experiments have been performed at near solidus temperatures.

The experiments were performed at the temperatures of 500°C, 800°C, 900°C, 1000°C, 1100°C, 1200°C, 1300°C and 1400°C, and the compression 0,15MPa on a thermal physical simulator Gleeble 3800. Experiment parameters determination was based on the numerical simulation.

The investigations have enabled to set temperature and time margins for diffusion connection between two materials in concern - it was found that the diffusion joint starts at 1200°C and two materials are fully bonded at 1300°C; furthermore it has been suggested that the holding time also plays the role - 30 seconds has been indicated as safe value

The aim of these experiments was the determination of the temperature of diffusion joint formation between high alloyed material (347H) and low alloyed (13CrMo4-5) material. Specimen dimensions were ø 8mm x 12 mm **Fig. 6** . The experiments were conducted in vacuum chamber of GLEEBLE 3800 physical simulator.

The samples were manually positioned between the jaws and loaded in compression F=0,5KN. The position of the samples shows **Fig. 7**. The samples were heated up to 500°C, 800°C, 900°C, 1000°C, 1100°C, 1200°C, 1300°C and 1400°C, heating rate of 10°C/s followed by hold of 120s and 240s and increased load of 0,15MPa. Samples were cooled freely in the chamber. The tests were doubled. The samples were metallographically analysed to describe the character of formed joint. The microstructure was observed and documented by means of light optical microscope OLYMPUS 51GX using magnification of 50 to 500x.

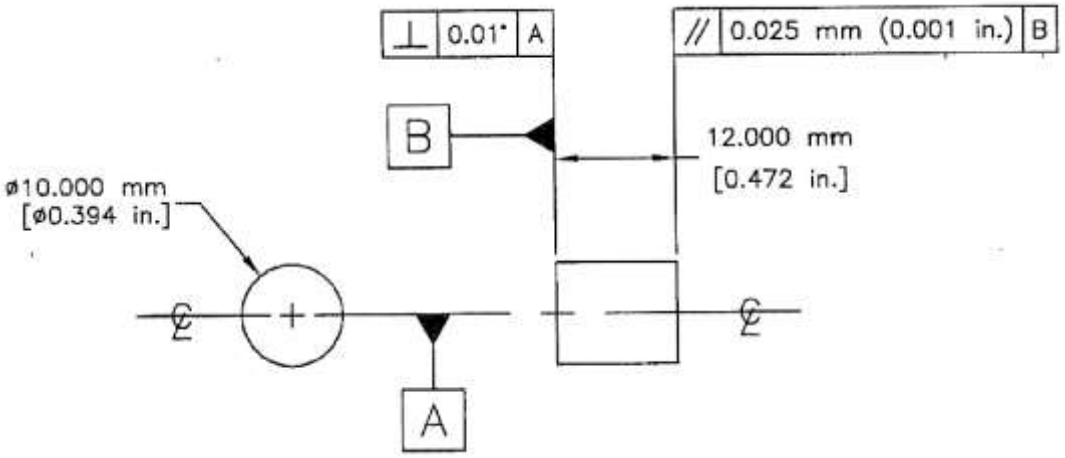

Fig. 6 Geometry of samples for physical simulation

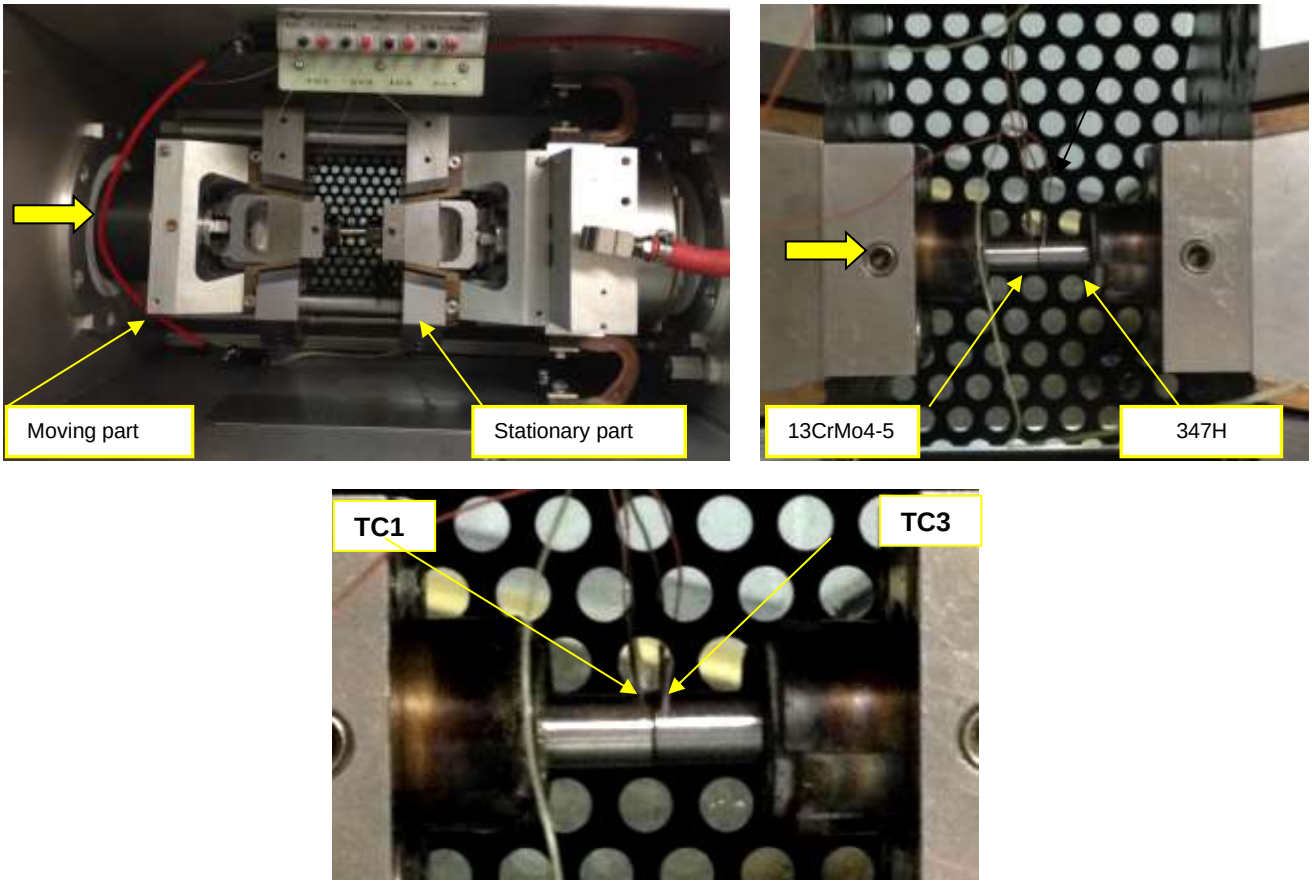

Fig. 7 Layout of sample in Gleeble working chamber

The results of the experiments are summarized in**. Fig. 8** and **Fig. 9** show appearance of specimen during the testing and after removing from jaws.

Tab. 2 Testing parameters

Number samples	Strain rate [°C/s]	Temperature [°C]	Hold [s]	Compression [MPa]	Cooling	Results
0	10	500	30	0,15	free	no fusion joint
1/ 2		900				no fusion joint
3/ 4		1000				no fusion joint
5/ 6		1100				no fusion joint
7/ 8		1200				partial fusion joint
9/ 10		1300				fusion joint
11		1400				fusion joint

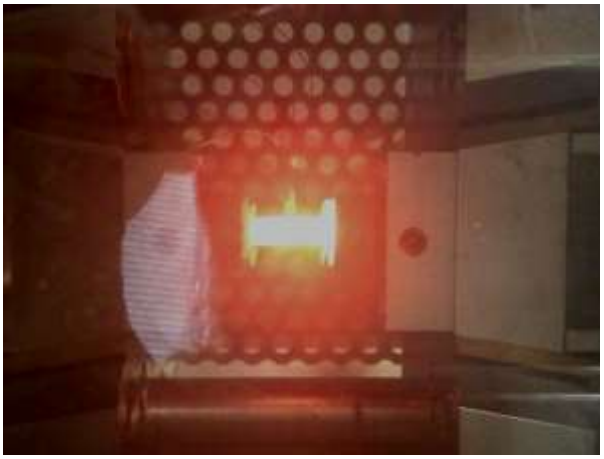

Fig. 8 Sample No 4 (Tmax. 1000°C)

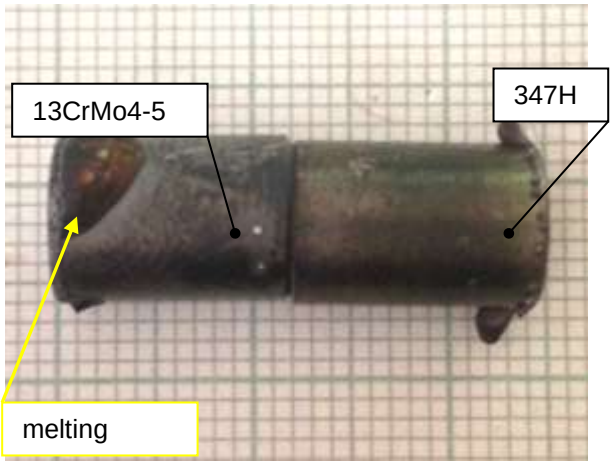

Fig. 9 Sample No 8 – without fusion joint

The aim of microstructural examination was to observe the character of joint formed during the test performed on GLEEBLE 3800 physical simulator. Sample no. 2 (900°C) showed some joint formation after extraction from the testing chamber, but metallographic examination proved no diffusion joint formation – see **Fig. 10**. documented metallographic section in un-etched condition. Sample no.7 (1200°C) shoved diffusion joint formation between the materials. The microstructure of the sample no.7 is documented on **Fig. 11** and **Fig. 12.** It can be concluded that poring temperature should be material temperature should be app. 1 250°C to 1300°C to obtain the diffusion joint formation between austenitic core and ferritic shell.

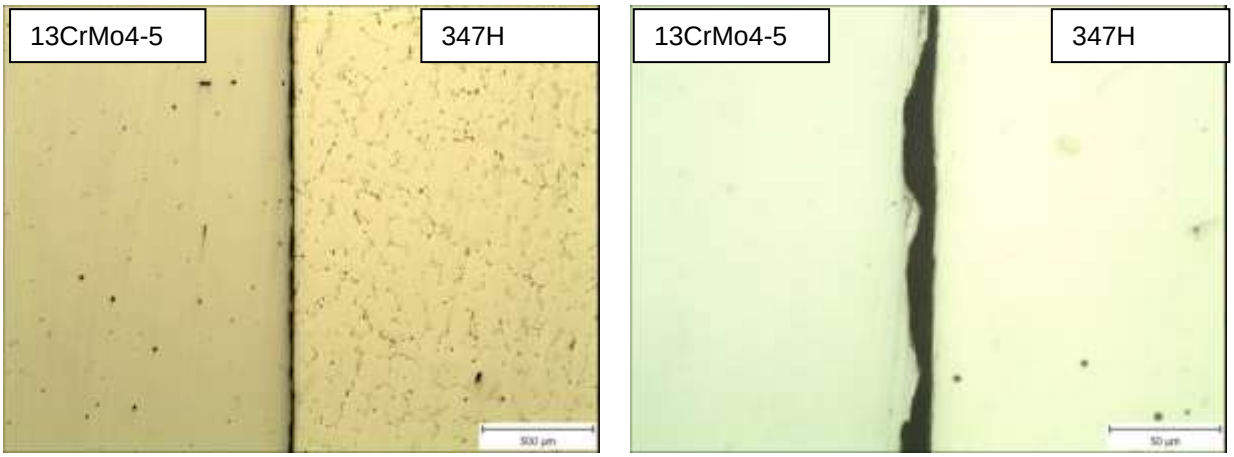

Fig. 10 Metallographic not etching of sample No 2

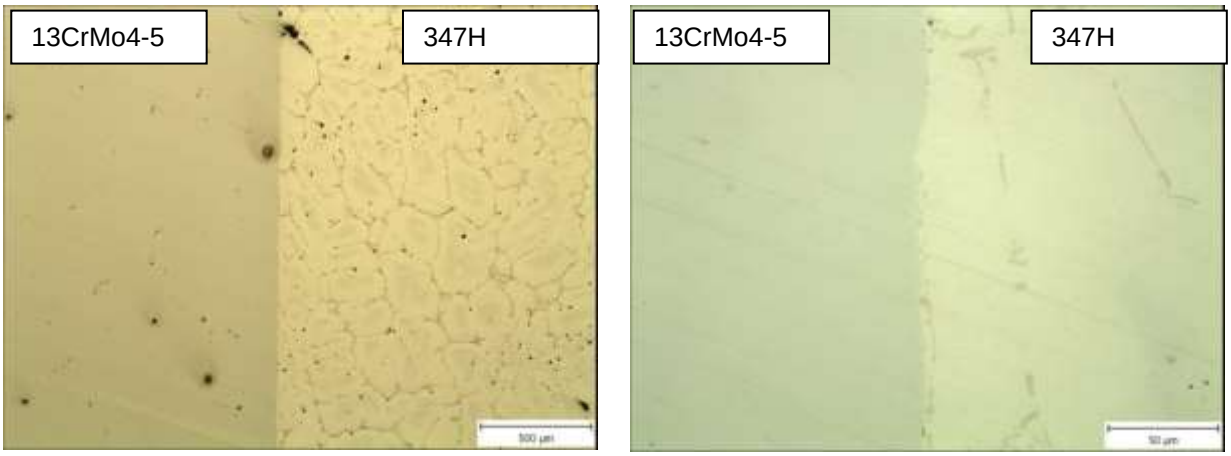

Fig. 11 sample no 7 - polished

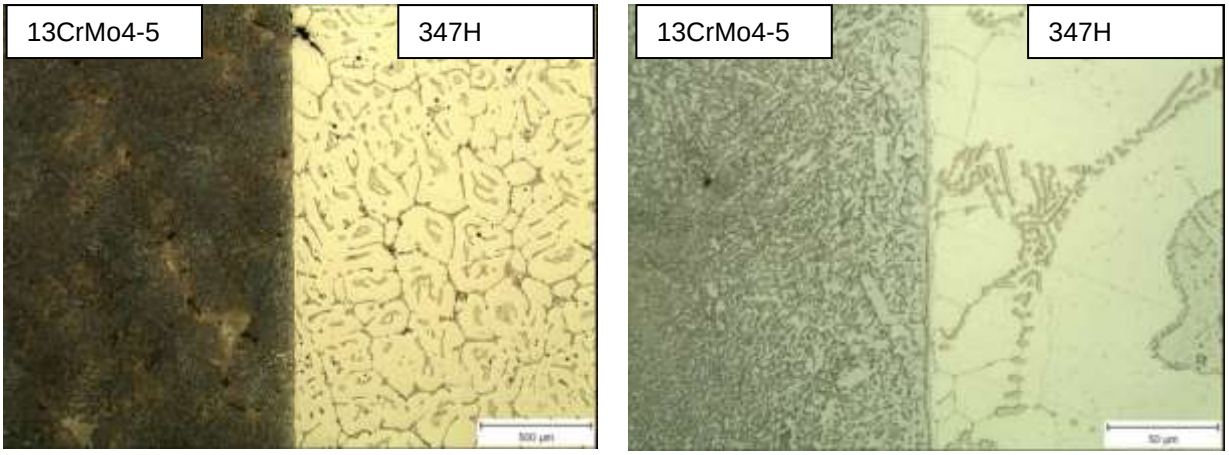

Fig. 12 sample no 7 – polished + etched

TASK 1.5 INDUSTRIAL TRIALS OF CASTING

Based on outputs from 1.1 – 1.4, the experiments have taken place to proceed gradient ingot manufacturing to industrial conditions. An experimental workplace has been be designed and

manufactured for trial purposes to confirm acquired basic knowledge about gradient material behaviour during casting processes. Design has been based on the knowledge obtained in previous tasks and modified subsequently based on feedbacks from trials. Experiments have been devoted to optimisation of casting parameters, shape, and through length geometry of high-alloyed layer in semiproduct devoted to rolling. Full-scale trials have been carried-out to manufacture semiproducts for subsequent rolling experiments.

It was planned to perform at least 40 full-scale industrial casting; during the project a total amount of **42 castings** has been delivered during a total amount of 6 industrial trials (6 + 7 + 9 + 20 pieces of castings).

- **1st industrial casting**

Based on first calculations (physical and numerical simulations) the **1st** industrial casting was performed: "small experiments" were set up in ZDAS foundry, see **Fig. 13**. Experiments were devoted to" a) checking the numerical calculations and b) providing real data. Many variables were tested: different shape and size of outer shell (12, 16, 20, 30 mm, conical tube), preheating, pouring temperature and mould design, temperature measurements.

"small" trial

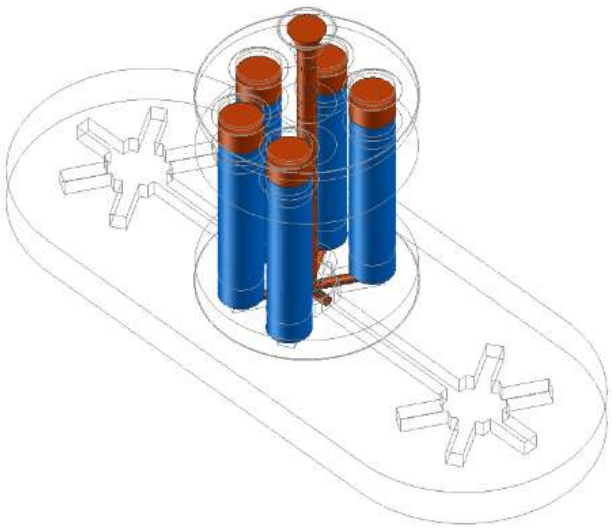

Casting plane layout

Fig. 13 "small" trial and casting plane layout

Main outputs from pre-industrial experiments: preheating of **700** °C allow to heat up austenitic steel shell to desired 1,250 °C (confirmed by physical simulation as proper ones for diffusion) joint creation. These temperatures are reached before solid layer of the ingot starts to contract and thus there is still a good contact between the two steel volumes.

The pouring temperature was set up **1,615** °C or more. If lower, the solidification of core ingot progress too fast and there is negligible chance of diffusive joint creation.

At the end of first stage, the general overview of the gradient tube problematic was completed. All test, laboratory, industrial, supported by physical and numerical simulation and metallography testing pointed at most critical parts of the project: reliable gradient product production. In following stages all available manpower was appointed to this issue.

- **2nd industrial casting**

Six pieces of round gradient cast were produced and shipped to the **Benteler r**olling mill one piece of square gradient cast was shipped to the **Podbrezova** rolling (corners without joint). Details are summarized in **Tab. 3** .Overview of the trials are seen in Fig. 14 and **Fig. 15.**

It should be noted here that the due to lack of commercially available tubes, those were made by expensive processes. Semi-products were produced from austenitic stainless steel – grade A182F347H acc. ASTM SA182 by EAF/LF/VOD/VD process and followed by bottom casting to the round moulds. Semi-products were forged by open die forging process to produce tubes.

Tab. 3 2nd industrial casting details

First Casting Plate	no. 1	ø 210mm x 1000 mm; h_{347H} = **12mm**	Approx. 550mm – accepted Local defect (app. 100mm^2)
	no. 2		
	no. 3		
	no. 4		
	no. 5	ø 210mm x 1000mm; h_{347H} = **12mm**	Approx. 600mm – accepted
Second Casting Plate	no. 6		Approx. 600mm – accepted
	no. 7	200mm x 200 mm x 1000mm; h_{347H} = **12mm**	Corners without diffusion joint, rest of the ingot without problems

Very conservative approach for ingot selection for rolling was made. The usage of the ingots based on NDT testing was set up to 60 %. It was, however shown that the local lack of the fusion, if it is not at the ingot both endings (in other word the lack of fusions are fully locked in material and consequently less oxidised), is not harmful neither for rolling process, nor for quality of gradient tubes. Appearance of ingots ready for delivery to Benteler is seen in figure **Fig. 15**.

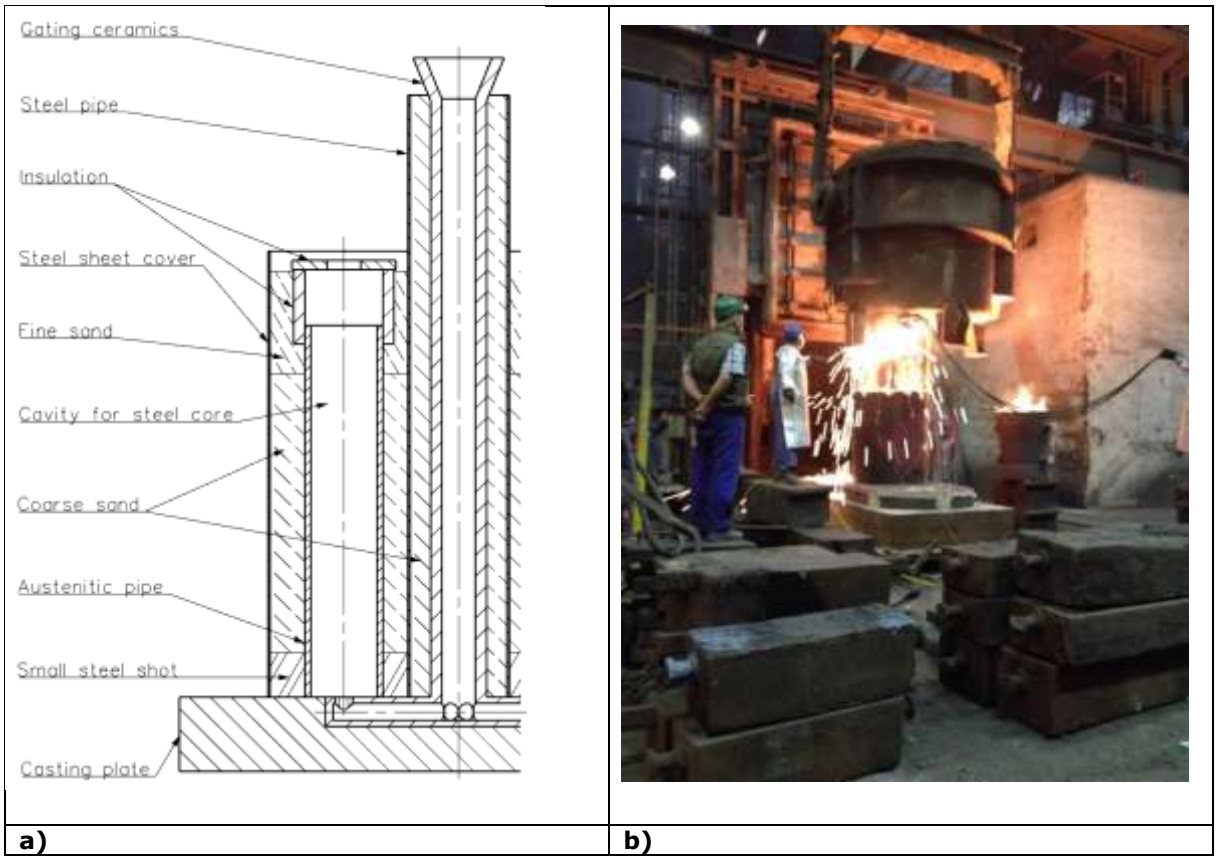

a) **b)**

Fig. 14 a) Construction of casting plane b) Casting process

Fig. 15 Gradient ingots ready for rolling in Benteler

- **3rd industrial casting**

The aim of the third industrial casting was the production of full-scale casts for rolling experiments in order to optimise the casting process in order to produce next generation of gradient tubes.

The main aim was to make progress in manufacturing the square semiproducts for Podbrezova rolling mill. Also, the knowledge gained from 2nd industrial cast was used to improve the quality of oval semiproducts for Benteler rolling mill.

Nine gradient ingots were prepared (3pcs. of the square gradient casts, 6pcs. of the oval gradient casts). Three oval gradient cast was forged by open die forging process.

Gradient cast no. 4, 5 and 9 were forged by open die forging process within the temperature interval from 1000°C to 1150°C followed by free cooling. Details are summarized in **Tab. 4**.

Tab. 4 Results of NDT testing of third industrial trial

Number of gradient casts	Geometry of shell	Thickness of shell (347H steel)	Geometry of gradient cast after open die forging	NDT Results/ UT acc. EN 10228-3 Level 3
no. 1	200mm x 200mm 1000mm; R40	h347H = 12mm	-	not accepted
no. 2	200mm x 200mm 1000mm; R60	h347H = 12mm,	-	not accepted
no. 3	200mm x 200mm 1000mm; R80	h347H = 12mm,	-	approx. 610mm accepted
no. 4	ø 235mm 1000mm	h347H = 12mm	200 mm x 200 mm	approx. 470 mm accepted
no. 5	ø 235mm 1000mm	h347H = 12mm	200 mm x 200 mm	approx. 520 mm accepted
no. 6	ø 250mm 1000mm	h347H = 15mm	-	approx. 501 mm accepted
no. 7	ø 210mm 1000mm	h347H = 12mm	-	approx. 550 mm accepted
no. 8	ø 210mm 1000mm	h347H = 12mm	-	approx. 770 mm accepted
no. 9	ø 200mm 1000 mm	h347H = 12mm	200 mm x 200 mm	approx. 700 mm accepted

The ingots No. 8 a No. 9 were most promising: 770 mm (the best result within the project) mm and 700 mm of the length were accepted.

Six pieces of gradient ingots with acceptable NDT were produced and shipped to the Podbrezova/Benteler (Fig. 16.) rolling mills. It has been assessed that the R80 seems the be most promising corner radius for square billets casting.

However, a 100% diffusion joint has not been reached.

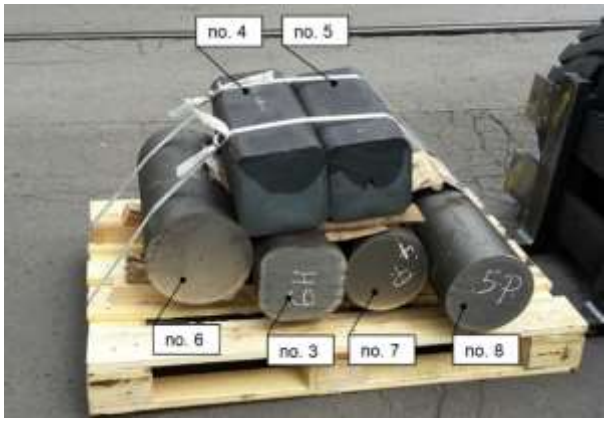

Fig. 16 Some gradient ingots ready for rolling in Benteler (oval) and Podbrezova (square)

Summary of 3rd industrial casting and outputs for the further work

To ensure optimisation of casting and rolling processes and related heat treatment it has been necessary to deal with the issues of better diffusion layer along the produced tube, less surface defects, smaller decarburisation and sensitization layers at the interface, and no large residuals from the interface.
Additionally, the problem (identified as main encountered in the midterm report) of persistent problems with insufficient diffusion joint between the outer layer and the inner core in the corners of gradient square casts (demanded by Podbrezova rolling mill) has been tackled again.

Since the last experiments with 1 m long steel tubes were satisfactory, next logical step was to use longer tubes. That should lead to improvement of liquid metal mass yield. The length of new steel tubes was 1,700 mm. At the same time there was an idea of possible innovation which was reduction of whole pouring system size. That consists in moving all ingots closer to each other and decreasing diameter of steel frame. Such innovation could speed up process of preheating and usage of material. That should lead to better economy of whole production.

4th, 5th and 6th (instead of two planned trials) industrial casting trial was performed to validate optimised casting technological parameters and to produce full-scale casts for further rolling experiments in Podbrezova and Benteler.
Optimisation of casting sequence to increase the casting efficiency was the primary target. The experiments were focused mainly on length extension of cast gradient ingots in order to get more semi product for rolling experiments. The liquid to solid material casting was of the main concern; however, some laboratory experiments devoted to liquid materials co casting were conducted.

- **4th industrial casting**

Main aim was to investigate a) increase of the gradient ingot length from former 700 mm to 1 700mm and b) changes in casting layout on quality of the process.

New geometry proposed for new trials
In order to obtain more economical solution three nests were placed on one pad.

The shell dimensions: height 1,700 mm x D212 mm x 12/13 mm

Due to heat output of the preheating furnace which would not allow to preheat an increased number of ingots, the casting layout was changed to get the tubes closer, which brought about the problems with melting of ingots with closer layout (few cm). Ingot layout on pad with wider span between the shells before pouring (app. 10 cm) brought about better results - **Fig. 17**.

a) Lower parts of cast ingots, melted sand

b) three ingots with closer layout damaged during casting in lower parts (melt sand), separate ingot (right in the figure) without any problems

Fig. 17 4th industrial casting

- **5th industrial casting**

Based on 4th industrial casting, the new layout was proposed. The tubes were positioned in way where the heat flux from other tubes was mitigated**.**

1. Oval shaped ingots **D212/t12mm** were delivered to Benteler for industrial rolling, see **Fig. 18**.

2. Oval shaped ingots **D232/t13mm** were forged onto square in Ždas. Forging temperatures varied between 900 and 800°C. After forging, the ingots passed quality control and then they were sent to Podbrezova.

Only 100 % sound parts of ingots were selected for rolling – **which was app. 800 mm from the length of 1700 mm. Rest of the ingots contained following defects (lack of fusion, shrinkages, pores). This was not satisfactory.**

	
ingots + runners	**ingots after steel pellet blasting**

Fig. 18 a) 5th industrial casting – ingots + runners. b) 5th casting – ingots after steel pellet blasting.

- **6th industrial casting**

6th industrial casting was following up of 5th experiment. Slight changes were made in tubes layout. 3 ingots **D232/t13mm** were selected for forging. The forging temperature was kept at 800°C to 900°C. Then they were sent to Podbrezova.

In general, the progress, despite of tremendous effort was very small:

1. Extension of cast gradient ingots, despite of a lot of effort, did not bring the desired results. Therefore – the optimised length of cast ingots was chosen for final generation of gradient tubes.
2. It is very difficult to make gradient ingots in form of square ingot (ŽP rolling sequence). The thermal flux on the corners causes non diffusion joints – this phenomenon is unbeatable. **The best way to get ingot for ŽP rolling sequence is to forge the oval gradient ingot to the square one. Oval ingots for the Benteler rolling sequence did not encounter any problems to rolling sequence**.

FINAL CONCLUSIONS FROM WP METALLURGY

Successful production of gradient ingots is a very sensitive process. The main problems: melting of steel tube shells at ingot bottoms (oval semiproduct) and lack diffusion joints at corners (square semiproduct).

The summary of acquired knowledge can serve as a recommendation for future industrial production:

- Geometrical point of view on mould and ingots
    - Inlet should be longer in vertical direction to prevent melting at the bottom of steel tube and metal penetration to sand.
    - Shorter preheating time for bigger mould would cause important temperature differences in whole system. It is not recommended to use tight type of assembly where are 6 ingots in one nest. Only 3 ingots were consequently used (every second one in nest).
    - It is not recommended to use top filling. Bottom filling is preferable because it is easier to control filling process.
    - Height, diameter and thickness of steel tube changes other technological parameters. At the first place pouring temperatures and preheating temperatures must be evaluated when shape of tube is changed.
- Preheating
    - Preheating process is necessary and cannot be skipped. At the same time preheating must be done to precise temperature otherwise proper joining of material cannot be obtained. The preheating temperature will be different for different types of gradient ingot materials. The preheating temperature also depends on size of ingots, geometry of the casting plates (pads) – in other words – there in no general recommendation for this temperature. The preheating temperature 700°C is necessary to get the proper metallurgical bonding between shell and liquid metal. The homogeneity of thermal fields inside the should be kept a slow as possible - there is no straight rule to achieve this
    - Temperature distribution amongst mould assembly must be as homogenous as possible. That can be reached by homogenization in furnace when constant temperature is used from some moment of preheating and homogenization by air natural convection doesn't work.

  Diffusion joint between materials 11CrMo910 and 347H is created when temperature of tube at joining surface is app. 1 300 °C. If the temperature is above 1 370°the shell can reach the melting temperature. Other combination of materials will have different range of proper temperatures. Pouring temperature (10CrMo9-10) should be at least 1615°C. As fast pouring as technically possible is recommended.

  Significant amount of know-how was gathered since the beginning of project and there are still unknowns which must be revealed and solved before industrial production can fully begin. Results of simulation could help with understanding of processes and support further research and technological development.

- **Cross section of ingots**

It is not recommended to use squared type of steel profiles. In such case with present technology it is nearly impossible to get good quality of gradient ingots. In most of cases joints are not created at corners. It is recommended to continue with work only on round ingots. The square semiproduct (feedstock for Podbrezova production line) did not provide the proper fusion when manufactured as a square - see

Fig. 19 and **Fig. 20**.

The heat fluxes on the corners of outer shell were much faster that on shell sides during the pouring the low alloyed metal to square high alloyed shell. These inhomogeneities in cooling speed are intrinsic part of the cooling process and cannot be mitigated. As a result, the diffusion joint in corner was very weak, or in many trials did not exist. In addition, the first step of tube production – piercing mill – did not forged the two materials in corners together as we expected. As a result the gradient tubes made from square semiproduct were not as good as expected. On the other hand, when the square semiproduct made by forging from oval cast ingot were used as a feedstock to Podbrezova rolling mill, the quality of final gradient tubes was comparable to those produced in Benteler mill. However, in general, the forging increase the price of the final product.

a)

b)

Fig. 19 Typical appearance of gradient ingots quality a) oval for Benteler b) square for Podbrezova

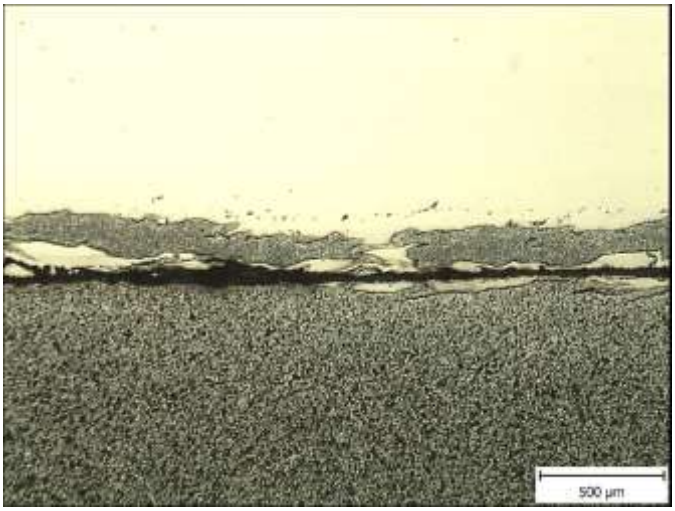

Fig. 20 Typical appearance of interface without fusion joint - square semiproduct

Process sensitivity

The process sensitivity of casting is one of the biggest issues of the project solved. However, the lessons learned from the experiments gave the possibility to select the principal parameters which are overshadowing those less important. The principal variables influencing the quality of the final gradient ingot can be split onto three main groups:

1. Gradient ingot geometry:
   Note: the margins for the variables are given for the desired gradient semiproduct dimensions (oval app. 200 mm in diameter for Benteler rolling mill, square app. 200 mmx 200 mm in case of Podbrezova rolling mill).
   a) Thickness of outer shell (oval, square) app. 12 mm.
   b) Height of outer shell up to 1000 mm (app. 800 mm of ingot prepared for rolling).

2. Casting set up geometry:
   a) The insulation in sand is the most effective.
   b) The nest of 3-4 shells equipped with one pouring channel. The shells are circumferentially located around the pouring channel. The distance in between shells should be 100 mm at least to avoid the mutual heat flux after casting and during cooling down.
   c) The bottom pouring is proven to be then most convenient.
   d) Heavy insulation casting plate should be used to avoid the heat flux from the bottom of casting set up.
   e) Optimum feeder height is 200 mm

3. Pouring parameters:

   a) The preheating temperature 700°C is necessary to get the proper metallurgical bonding between shell and liquid metal. The homogeneity of thermal fields inside the should be kept a slow as possible - there is no straight rule to achieve this.
   b) Pouring temperature (10CrMo9-10) should be 1615°C.
   c) As fast pouring as technically possible is allowed.

Work package 2: Forming

TASK 2.1 NUMERICAL SIMULATION OF ROLLING

The FEM numerical simulation have been used in order to describe and optimise the gradient tube forming process and provide the following:
- risk estimation of gradient tube rolling process
- proposal on gradient ingot layout and geometry
- model of rolling sequence

The simulations have been upgraded periodically, as new data from physical simulation; and especially from real rolling trials and outcoming new generations of rolled tubes have become available.
The aim of numerical simulations was to develop a method which would enable to simulate any forming process during Benteler and Podbrezova gradient tubes production. Generally, there are many numerical simulations concerning tubes rolling. However, all these numerical simulations deal with *rolling only single material.* The purpose was to find a simulation method which allows solving all gradient tubes processes, i.e. symmetrical (2D problems) or asymmetrical (3D problems) processes. The method for simulating the gradient tube production has been established. The principle of this method consists in simulating a gradient tube as two separated objects (a body and a shell). The body and the shell are represented by two objects with two separated FE-meshes connected through a contact condition to a gradient tube (see **Fig. 21**).

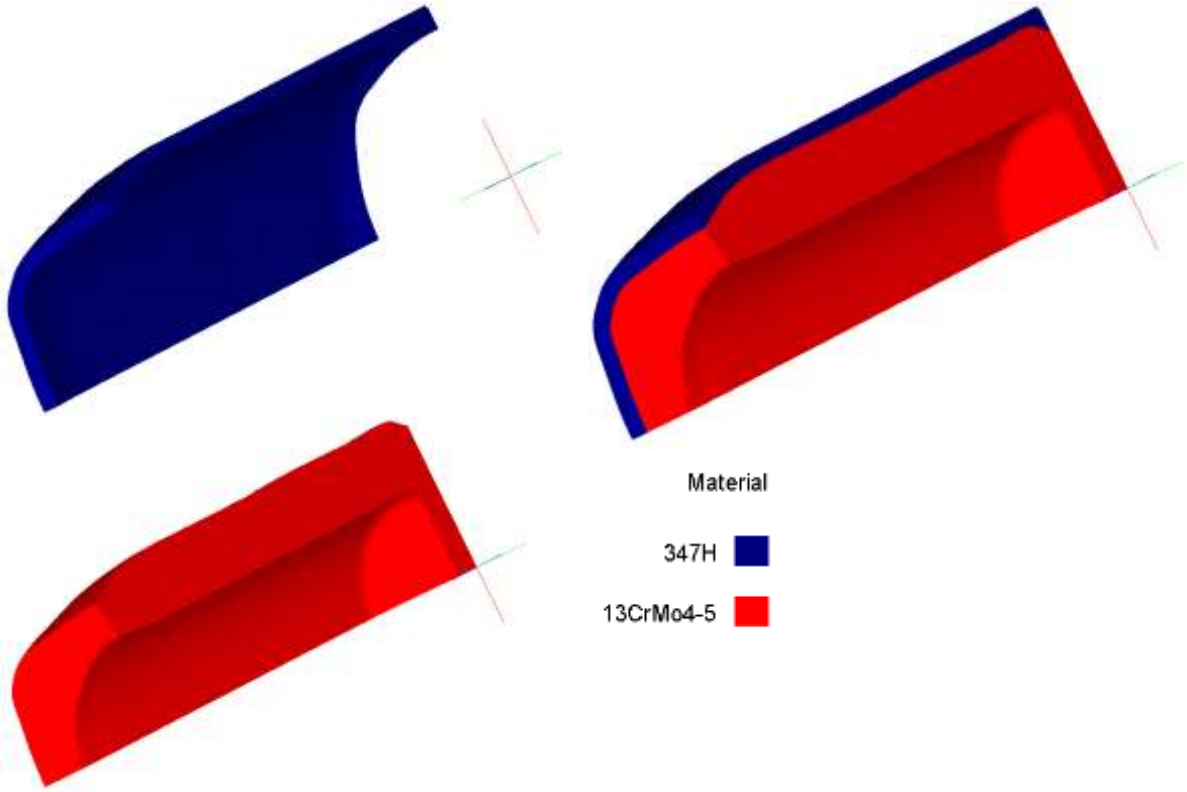

separated shell (blue) and body (red) *shell and body together*

Fig. 21 The representation of the gradient tube created by two objects with two FE-meshes

It was a best alternative from alternatives investigated at the beginning of the project because:
- It enables to accurately define the interface between a body and a shell which allows measuring the shell wall thickness in any direction,
- And to apply this method for any forming process (not only axisymmetric process)

Based on the physical simulations (isothermal compression tests) were carried out series of numerical computations with the aim to find material constants of the Jonson-Cook flow stress model. This model allows eliminating potential numerical problems connected with convergence of a numerical computation which can occur in the case of the use of a tabular format of the flow stress data.
The equations describing flow stress behaviour by means of the Johnson-Cook model are as follows:

$$\overline{\sigma} = \left(298.13 + 250.11 \cdot \overline{\varepsilon}^{0.33}\right) \cdot \left(1 + 0.087 \cdot \ln\left(\frac{\dot{\overline{\varepsilon}}}{\dot{\overline{\varepsilon}}_0}\right)\right) \cdot \left(1 - \left(\frac{T - T_{room}}{T_{melt} - T_{room}}\right)^{0.99604}\right) \quad \text{(Eq. 1)}$$

$$\overline{\sigma} = \left(497.27 + 262.55 \cdot \overline{\varepsilon}^{0.38}\right) \cdot \left(1 + 0.081 \cdot \ln\left(\frac{\dot{\overline{\varepsilon}}}{\dot{\overline{\varepsilon}}_0}\right)\right) \cdot \left(1 - \left(\frac{T - T_{room}}{T_{melt} - T_{room}}\right)^{0.97186}\right) \quad \text{(Eq. 2)}$$

describe flow stress behaviour of 13 CrMo4-5 and 347 H steel grades respectively.
The further aim of numerical simulation was to map an influence of the change of the initial shell wall thickness on the eventual shell wall thickness.
The virtual slice method was used for the shell wall thicknesses measurement. The assessment of the change of the shell wall thickness was performed for initial shell wall thicknesses of 12, 16, 18 and 20 mm, see **Fig. 22** and

Fig. 23. Initially, it was assumed that these shell wall thicknesses would be tested in industrial trials. According to ascertainment in WP1, it was proven that the initial shell wall thickness of 12 mm is the best alternative with respect to the diffusion joint quality and therefore the initial shell wall thickness of 12 mm was used in industrial trials. However, just to be clear, the obtained results are shown for all initial shell wall thicknesses (figures below). Because the ¼ model of the simulated workpiece was used to save the CPU-time, the shell wall thickness was evaluated only in C, F and B positions.

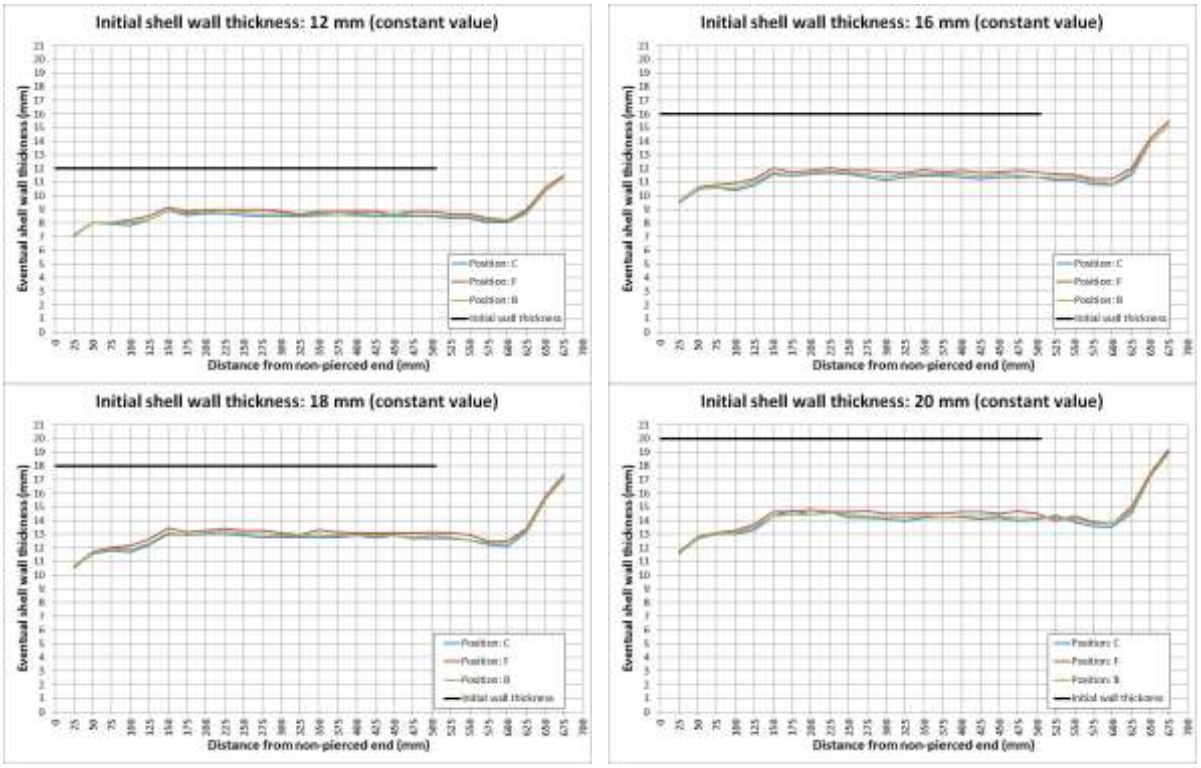

Fig. 22 The change of the shell wall thickness while piercing in the piercing press in Benteler (the billet cross-section – the circle)

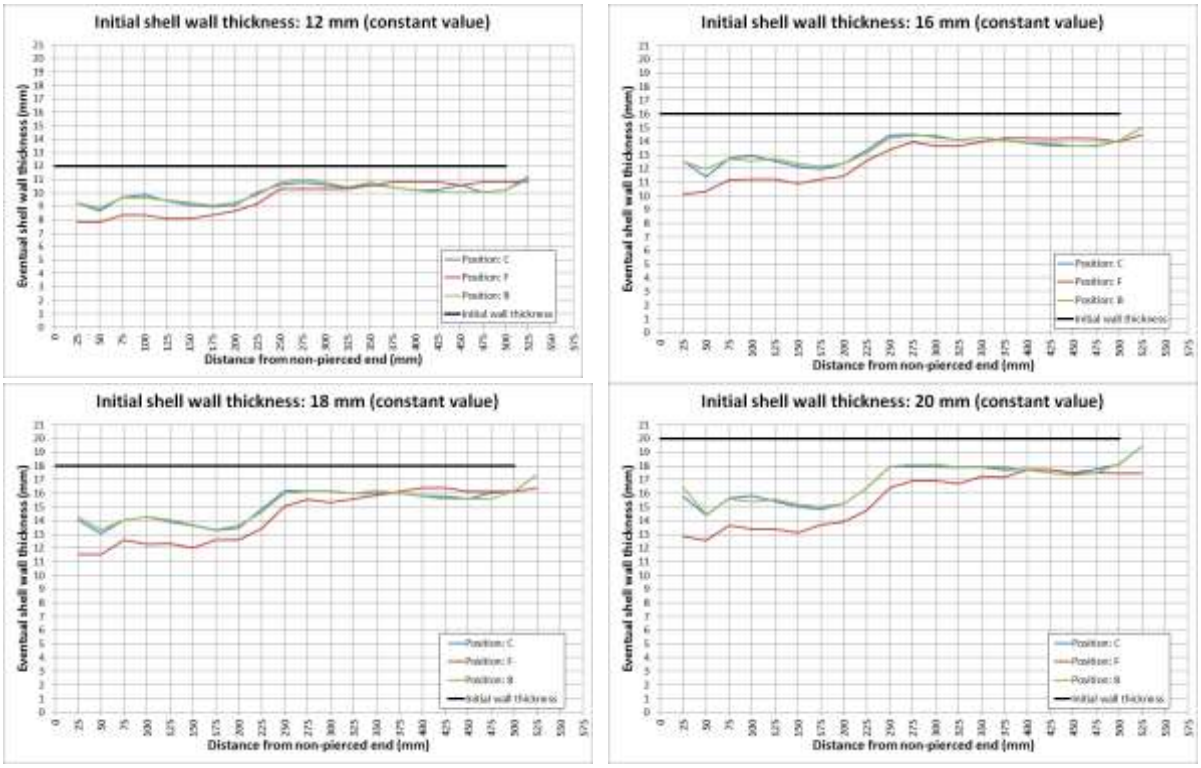

Fig. 23 The change of the shell wall thickness while piercing in the piercing press in Podbrezova (the billet cross-section – the circle)

Preheating is very important part of rolling process, since materials with different physical properties are heating up to 1300°C before rolling. It was necessary understand the of As for numerical simulations, Benteler and Podbrezova provided COMTES FHT (COM) with temperature modes used for the heating of gradient billets in a rotary heart furnace during the last industrial trials. COM on the basis of these temperature modes created a temperature model for the description of temperature behaviour of a billet in the rotary hearth furnace. Also, the subsequent cooling during transport and forming were being solved (see

Fig. 24).

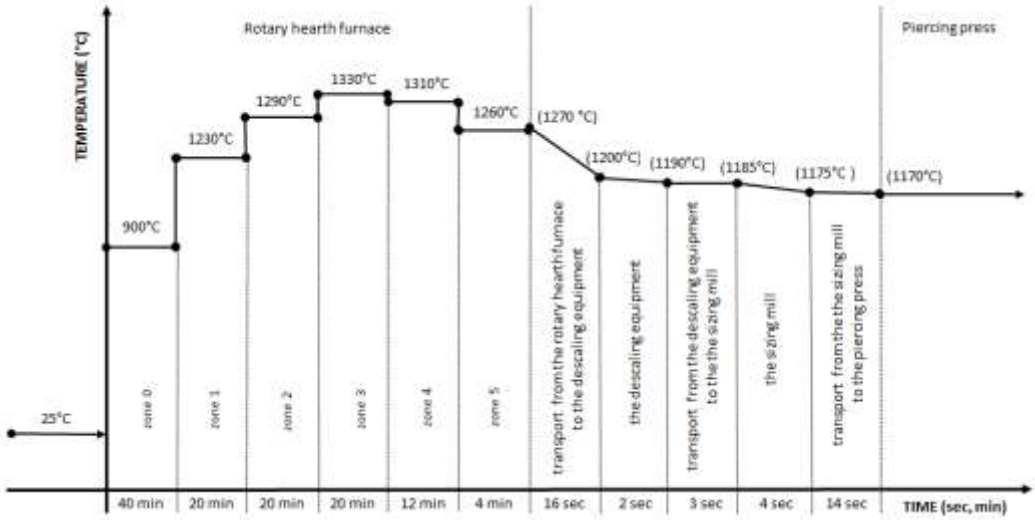

Fig. 24 Benteler (above) and Podbrezova (below) temperature characterization in the process chain

Also, a series of numerical simulations were carried out with the aim to create an alternative mode of the gradient billet heating in a rotary hearth furnace - see **Fig. 25**. The alternative mode should assist with minimising the aforementioned imperfections. The modes for both plants (Benteler and Podbrezova) are displayed in. They were suggested on the basis of theoretical knowledge (a literature

review), know-how of all partners in the GRAMAT consortium and a facility limitation (the nominal force of the piercing press) in Benteler and Podbrezova.

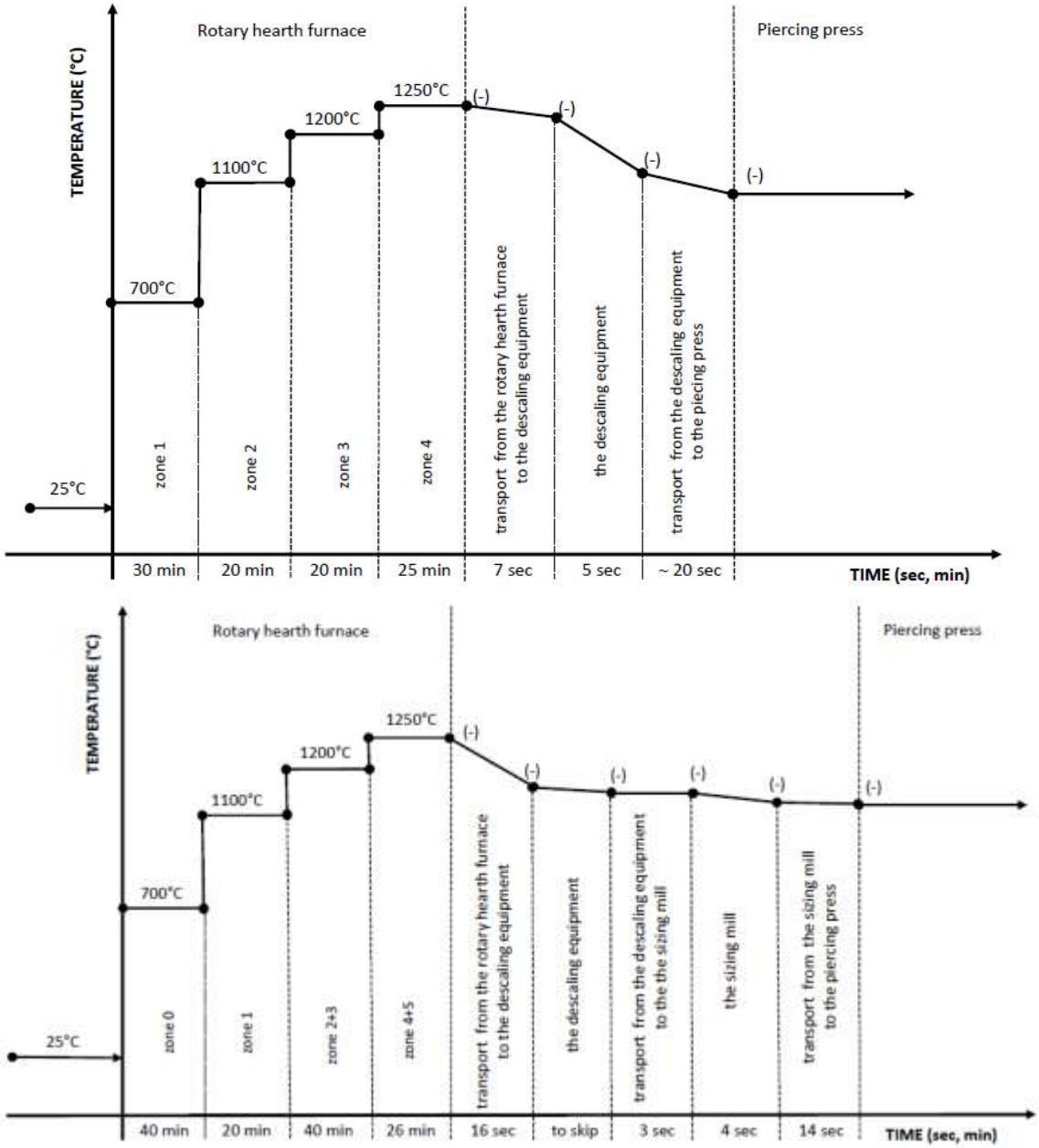

Fig. 25 Benteler (above) and Podbrezova (below) alternative modes for the gradient billet heating in a rotary hearth furnace. Note: (-) – without measurement

The temperature, strain and strain rate courses were analysed in the point P (see **Fig. 26**). The obtained courses served as input data for the physical simulations. Some of these courses, by way of illustration, are displayed in **Fig. 27**.
By combining the numerical and physical simulations, it is possible to assess the influence of the heating, cooling and forming operations on imperfections genesis. Based on this assessment, potential changes/corrections of the current technology can be done.

Fig. 26 The point position P at the beginning of the numerical simulation

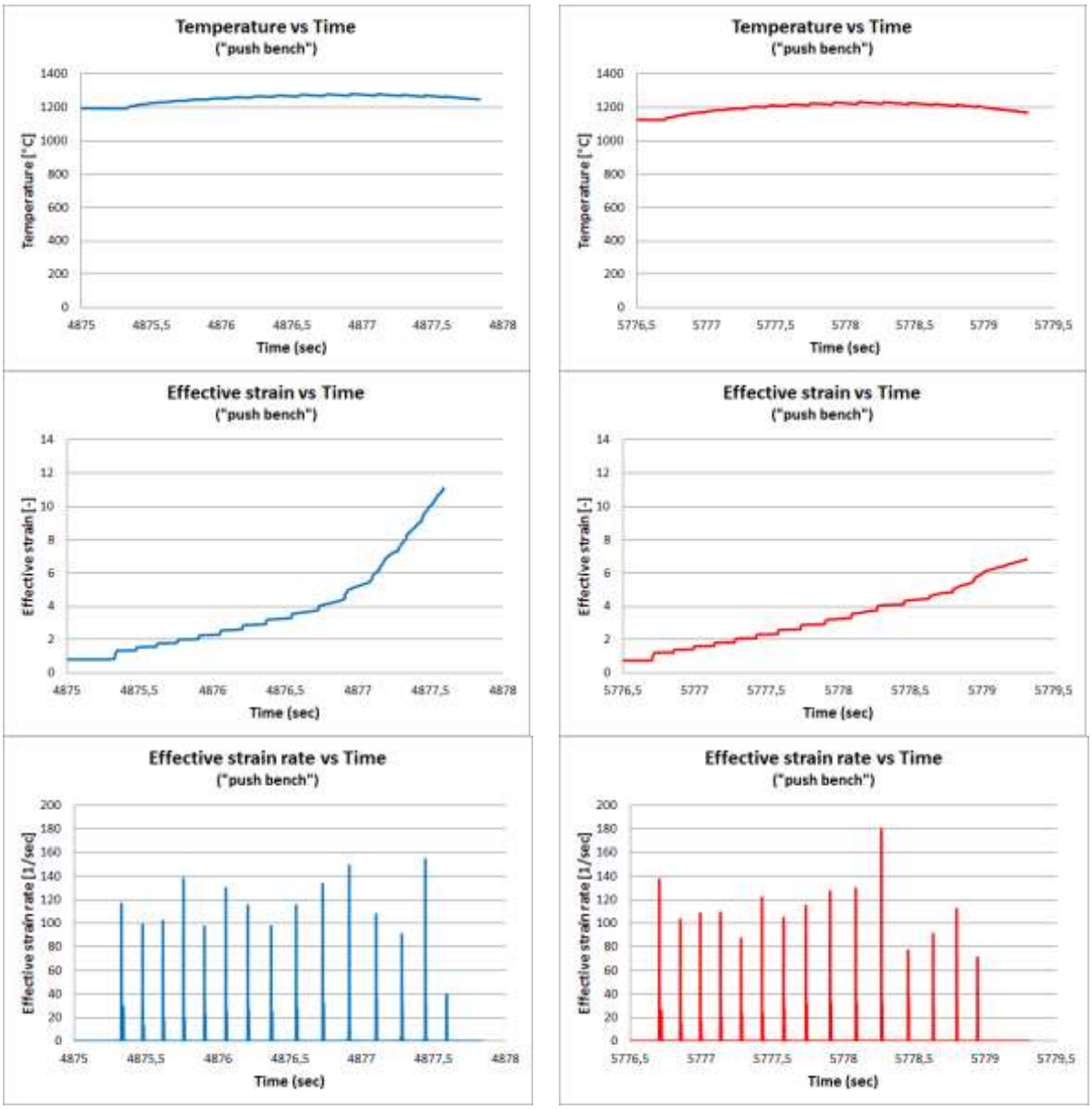

Fig. 27 Illustration of the temperature, strain and strain rate course in the selected point in different time intervals (blue interval, red interval)

TASK 2.2 PHYSICAL SIMULATION OF ROLLING

Within physical simulation tests, data inputs have been provided to numerical simulation models, flow stress data were measured and assessment of the cracking at higher temperature was performed. Besides several ordinary tests, two most important issues have been solved.

1. The behaviour of gradient interface during the strain stress exposure.
2. High temperature ductility of material 347H (shell)

1. The behaviour of gradient interface during the strain stress exposure

The aim of the physical simulation in the first phase was to provide numerical simulation with data to be used for the creation of the Johnson-Cook flow stress model. Isothermal compression tests were performed at the temperatures of 800 °C, 900 °C, 1000 °C, 1100 °C and 1200 °C, and at the strain rates of 1 s-1, 10 s-1 and 100 s-1 on thermal physical simulator Gleeble 3800. Test parameters determination was based on technological parameters of the rolling process (rolling mills: Podbrezova, Benteler). The influence of the temperature and the strain rate on flow stress values was observed.

The isothermal hot compression tests were conducted on a Gleeble-3800 thermo-simulation machine. The Gleeble 3800 is fully integrated digital closed loop control thermal and mechanical testing system.

Specimens of ø10mm x 12mm were used for both steels (specimens A from 13CrMo4-5 steel, specimens B form 347H steel). Experiments were conducted in chamber at 10^{-6} torr vacuum. Temperature was measured by means of thermocouple type K, Ni-Cr (+)/ Ni-Al (-), 0-1250°C and type R, Pt-13%Rh(+)/ Pt(-) 0-1450°C. The specimens were resistance heated to 1200°C at a heating rate 10°C/s. The temperature was held for 120s for the austenite fully homogenized. The specimens were then cooled to the deformation temperature at a cooling rate 5°C/s. The specimens were given a heat soak for 30s to eliminate the internal temperature gradients before testing. **Fig. 28** show the schematic diagram of heating process. The tests were done using temperatures of 1200°C, 1100°C, 1000°C, 900°C and 800°C. The strain rates tested were $1s^{-1}$, $10s^{-1}$, $100s^{-1}$ and the deformation was 60%. To reduce experimental error caused by friction between the specimen and testing fixtures, the tests were carried out in a vacuum, with both ends of the specimen coated with nickel-base high temperature lubricant and capped with graphite foil 0,25mm. The graphite was a disc with the diameter being about 2mm larger than the initial specimen diameter and inserted between the anvil and the specimen. The results obtained are mean value out of two tests.

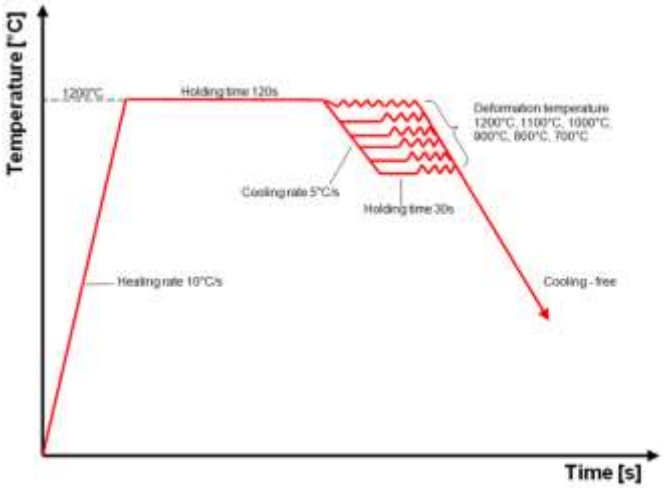

Fig. 28 Diagram of heating process

The compressive stress–strain curves obtained from the hot compression tests of 13CrMo4-5 steel and 347H steel are summarized in **Tab.** 5. The flow stress as well as the shape of the flow (strain – stress) curves is sensitively dependent on deformation temperature and strain rate. The flow stress increases monotonically from beginning to end at the temperature, showing dynamic work-hardening. In most instances, the stress level decreases with temperature increase and strain rate decrease because lower strain rate and higher temperature provide longer time for the energy accumulation and higher mobility at boundaries which result in the nucleation and growth of dynamically recrystallized grains and dislocation annihilation.

Tab. 5 The peak stress of both investigation steels (13CrMo4-5/ body and 347H/ shell)

Deformation temperature	Cooling rate	Hold	Strain rate	No. sample*	13CrMo4-5	347H
[°C]	[°C/s]	[s]	[s^{-1}]	[-]	[MPa]	[MPa]
800	5	30	1	A1/B1	**380**	**337**
			10	A2/B2	**368**	**459**
			100	A3/B3	**437**	**484**
900	5	30	1	A4/B4	**287**	**252**
			10	A5/B5	**304**	**389**
			100	A6/B6	**338**	**434**
1000	5	30	1	A7/B7	**254**	**170**
			10	A8/B8	**232**	**297**
			100	A9/B9	**297**	**343**
1100	5	30	1	A10/B10	**170**	**135**
			10	A11/B11	**186**	**217**
			100	A12/B12	**241**	**307**
1200	---	---	1	A13/B13	**112**	**105**
			10	A14/B14	**134**	**153**
			100	A15/B15	**198**	**184**

***A1/15 – 13CrMo4-5 (body)/ B1/15 – 347H (shell)**

In contrast, for a fixed temperature, the flow stress generally increases as the strain rate increases due to the increase of dislocation density and the dislocation multiplication rate. When the flow stress relative to the temperature is compared to the flow stress relative to the strain rate, there is no doubt that the effect of temperature on the flow stress is more pronounced than that of the strain rate on flow stress.

2. High temperature plasticity material 347 (shell)

Due to concerns on possible cracking of 347H steel at higher temperature, experiments on liquation cracking susceptibility of 347H steel were performed. The GLEEBLE 3800 physical simulator was used for the evaluation of Nil-Strength Temperature, Nil-Ductility Temperature and Nil-Ductility range. Nil-Strength Temperature of 1338 °C, Nil Ductility Temperature - on heating of 1328 °C, Nil Ductility Temperature - on cooling of 1318 °C and Nil- Ductility range of 20 °C was specified for the tested sample of steel. The results are summarized in **Tab. 6** and **Fig. 29**.

Tab. 6 Experimental results for 347H steel

Material	347H
Nil-Strength Temperature NST	**1338°C**
Ductility Temperature NDT – on heating	**1328°C**
Ductility Temperature NDT – on cooling	**1318°C**
Nil- Ductility range NDR (NST – NDT on cooling)	**20°C**

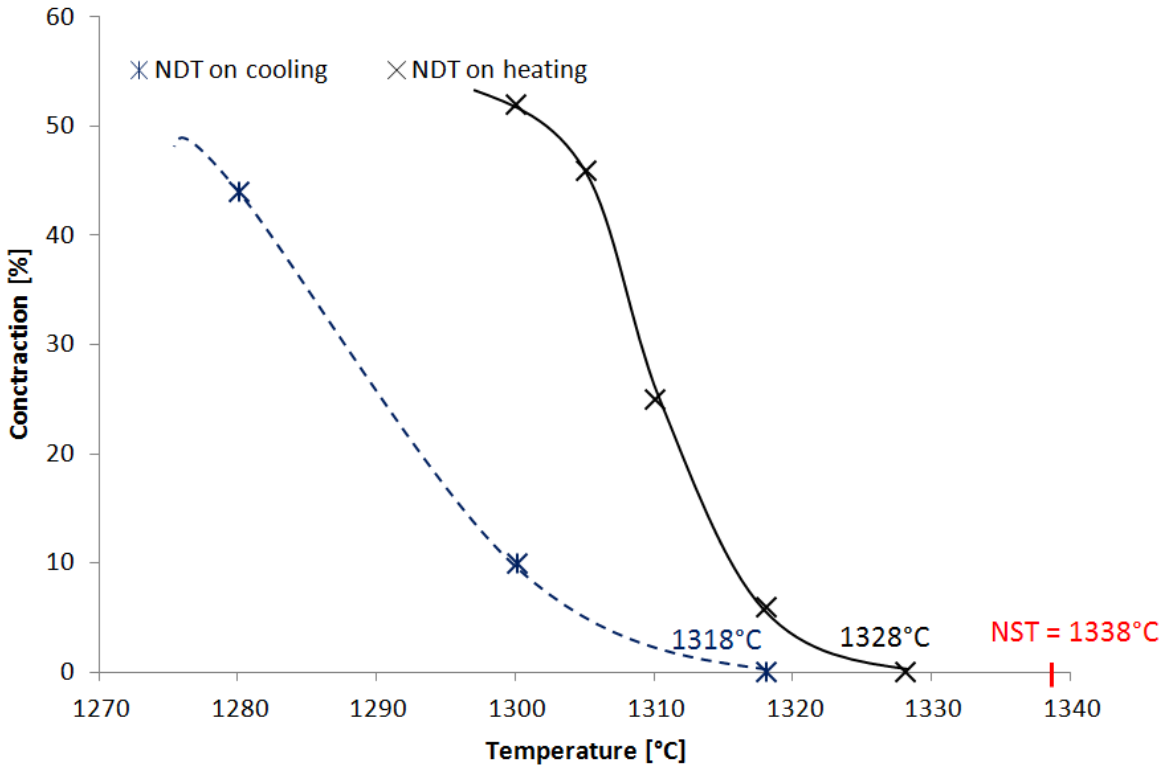

Fig. 29 "On-heating" and "on-cooling" ductility curve (347H)

Physical simulations determined that working temperature in any forming operation should not exceed 1300 °C due to danger of cracking of 347H at higher temperature.

TASK 2.3 TRIALS OF GRADIENT INGOTS ROLLING

- **1st generation**

The gradient billets from first industrial trials s were used in this stage.

The course of forming operations in Benteler/Podbrezova was carried out in the following order: Heating in a rotary heart furnace – piercing press processing – elongation mill -push bench rolling – detaching mill rolling – heating in a reheating furnace – stretch-reducing mill rolling

In Benteler, all process steps of the seamless hot-rolled tubes manufacturing were successfully passed. The appearance of the gradient hollow block after withdrawing from piercing press is seen in

Fig. 30. The smooth diffusion join between core and shell is clearly seen.

Fig. 30 Hollow block after piercing press.

The body and shell in the gradient billet/semiproduct did not separate during the whole rolling sequence. Therefore, Benteler was able to produce the first successful gradient tubes (**Fig. 31**).

Fig. 31 The gradient tubes on cooling bed after final rolling operation stretch-reducing mill

After the successful tube production from the oval gradient billets at Benteler rolling mill, all tubes (also semi-products withdrawn from production lines) were sent to WRI in Bratislava for quality testing. **The first generation of gradient tubes passed all A AFW requirements for the commercially available boiler tubes**. As a result, A AFW has decided to place in a power for long-term testing.

Podbrezova also carried out the industrial trial of the first-generation gradient tubes rolling. As for the course of the industrial trial, two **square** shaped gradient billets were rolled. The billet made in WRI laboratory was not completely rolled up to a final gradient tube. The shell (outer material) was disintegrated after rolling in the elongator and therefore this semi-product was withdrawn after this mill. The ZD billet was rolled up to a final gradient tube, however, the final tube had several surface defects and there was only short part with the sufficient surface quality (ca. 1.8 m) – see **Fig. 32**.

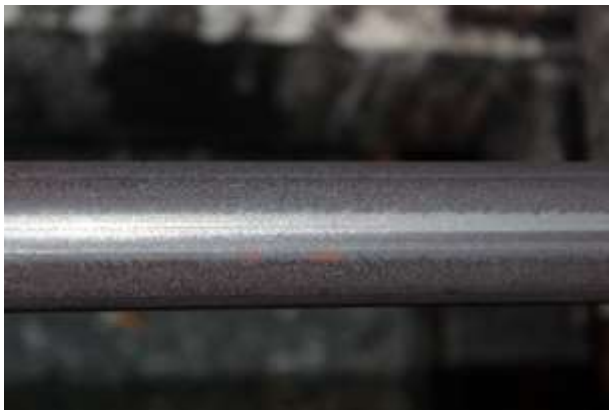

Fig. 32 Approximately 1.8 m of gradient tube with the outer surface without defects

- **2nd generation**

The gradient billets from second industrial trials s were used in this stage.
Work towards the second generation of rolling was concentrated to **the optimisation of the overall billet shape and other shell geometry to improve the quality of gradient tubes**. Six industrial gradient billets were prepared for rolling. This rolling was carried out in Podbrezova. The brief characteristic of the gradient billets is mentioned in **Tab. 7.** The cross-sectional overview of the billets is shown in **Fig. 33**.

Tab. 7 The most important attributes of the gradient billets

Billet No.	Cross-section (mm)	Cross-sectional geometry (mm)	Length (mm)	Body material	Shell material	Shell wall thickness (mm)
1	Round	∅ 250	495	11CrMo9-10	347H	12
2	Square	205 x 205 R60	517	11CrMo9-10	347H	12
3	Square	205 x 205 R40	460	11CrMo9-10	347H	12
4	Round	∅ 210	548	11CrMo9-10	347H	12
5	Round	∅ 210	772	11CrMo9-10	347H	12
6	Square	200 x 200 R80	611	11CrMo9-10	347H	12

Fig. 33 The gradient billets after dimensional inspection

The rolling strategy was divided into two main courses.
The 1st course of forming operations was carried out in the subsequent order:
Heating in a rotary heart furnace – piercing press processing – push bench rolling – detaching mill rolling – heating in a reheating furnace – stretch-reducing mill rolling. No elongating mill processing was intended to avoid tearing the surface austenitic layer in this technological operation. By this course, the gradient billets No.4 and 5 were selected for next processing.
The 2nd course of forming operations was carried out in the subsequent order:
Heating in a rotary heart furnace – piercing press processing – elongation on an elongating mill – push bench rolling – detaching mill rolling – heating in a reheating furnace – stretch-reducing mill rolling. By this course, the gradient billets No.1, 2, 3, and 6 were selected for next processing. These billets were processed by the standard technology.
Gained results were as follows.
The gradient billet No.4 was successfully rolled over all technological operations. However, a load of the piercing press was largely increased during piercing. When piercing the gradient billet No.5, a piercing press load exceeded a critical level and the gradient billet was removed from further rolling. Based on these circumstances, the rolling of the gradient billet No.1 was cancelled. The explanation of the increased piercing press load during round billet piercing is the fact that a round cross – section is not a standard input format for the rolling line in Podbrezova. A standard input cross – section is a square billet with preferred sideways material spreading in contrast to upward material spreading in case of round billets.
Subsequently, all 3 square billets No. 2, 3 and 6 were set for rolling. There were no problems during rolling in terms of the piercing press, elongating mill, push bench, detaching mill or stretch-reducing mill.
Altogether 4 tubes were rolled. Cross-sectional dimensions of the tubes after stretch-reducing mill were 38 x 5 mm (outer diameter x wall thickness). The length of these tubes was 30 metres. These tubes were subsequently cut into two 14 – 15 metre pieces.
After all industrial rolling trials had been finished, visual and NDT (Non-Destructive Testing) analyses of the gradient tubes were performed. The visual analysis of tubes surface after rolling has proved that the best results were reached on tubes from the square gradient billet No. 6. Based on the NDT (an Eddy current test + ultrasonic inspection) analyses, the best results were reached on the tubes from the square billet No. 3, especially on the first 15-metre part. Typical random defects on all Podbrezova gradient tubes are seen in **Fig. 34**. The genesis of these defects was analysed. It was assumption that these defects were caused by a high temperature of heating in a rotary hearth furnace; and they were in fact mitigated by lowering the temperature in rotating furnace.

Fig. 34 Tubes surface defects

- **3rd generation**

The gradient billets from 5th industrial trials s were used in this stage.

The third rolling of industrially casted gradient billets was conducted in both Benteler (3 billets) and Podbrezova (3 billets).
All of those 6 billets had the metallurgical bond in the range of 30-70%.
Rolling trial at Benteler was not successful. First billet did not pass behind the elongator and the process had to be stopped. Rolling trial at Benteler was not successful. Billet did not pass behind the elongator and the process had to be stopped - **Fig. 35**.

Fig. 35 Semiproduct taken out of the elongator with stripped outer shell

In Podbrezova, 1st billet was rolled successfully over the all technological steps. The final tube dimension: OD (outer diameter) 37.97 mm, WT (wall thickness) 5.07 mm and 38.5 m in length (without crop ends). Approximately 30 % of the final tube length (the front end) was found with visible surface defects. The rest of the tube length was found visually good (**Fig. 36**). The tube surface over the whole length corresponds with the fact that both descaling units were turned off.

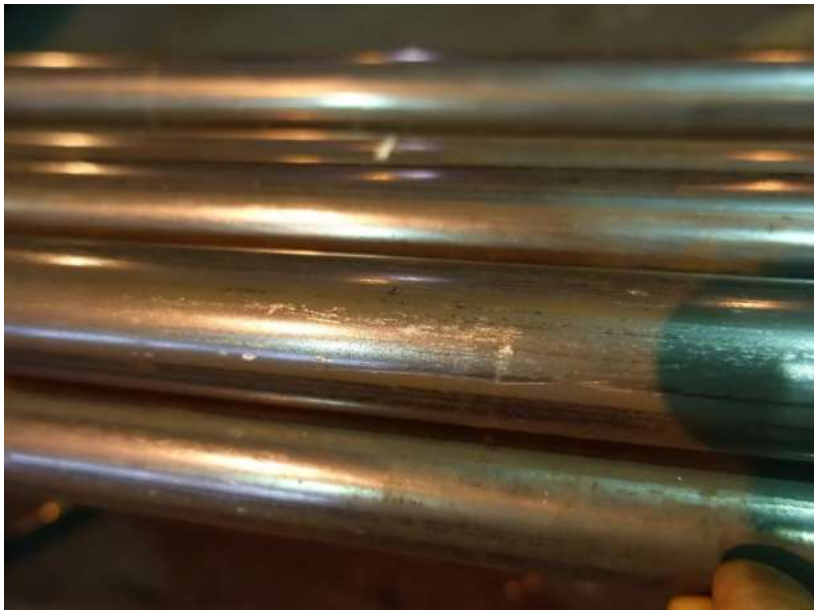

Fig. 36 The parts of the final gradient tube without the surface defects

The third industrial rolling of industrially casted gradient billet has proved that in the case of good diffusion joint between austenitic and ferritic layer, the chosen technological parameters of heating, piercing and rolling are suitable for the production of gradient tubes.

The third rolling of industrially casted gradient billets was conducted in both Benteler (3 billets) and Podbrezova (3 billets).

The 2nd and 3rd gradient billets were heated, pierced and elongated. After elongation, the outer austenitic layer was disintegrated from the ferritic core, and the pieces could not be further processed - **Fig. 37**.

Fig. 37 The cross sections of the gradient semi-products made of the 2nd (left) and 3rd (right) gradient billets after the elongation.

The third industrial rolling of industrially casted gradient billet has proved that in the case of good diffusion joint between austenitic and ferritic layer, the chosen technological parameters of heating, piercing and rolling are suitable to produce the gradient tubes.

FINAL CONCLUSIONS FROM WP FORMING

All three tasks: both numerical (2.1) and physical (2.2) simulation and rolling trials (2.3), contributes to the first WP 2 objective to obtain basic knowledge to define gradient tube rolling process. **The original project assumption that the gradient tubes can be produced at existing rolling plants with minimal process changes was proved to be true**. However, the simulations and the industrial trials show that the process stability is strongly related to the quality of gradient billet (feedstock). Oval gradient billet brought about better results than the square ones.

When there was a oval billet with good diffusion joint between the layers, the rolling process was running steadily. Square billets, chronically starving to insufficient diffusion joints at corners, causes rolling instabilities either during piercing operations or later during elongation steps.

Both tube manufacturers (Benteler, Podbrezova) successfully produced gradient tubes only at limited lengths corresponding to the areas of high-quality diffusion joint of billet material. On the other hand, the quality of tube was high enough to pass all qualification tests required by A AFW for real-life boiler testing. Coil made of GRAMAT gradient tubes in the first half of the project was installed in boiler and so far successfully passed 4 years of testing at operating conditions.

Three generations of tubes which are roughly corresponding to the second, third and fourth year of project duration. All three generations were based on the same material combination:

Outer material: 347H (1.4912)

Inner material: 11CrMo9-10 (1.7383) or a very close material 13CrMo4-5

Thorough metallographic analysis and boiler qualification tests of the first generation followed by numerical and physical simulations enables reaching the better understanding of all metallurgical and physical phenomena of gradient tubes rolling. The most difficult issues consortia met during the project are listed below along with the proposed corrective measures.

1) Grain size of austenitic outer surface layer (347H)
   Precaution: Lowering of rotary hearth furnace temperature to stay below critical grain growth temperature
2) Surface imperfections (voids and cracks)
   Precaution: Increase the final rolling temperature to keep austenitic material in good formability region by increasing reheating furnace temperature before stretch-reducing mill. Decreasing of surface zone grain size also helped to improve formability and consequently also it improves the surface quality
3) Large carburized zone at outer part (347H) of gradient zone and large decarburized zone at inner part (11CrMo9-10) of gradient zone.
   Precaution: Modified heat treatment to minimize undesired carbon diffusion and maintain the required mechanical properties in the same time.

Work package 3: Utility properties

TASK 3.1 HIGH TEMPERATURE CORROSION AND STEAM OXIDATION RESISTANCE

In this section, the most important outputs from corrosion testing are stressed out. The high temperature corrosion properties are the key feature for gradient tubes implementation in biomass boilers.
Corrosion properties of body and shell materials have been determined for selected boiler conditions in high temperature corrosion laboratory and supercritical autoclave.

The testing conditions:
the exposure: 550°C for 164h (one week),
the exposure atmosphere:
Air + (2000) ppm HCl + (200) ppm SO_2 + (15%) H_2O
corrosion accelerator: NaCl-KCl-Na_2SO_4 (6.5/34.5/ 59 wt.-%) mixture

The corrosion rates of both gradient tube and conventional 347H tube is compered in **Fig. 38**. In general (comparison of column 1 and column 4 in **Fig. 38**), **the results are very promising for the as-received gradient tube** heat treated according to the 11CrMo10-9 requirements. The corrosion of both whole austenitic tube and gradient tube respectively is the same.

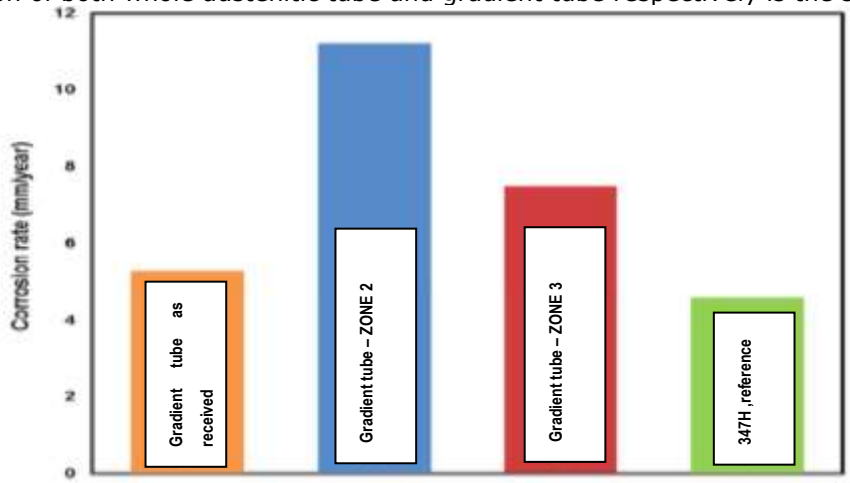

Fig. 38 Corrosion rate – high temperature corrosion with deposit

The deeper investigation shows that austenitic shell consists of three different microstructures - (see **Fig. 39**).
ZONE 1: highly deformed zone at outer diameter, possible location of the defects
ZONE 2: ordinary austenitic microstructure (revealed after grinding of the zone 1)
ZONE 3: sensitized microstructure (carbon diffusion from ferritic body during metallurgical processes).
To test each zone, the shell material was "peeled out" from the gradient tubes by machining. The extent of machining was set by measurement the each above mentioned zone. The results are summarized in columns 2 and 3 in **Fig. 38.**

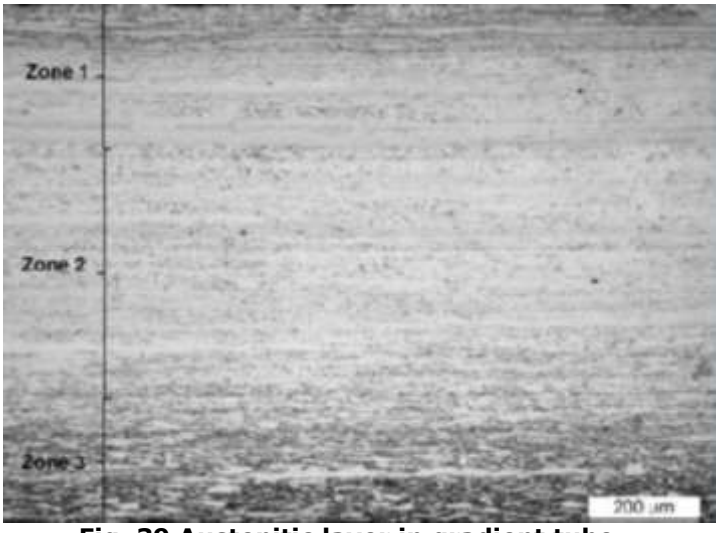

Fig. 39 Austenitic layer in gradient tube

Although overall corrosion of gradient tubes similar to 347H material, the ZONES 2 and 3 showed higher corrosion during the laboratory testing. The only explanation is that the mitch match occurred when not exactly symmetric tubes were "peeled". The only relevant output from this test is following: the internal parts of austenitic shell are less corrosion resistant when comparing the outer parts, mainly due to carburisation/sensitisation of the ferritic/austenitic interface.
To conclude, the thickness and microstructural state of the austenite layer as well as possible surface defects of the gradient tube have a great influence on the high temperature corrosion rate of the gradient material, as well as the size of the heat affected zone.
The lessons from corrosion tests are as follows: ZONE 1 should be manufactured without big defects. ZONE 3 should be as narrow as possible. Both phenomena relate to forming technology.

The laboratory corrosion test results presented are accelerated laboratory scale test results and are only indicative not showing a real service performance. The real long-term performance of gradient tube material is obtained from in real service environment test.

- **Partial conclusions**

Finally, the materials selected for the gradient tube have good high temperature corrosion resistance as well as needed steam oxidation resistance for the high temperature components of biomass boilers. To obtain optimal high temperature corrosion resistance the shell material layer should be approximately 1 mm thick, without any surface defects.

TASK 3.2 WELDABILITY AND ALLIED PROCESSES

- **Introduction**

The welding of the gradient tubes is other critical issue in terms of utility properties. Main task was to perform first circumferential welds on gradient tubes samples to investigate influence of welding thermal cycle on utility properties of welded tubes and to provide a first proposal of welding procedure to the boiler manufacturer (AFW). During the experiments described by this report, commercially available consumables have been selected and used for welding experiments and optimal welding procedures, including preheat, bead size (especially in cap region) and sequence were investigated.

- **Experiments**

The seamless hot – rolled gradient tubes (38mm outer diameter, 5mm wall thickness from which austenitic shell is ~1mm thick), made of material low alloyed body (11CrMo9-10) and austenitic shell (A182F347H) were used for weldability investigation, see **Tab.** 8 and **Tab. 9**. The tubes were delivered in quenched and tempered condition in accordance with EN 10216-2 for no. 1.7383 (11CrMo9-10). Gradient tubes were rolled in Benteler from gradient cast manufactured by unique casting technique (ŽDAS, Inc.).

The gradient tubes were welded by TIG welding in the shielding gas Ar 100% (12 l/min– direct protection and 8l/min root protection), employing ø2mm EN ISO 14343-A: W 19 9 Nb, EN ISO 14343-A: W 23 12LSi and EN ISO 21952-A: W CrMo2Si consumables – see also **Tab. 10**. Polarity was "-"in all cases. Selected welding parameters are shown in

Tab. 11. After welding, the welds were cooling down in protection covers till 50°C. No PWHT was applied.
The testing methods and standards are summarized in
Tab. 12.

Tab. 8 Chemical composition - 347H (wt. %) – outer shell

	C	Si	Mn	P max.	S max.	Cr	Ni	Nb	N
Standard ASTM SA182 Grade A182F347H	0.04 - 0.10	≤ 1.00	≤ 2.00	0.040	0.015	17.00 - 19.00	9.00 - 12.00	8xC 1,20	≤ 0.1100
HEAT	0,06	0,47	1,47	0,022	0,007	17,95	11,20	0,57	0,0118

Tab. 9 Chemical composition - 11CrMo9-10 (wt. %) – body

	C	Si	Mn	P max.	S max.	Cr	Mo	Ni	Al	Cu
Standard EN10222-2 Grade 11CrMo9-10	0,08 - 0,15	≤ 0,50	0,40 - 0,80	0,025	0,020	2,00 - 2,50	0,90 - 1,10	≤ 0,30	≤ 0,040	≤ 0,30
HEAT	0,10	0,21	0,59	0,007	0,001	2,25	0,96	0,20	0,006	0,10

Tab. 10 Chemical composition – consumables used (wt. %)

	C	Si	Mn	Cr	Mo	Ni	Cu
EN ISO 14343-A: W 19 9 Nb	0,05	0,5	1,8	19,6	-	9,5	0,05
EN ISO 14343-A: W 23 12LSi	≤ 0,03	0,8	1,8	24	≤ 0,3	13	≤ 0,3
EN ISO 21952-A: W CrMo2Si	0,08	0,60	0,92	2,45	1,00	-	-

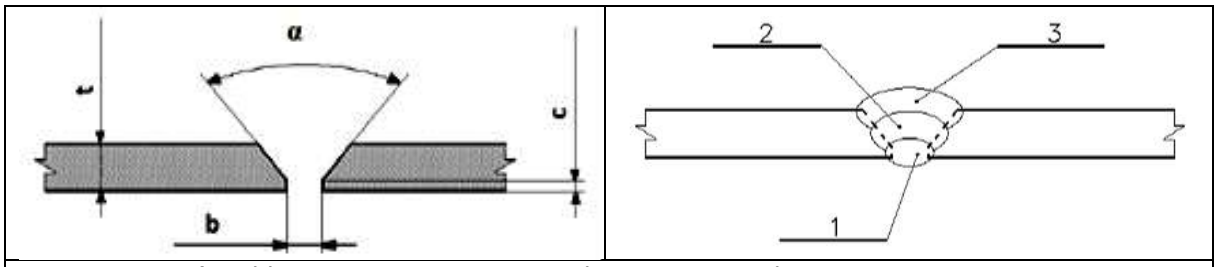

a) weld joint 1, 2, 3, 4, 5; joint shape: α = 60°, b = 2 mm, c = 2 mm

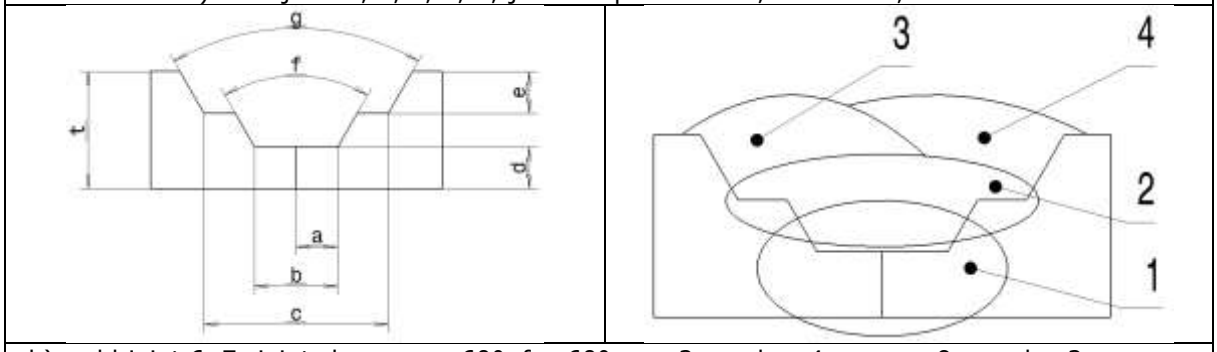

b) weld joint 6, 7; joint shape: g = 60°, f = 60°, a = 2mm, b = 4mm, c = 9mm, d = 2mm, e = 2mm

Fig. 40 Weld joint preparation and bead sequence

Tab. 11 Welding parameters

Weld joint	Beads	Wire	Welding current [A]	Welding Voltage [V]	Inter-pass (°C)	Welding speed [mm/s]	Heat input [kJ/mm]
1a	Root	19Cr9NiNb	100-115	10-12	220	0,75	0,9-1,3
	Filling	19Cr9NiNb	100-115	10-12		0,75	0,9-1,3
	Cap	19Cr9NiNb	116-125	11-13		1,1	1,0-1,2
1b	Root	19Cr9NiNb	100-115	10-12	220	0,75	0,9-1,3
	Filling	19Cr9NiNb	100-115	10-12		0,75	0,9-1,3
	Cap	19Cr9NiNb	116-125	11-13		1,1	1,0-1,2
2	Root	23Cr12NiLSi	100	10-11	150	1,0	0,6
	Filling	23Cr12NiLSi	100	10-11		1,0	0,6
	Cap	19Cr9NiNb	100	10-11		1,0	0,6
3	Root	23Cr12NiLSi	95-100	10-12	150	1,0	0,6-0,8
	Filling	23Cr12NiLSi	95-100	10-12		1,0	0,6-0,8
	Cap	19Cr9NiNb	95-100	10-12		1,0	0,6-0,8
4	Root	-	95-100	10-12	150	1,0	0,6-0,8
	Filling	23Cr12NiLSi	95-100	10-12		1,0	0,6-0,8
	Cap	19Cr9NiNb	95-100	10-12		1,0	0,6-0,8
5	Root	-	95-100	10-12	150	1,0	0,6-0,8
	Filling	23Cr12NiLSi	95-100	10-12		1,0	0,6-0,8
	Cap	19Cr9NiNb	95-100	10-12		1,0	0,6-0,8
6	Root	-	60-70	9-10	150	1,2	0,9-1,0
	Filling	23Cr12NiLSi	75-85	10-11		1,0	0,6-0,8
	Cap	19Cr9NiNb	87-95	11-13		1,0	0,6-0,8
7	Root	-	58-66	9-10	150	0,6	0,7-0,9
	Filling	CrMo2Si	70-80	10-11		0,6	0,8-1,2
	Cap 1	19Cr9NiNb	77-85	10-12		1,0	0,5-1,0
	Cap 2	19Cr9NiNb	77-85	10-12		1,0	0,5-1,0

Tab. 12 Test method of weld joint

Weld joint	Test method		Test standard
1 - 7	**Non-destructive testing**	Visual examination	EN ISO 5817, EN ISO 17637
		Penetrant testing	EN ISO 23277, EN ISO 3452-1
		Radiographic examination	EN ISO 17636-, EN ISO 10675-1
1 - 3	**Destructive testing**	Tensile test at room temperature	EN ISO 6892-1:2010
		Tensile test at elevated temperature (450°C)	EN ISO 6892-1:2010 EN ISO 6892-2:2011
1 – 7	**Macroscopic examination**		EN ISO 17639
1, 3, 7	**Microscopic examination**		EN ISO 17639
1, 3, 7	**Hardness test**	Vickers hardness test (HV5)	EN ISO 9015-1, EN ISO 6507-1
1	**Bend test**		EN ISO 5173:2010-10

- **Results**

Results of NDT test were evaluated as acceptable according to all standards mentioned in

Tab. 12. Macrographs of welded joints 1 - 7 are seen in **Fig. 41**. The welds were sound without pores but weld joint 4, 5, 6 showed an extensive inter pass lack of fusion. The HAZ is relatively wide for this kind of welds.

a) weld joint 1a

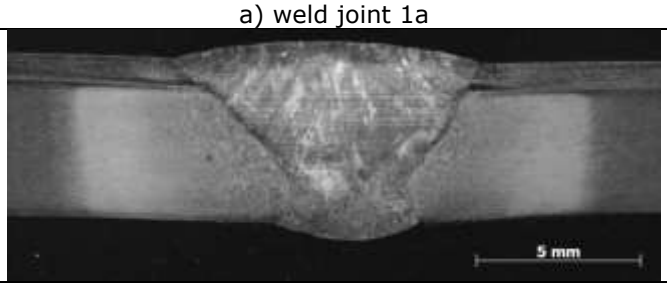

b) weld joint 1b

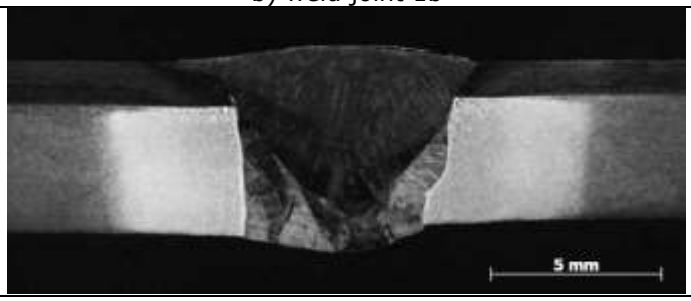

c) weld joint 2

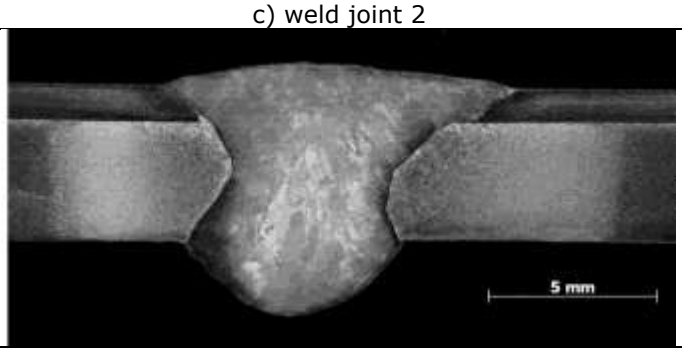

d) weld joint 3

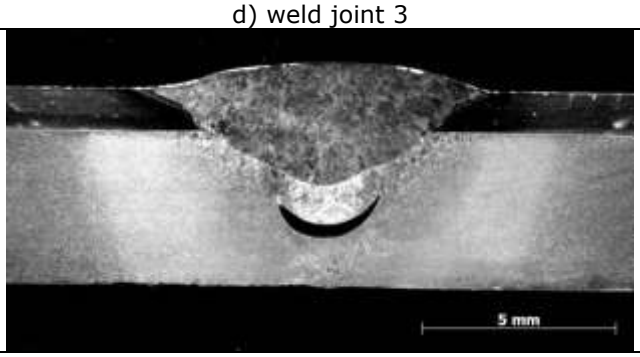

e) weld joint 4

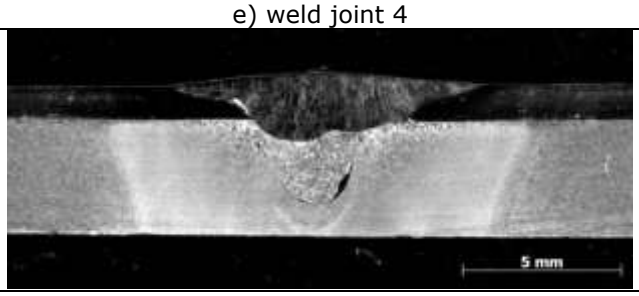

f) weld joint 5

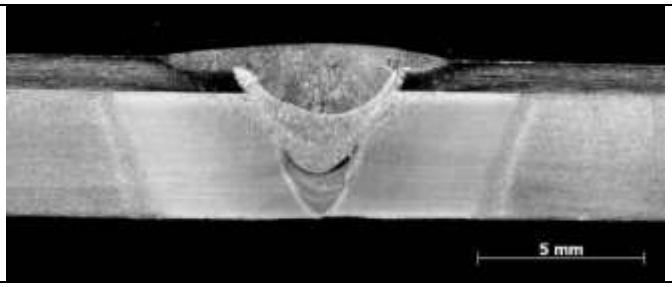

g) weld joint 6

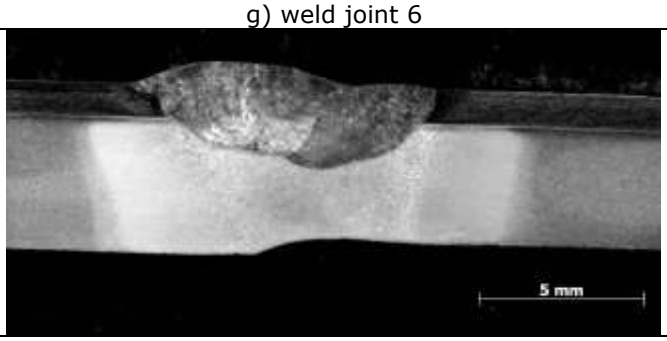

h) weld joint 7

Fig. 41 Macroscopic analysis of weld joints

The microstructure of shell (A182F347H) and body (11CrMo9-19) are seen in **Fig. 42**. Austenitic microstructure with low precipitation typical for solution treated material was observed in A182F347H steel. Mostly bainitic microstructure was dominating in 11CrMo9-10 steel.

The typical microstructure of HAZ triple point (shell + body + weld metal) and other important parts of weld 1a, b are summarized in **Fig. 43**.The microstructures are typical for given materials and welding technique. The triple point (**Fig. 43a**) is free from flaws or oxides. The borders in between microstructures are well defined, no brittle structure neither segregation bands were observed. The HAZ in between shell and weld metal is free from defects, 347H material grain size is slightly increased when comparing to base metal, however no grain boundary precipitation was observed, (**Fig. 43b**). Typical heterogeneous microstructure of low alloyed HAZ and high alloyed weld metal are in (**Fig. 43cd**). HAZ consist of coarse grained bainitic microstructure with no evidence of brittle martensite phases. Weld metal in cap and filling has typical austenitic cast microstructure containing several % of delta ferrite (**Fig. 43ef**). Cast microstructure is less visible in twice refined root parts (**Fig. 43f**). The same structure was observed in the weld joint 3 and 7 see **Fig. 44**.

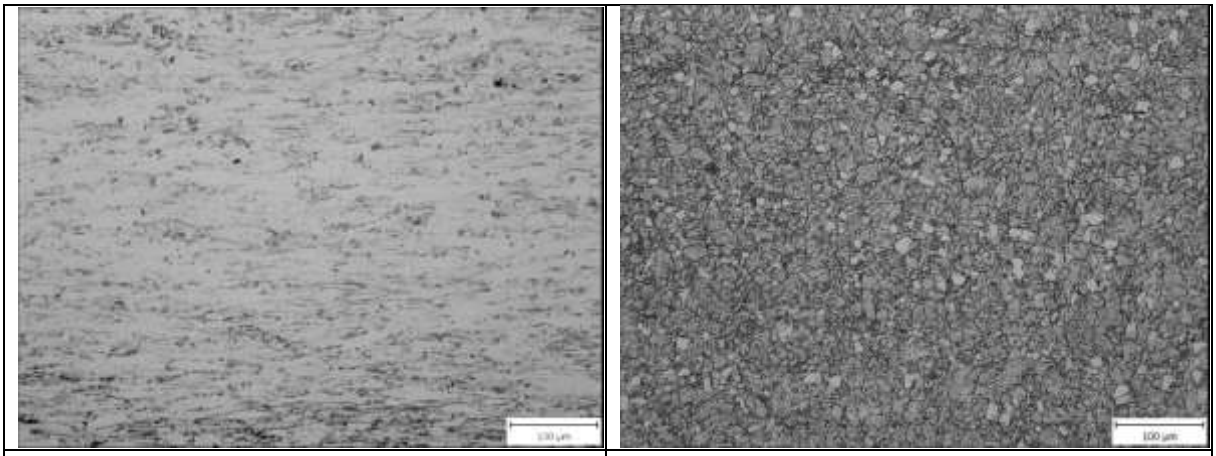

a) shell (347H)	b) body 11CrMo9-10

Fig. 42 Base metal microstructures

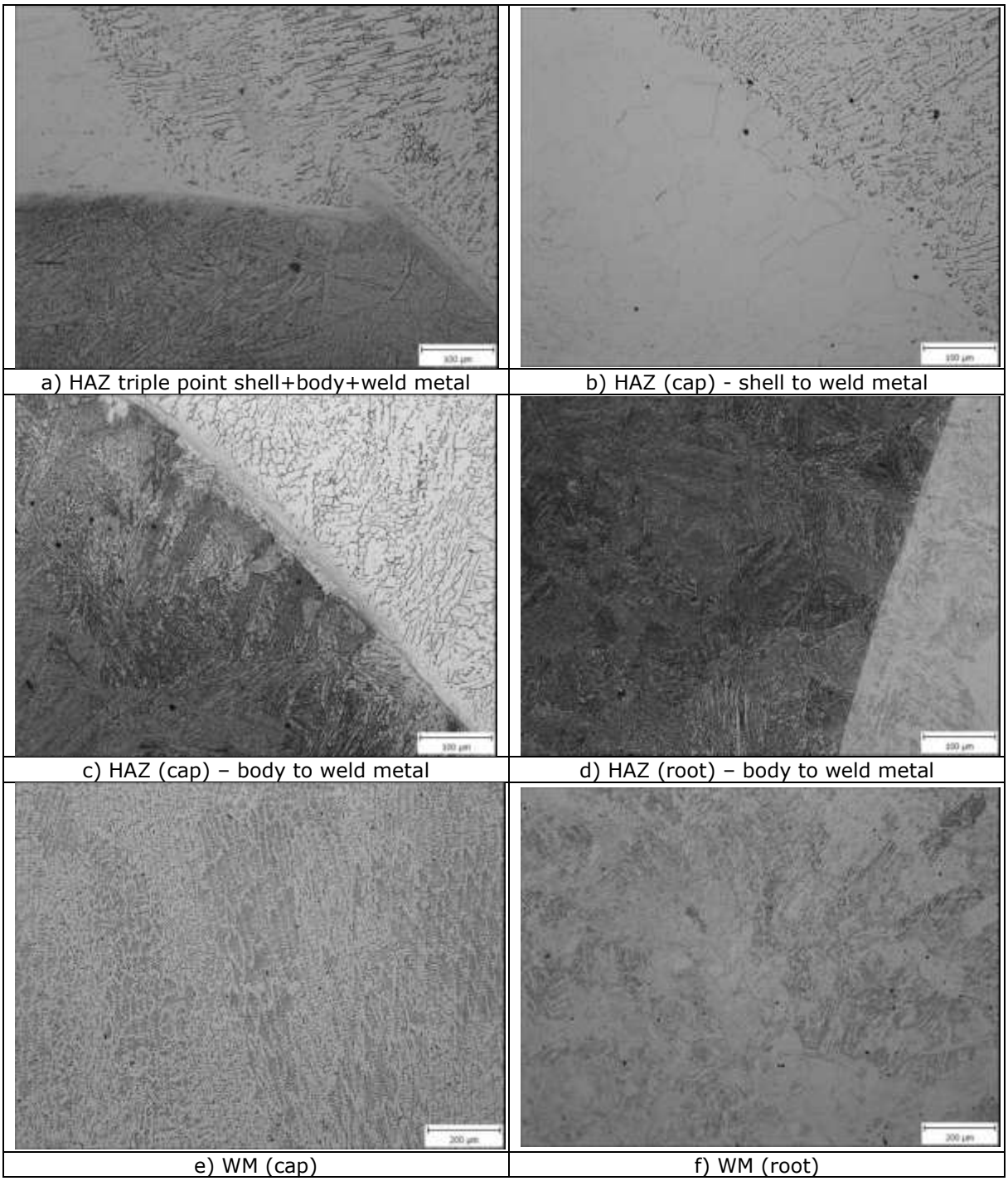

a) HAZ triple point shell+body+weld metal | b) HAZ (cap) - shell to weld metal

c) HAZ (cap) – body to weld metal | d) HAZ (root) – body to weld metal

e) WM (cap) | f) WM (root)

Fig. 43 Typical weld joint microstructures, weld 1a, b

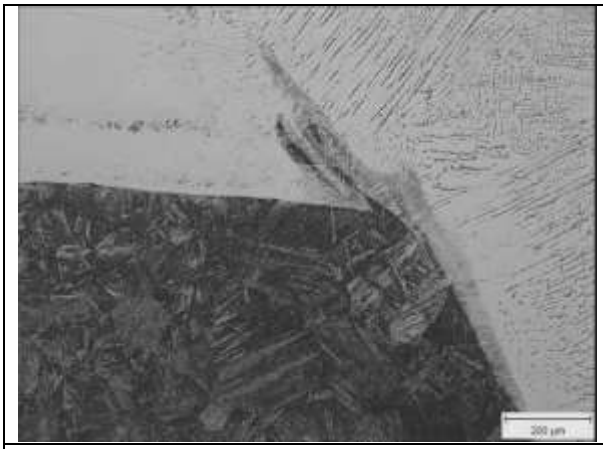

a) HAZ triple point shell+body+weld metal

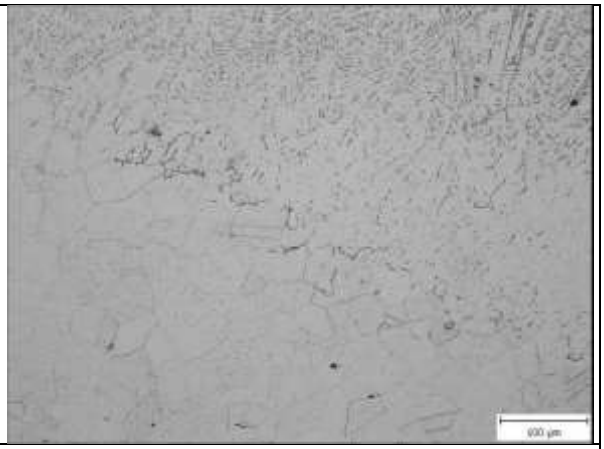

b) HAZ (cap) - shell to weld metal

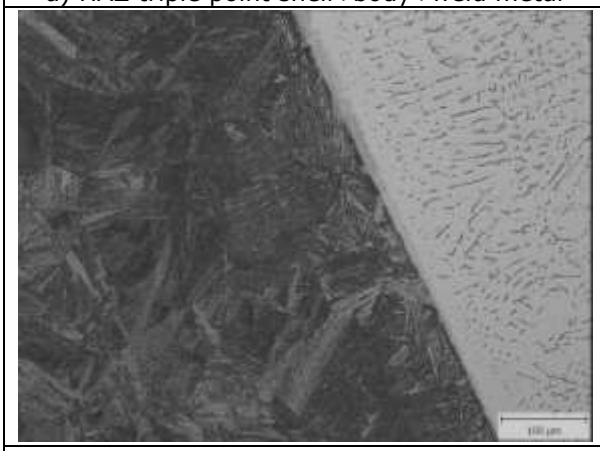

c) HAZ (cap) – body to weld metal

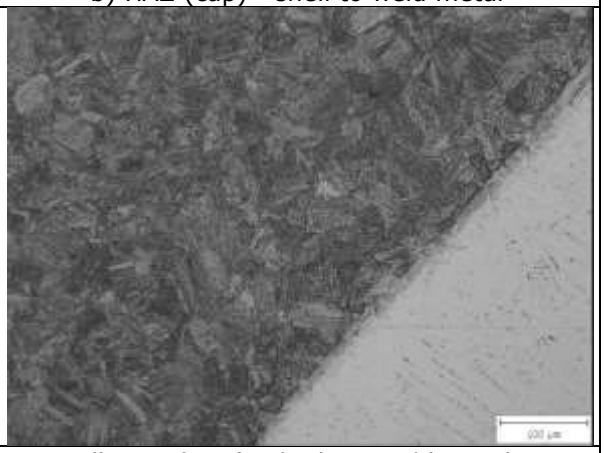

d) HAZ (root) – body to weld metal

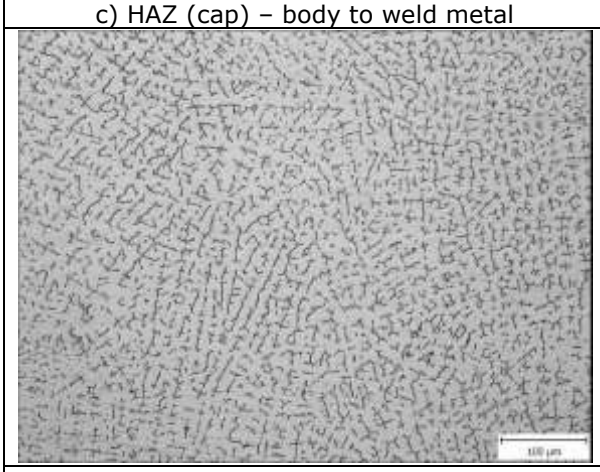

e) WM (cap)

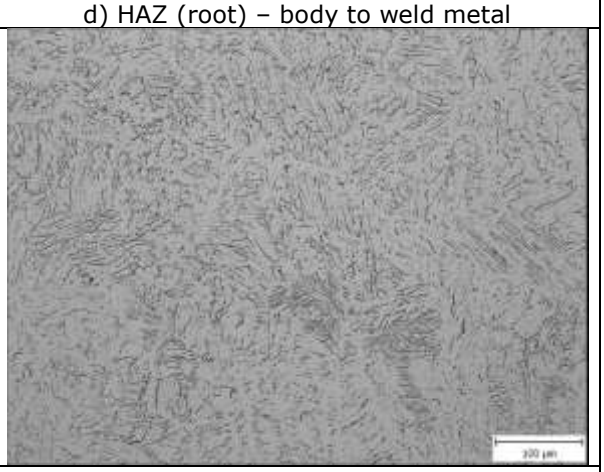

f) WM (root)

Fig. 44 Typical weld joint microstructures, weld 3

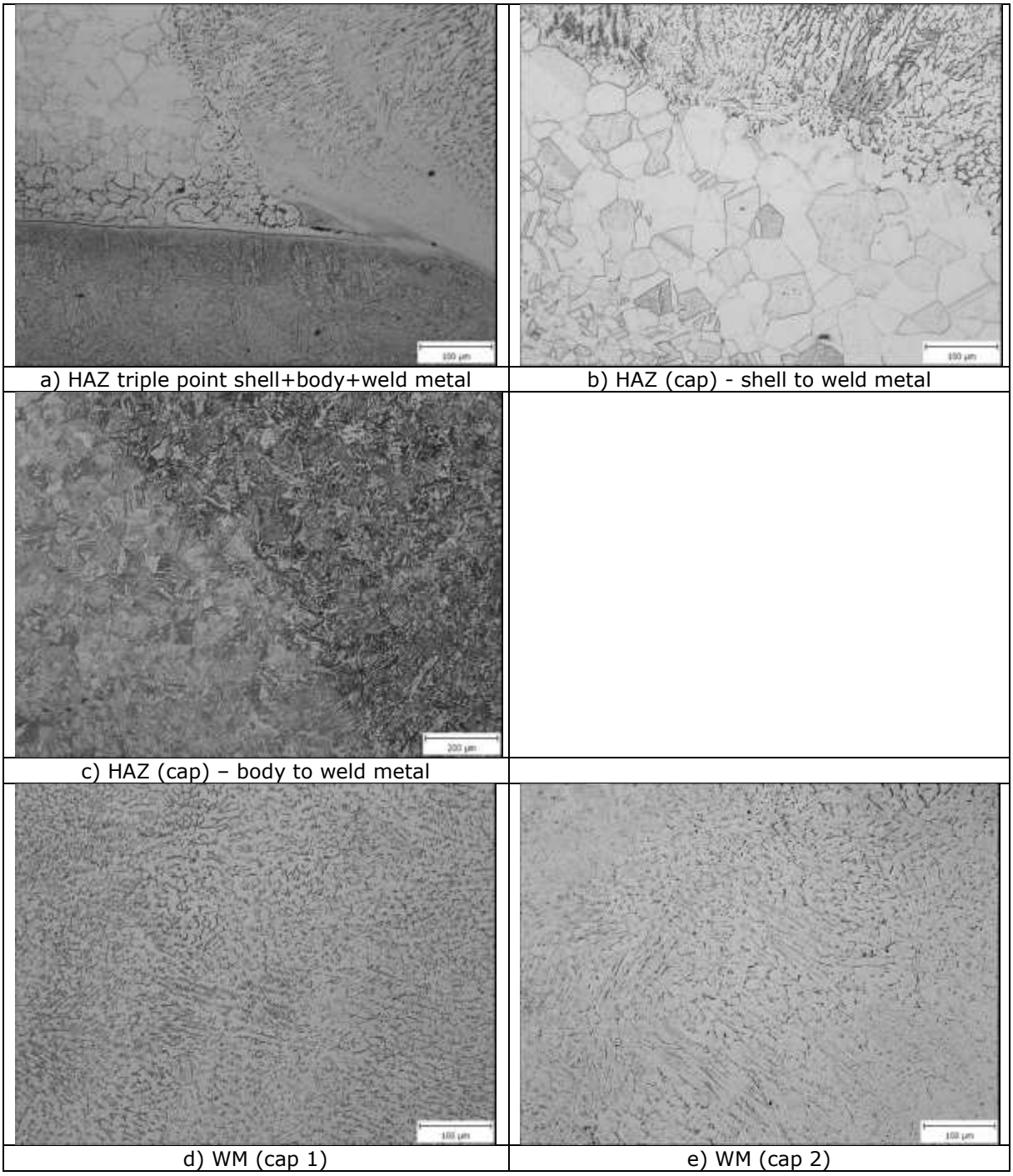

a) HAZ triple point shell+body+weld metal

b) HAZ (cap) - shell to weld metal

c) HAZ (cap) – body to weld metal

d) WM (cap 1)

e) WM (cap 2)

Fig. 45 Typical weld joint microstructures, weld 7

The quantitative profile of principal elements Fe, Cr and Ni from shell BM to the WM cap (weld 1a) was measured in order to check the level of reinforcement with low alloyed BM. The results are summarized in **Fig. 46**. No dramatic Cr/Ni drop was observed in across the whole weld.

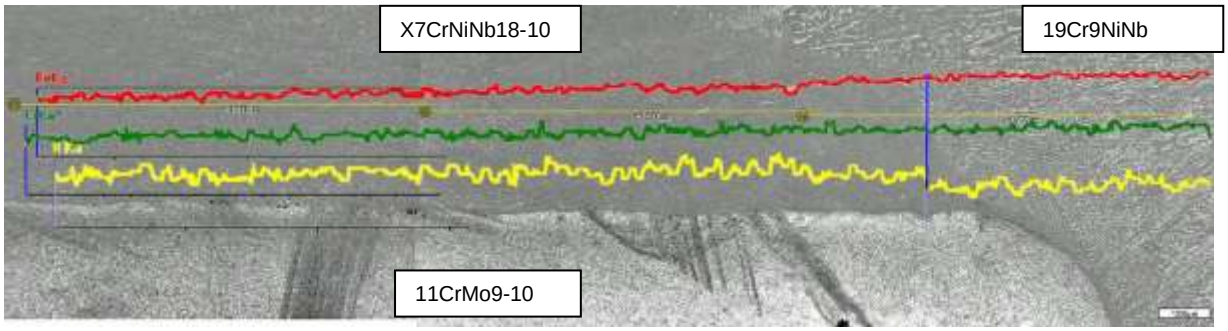

Fig. 46 EDX Fe, Ni, Cr line analysis. The line analysis starts shell BM (left) and end in WM (side)

Hardness surveys were measured in two lines, see **Fig. 47**. **Tab. 13** shows result of measurements on weld joint **1** (19Cr9NiNb – whole weld), **3** (19Cr9NiNb –cap - R1, 23Cr12NiLSi – filling/root – R2) and **7** (19Cr9NiNb –cap – R1, filling CrMo2Si).

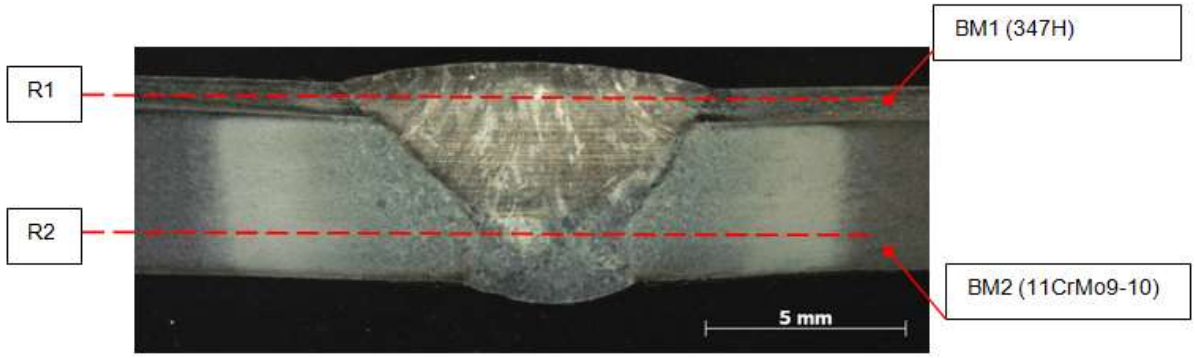

Fig. 47 Methodology of hardness measurements

Tab. 13 Results of hardness measurements HV5

Requirement HV5	**Max. 380HV5**			
Weld joint	**1a, b** 19Cr9NiNb whole weld	**3** 19Cr9NiNb –cap, 23Cr12NiLSi – filling/root	**7** 19Cr9NiNb – cap, CrMo2Si - filling	**Note**
BM1 (347H)	211 - 257			acceptable
BM2 (11CrMo9-10)	218 - 241			acceptable
HAZ 347 to WM	160 - 170			
HAZ 11CrMo0-10 to WM	360 – 371	358 - 381	313 – 286	acceptable
WM (cap of the weld)	174 - 180	160 – 164	328 – 336cap1 171 – 183cap2	acceptable
WM (root of the weld)	286 - 381	358-367	-	acceptable
WM (filling of the weld)	-	-	313 – 329	acceptable

The mechanical properties of the gradient tubes (base metal) are in accordance with the standard requirements.

Tab. 14 summarizes the mechanical properties of base metal and weld joint.

Tab. 14 Mechanical properties BM and WM

Steel		**Note**	**Tensile properties at room temperature**			**Tensile properties at elevated temperature (450°C)**	
			$R_{p0,2}$ min. [MPa]	**R_m [MPa]**	**A_{min} [%]**	**$R_{p0,2}$ [MPa]**	**R_m [MPa]**
			Wall thickness <16 mm		longitudinal		
11CrMo9-10		1.7383	355	540-680	20	257	-
X7CrNiNb18-10		1.4912	205	510-710	40	127	-
Base metal/ Gradient sample shell X7CrNiNb18-10, body11CrMo9-10		BM	491	648	61	443	544
1a	Weld joint		518	690	-	495 – WM fracture 501 – WM fracture	
1b		-	-	-	-	552 - BM fracture 467 – WM fracture	
2		-	-	-	-	547 - BM fracture 500 – WM fracture	
3		-	-	-	-	523 – WM fracture 522 – WM fracture	

Weldability – final conclusions

According to investigation of weldability of gradient tubes made of low alloy 11CrMo9-10 (body) and austenitic A182F347H (shell) steels we can conclude that:

The cross-weld specimens tested at ambient temperature also show the very good tensile properties comparable to base materials.

The weld manufactured with entirely 347 type consumable and tested at 450°C ruptured in weld deposit central line in one case, reaching the tensile stress of about 100 MPa less than those obtained in BM, see **Tab. 14**. The weld 1a/b where the root and filling passes were manufactured employing 309 types consumable was about the same results. In every weld, one of the specimens tested at 450°C fractured in weld metal. In this case the tensile properties are very similar to those obtained from BM, see. Other specimens tested at same temperature broke in BM far from HAZ; in this case the tensile stress was comparable to BM values. Also repeated testing at slightly different parameters (weld 3) gave the same unambiguous results. The welding heat input should be decreased perhaps more to get the rupture out of the weld deposit. The values of about 550 MPa (Rm - tensile properties at elevated temperature - 450°C) obtained are far beyond the working range expectations and therefore cannot cause any problems during testing loop operation. The bending tests, as well as hardness survey have revealed no big problems. Shell part remains solid after bent; and hardness of 11CrMo9-10 steel is just on the acceptance level.

The EDX line analysis shows no detrimental Cr/Ni decrease in shell to cup weld region.

TASK 3.3 MICROSTRUCTURE PROPERTIES

The aim of microstructure evaluation (precipitation processes, dislocation substructure evolution in gradient high-to-low alloy interfaces etc.) was mainly to determine possible degradation mechanisms in correlation to different processes parameters of casting, rolling, welding and heat treatment and their influence on the microstructure. Beside the microstructure investigation of as cast gradient ingots (indeed focused on interface), two other steps of rolling process have been defined as critical and thus systematically analysed from the microstructural point of view:
- piercing press
- elongator

As casted gradient billets

In following paragraph, the as cast gradient ingot microstructure is explained in general. So only general features are highlighted with no details.
The cast materials (small scale square shape and large scale oval shape) showed typical microstructures, though the grain sizes were relatively large without a proper heat treatment - **Fig. 48 (small scale laboratory trial)** and **Fig**. **49 (large scale laboratory trial).** In the casts the microstructure of the shell material was austenitic, and the body ferrite and perlite. The oval cast showed a relatively large diffusion zone and residuals (oxides and silicates).

In general, the diffusion layer between the shell and body materials is relatively thin. The diffusion layer between the shell and body materials is approximately 200μm, with some decarburisation on the low alloyed body material. The microstructure of the shell is austenitic, with relatively large precipitates at grain boundaries and minor ones within grains. The microstructure of the low alloyed body is ferrite and perlite. The grain size is relatively large, due to the lack of proper heat treatment.

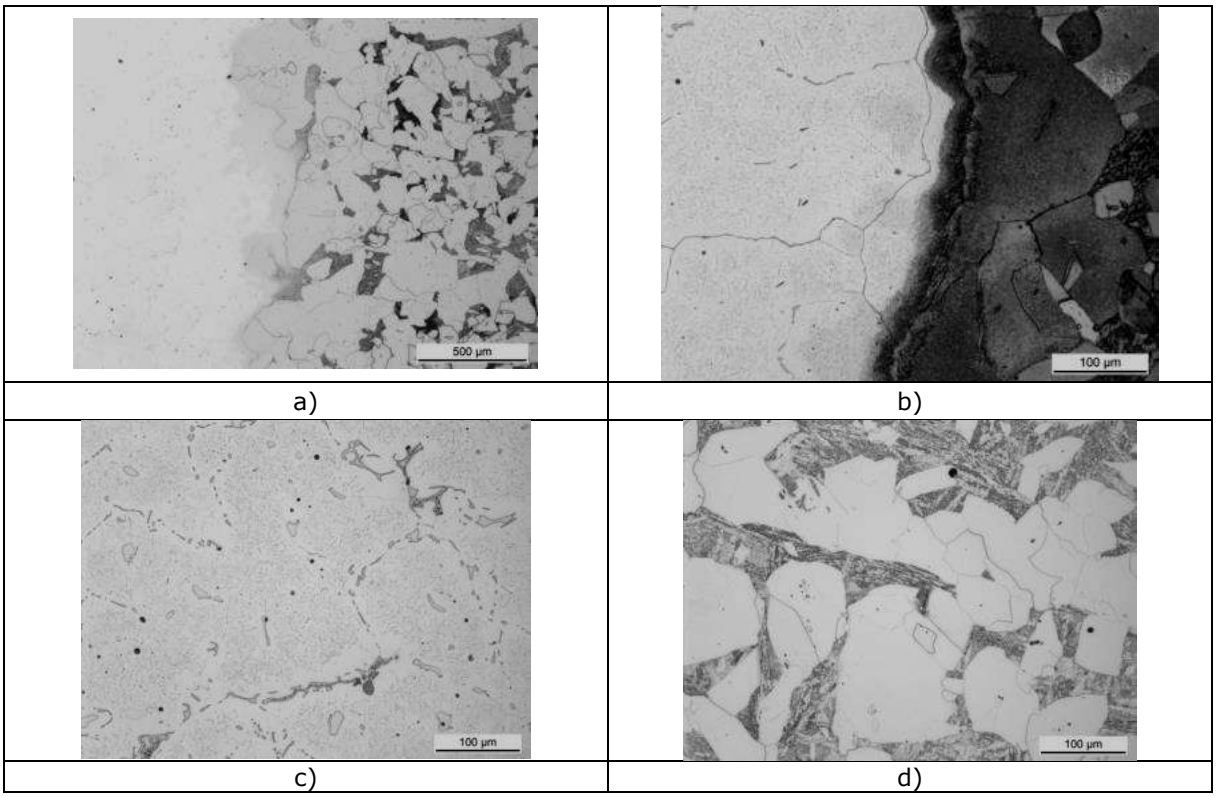

Fig. 48 Microstructure of the square cast no. 1 (small scale trial) a) interface with ferrite etchant, b) interface with austenite etchant, c) shell and d) body

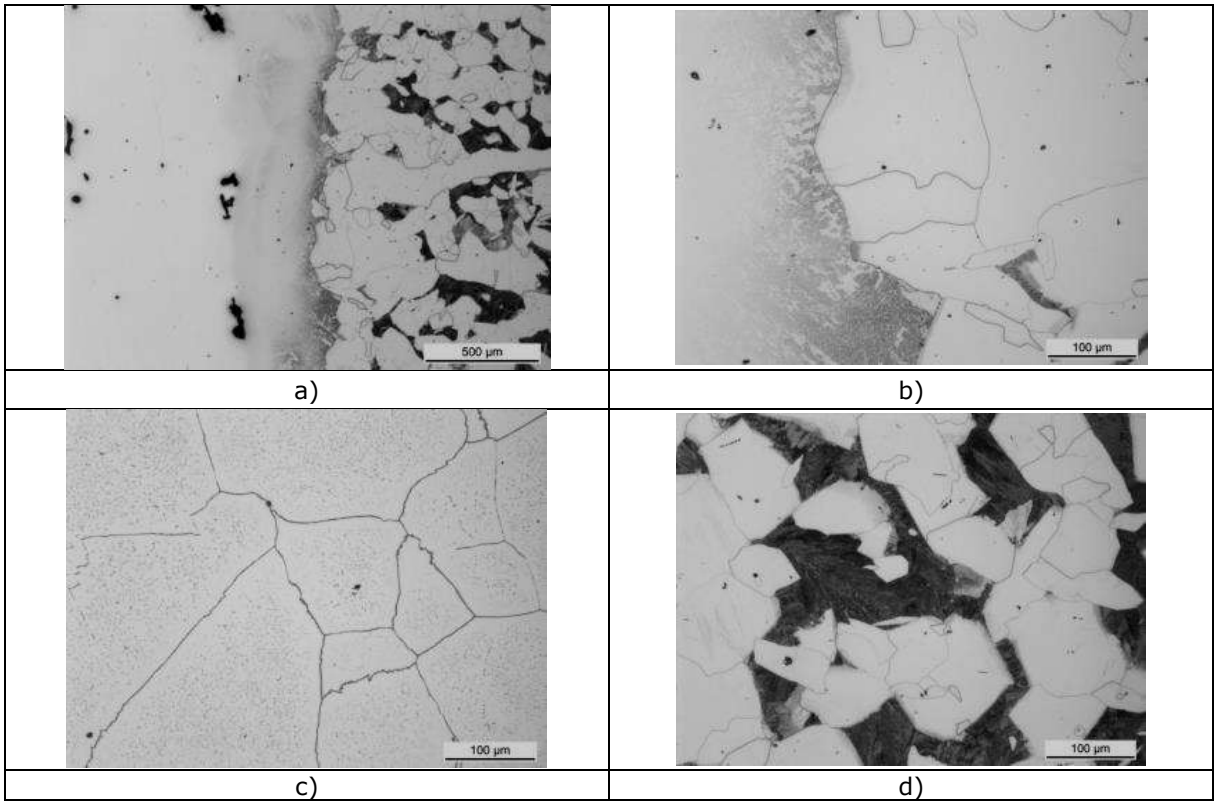

Fig. 49 Microstructure of the Oval cast no. 1 BEN (large scale trial) a) interface with ferrite etchant, b) interface with austenite etchant, c) shell and d) body

Piercing press semiproduct

The piercing-press product was analysed at four different locations (Sections A, B, C and D) with longitudinal and transversal from metallographic cross sections. The austenite layer of the piercing-press product was fairly uniform in thickness, only somewhat thicker at section B. Some voids were observed throughout the austenite layer, mostly in section A. Also surface defects (up to 2mm deep) mainly at section C were observed. At Section B and C a 2 to 3 mm deep area of a larger grain size was observed (**Fig. 50** and **Fig. 51**).

At the shell-body interface small areas were located with no diffusion layer, the locations were also detected with NDE. At the body a 100-300µm thick carbon depletion area was observed, the thickness of this layer varied a lot throughout the product. A corresponding sensitisation area was observed at the austenite shell side of the interface. The microstructure of the body material was martensitic (**Fig. 52** and **Fig. 53**).

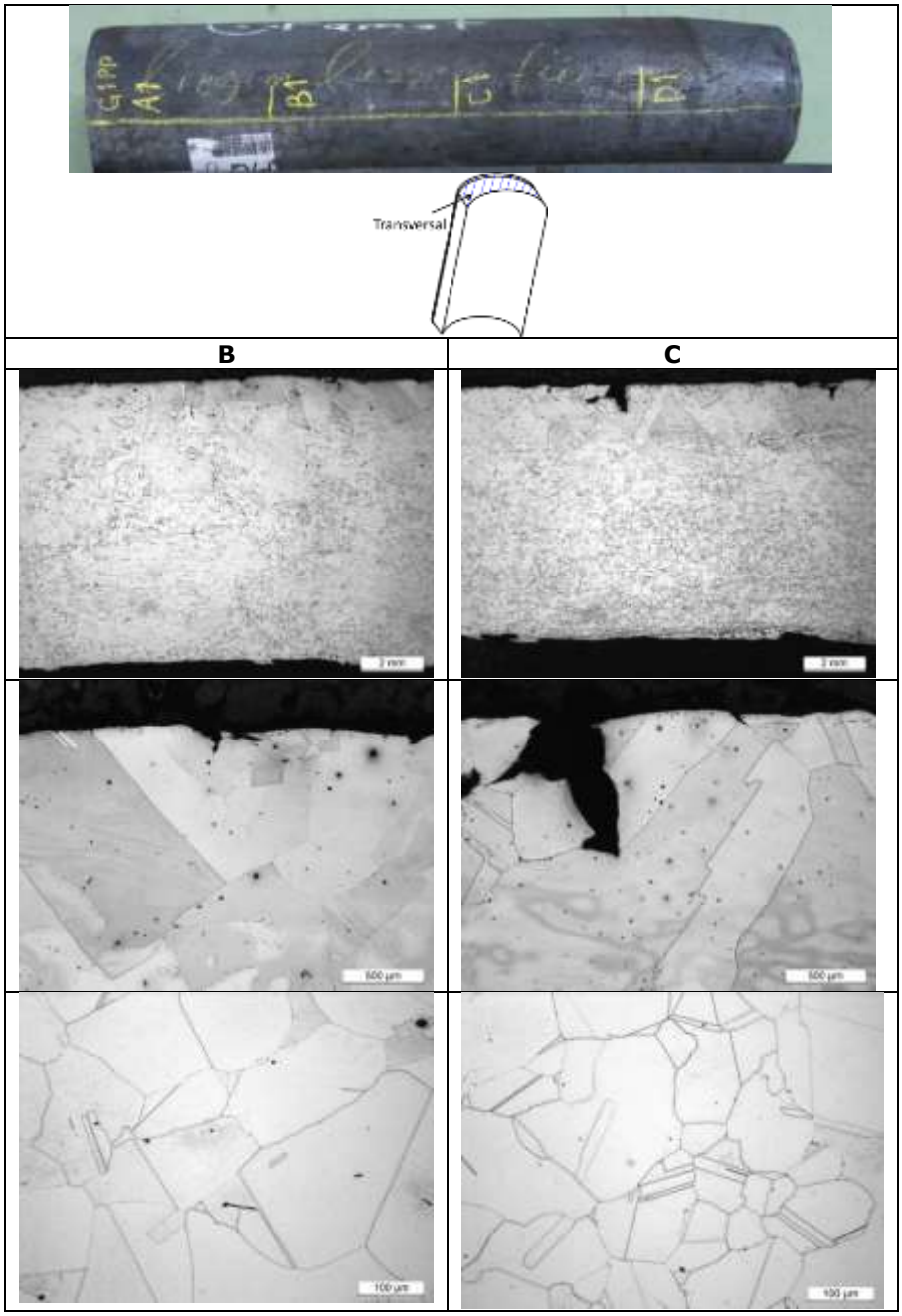

Fig. 50 The austenite surface of the piercing-press product, transversal cross-section

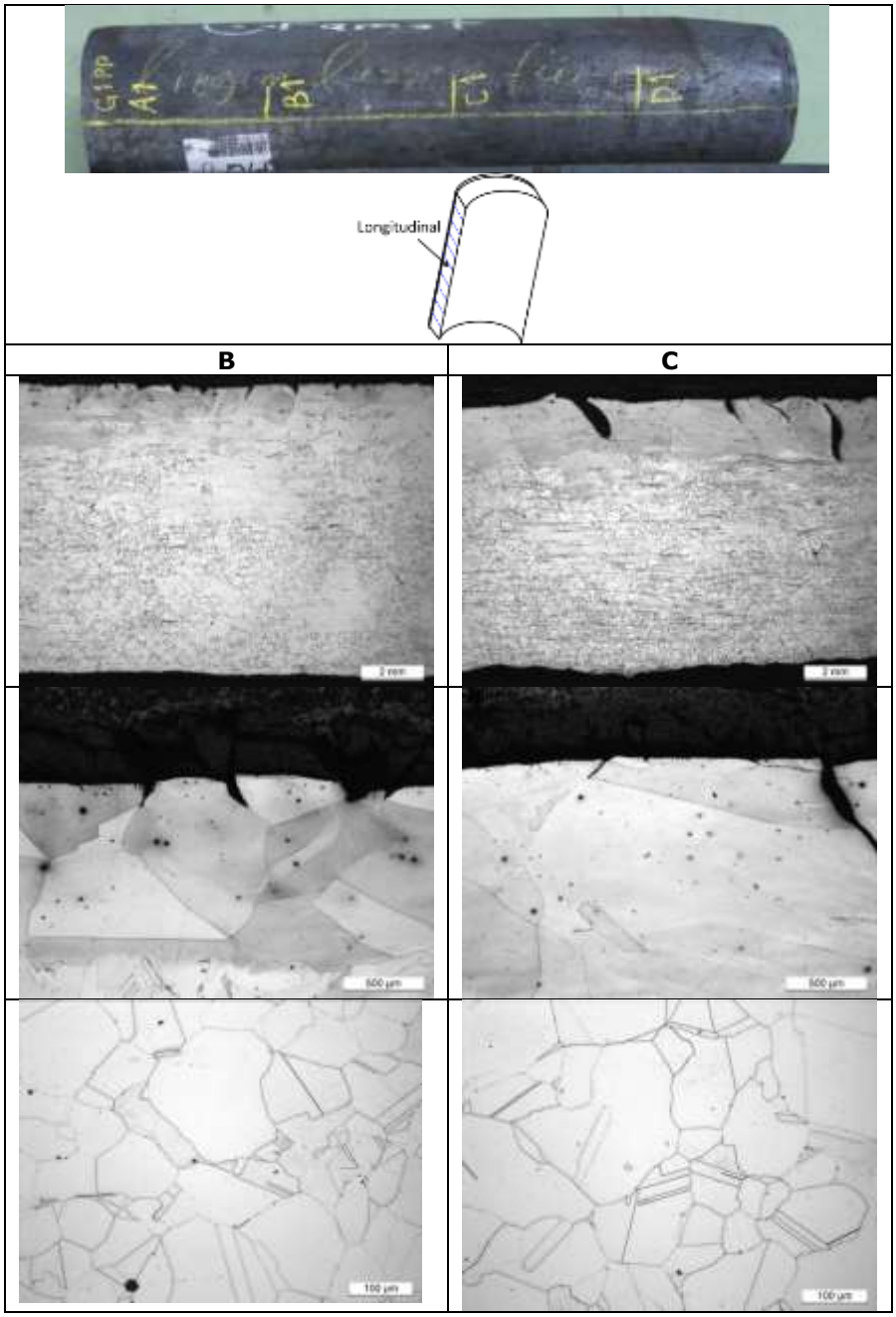

Fig. 51 The austenite surface of the piercing-press product, longitudinal cross-section

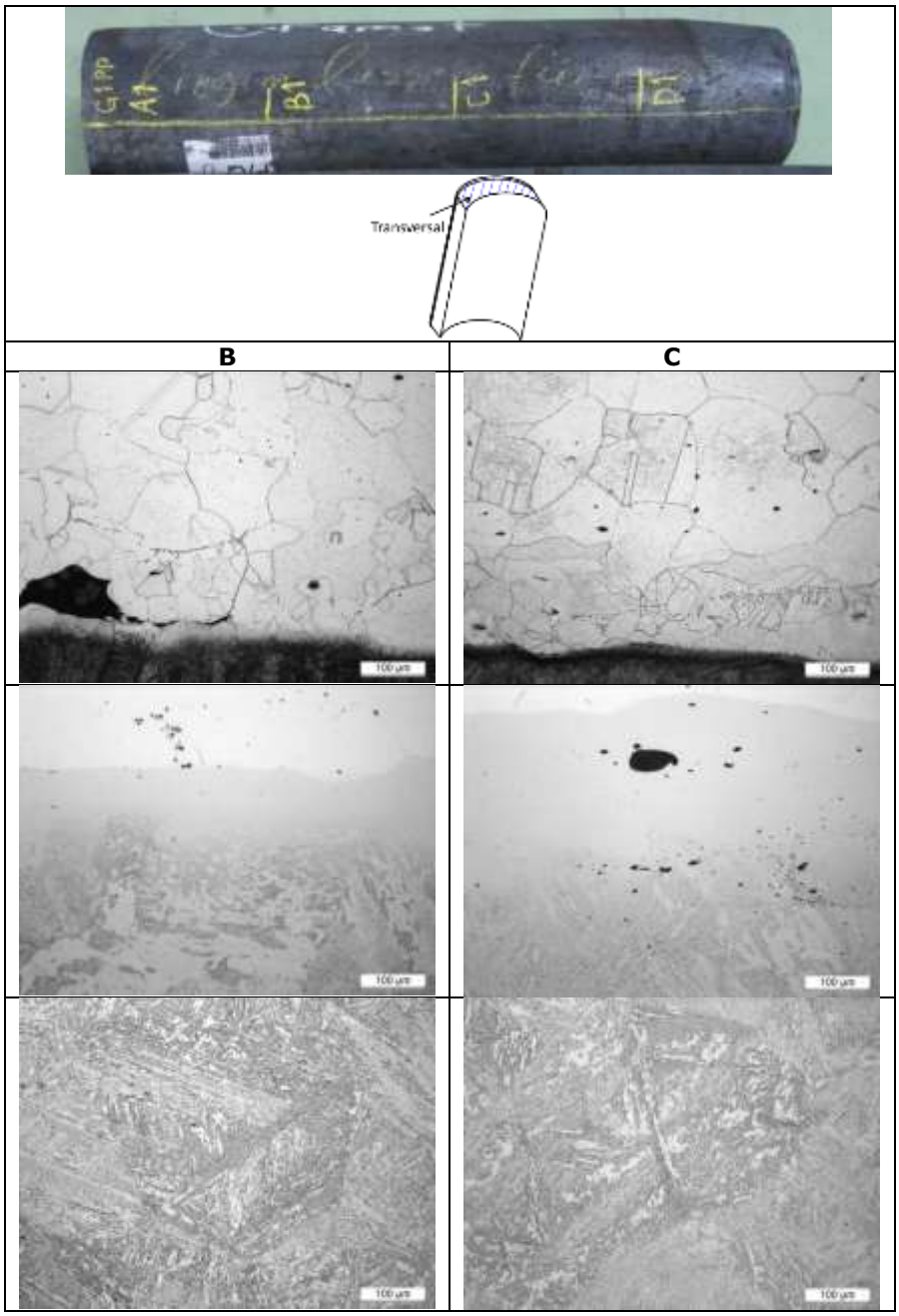

Fig. 52 The shell-body interface and the body microstructure of the piercing-press product, transversal cross-section

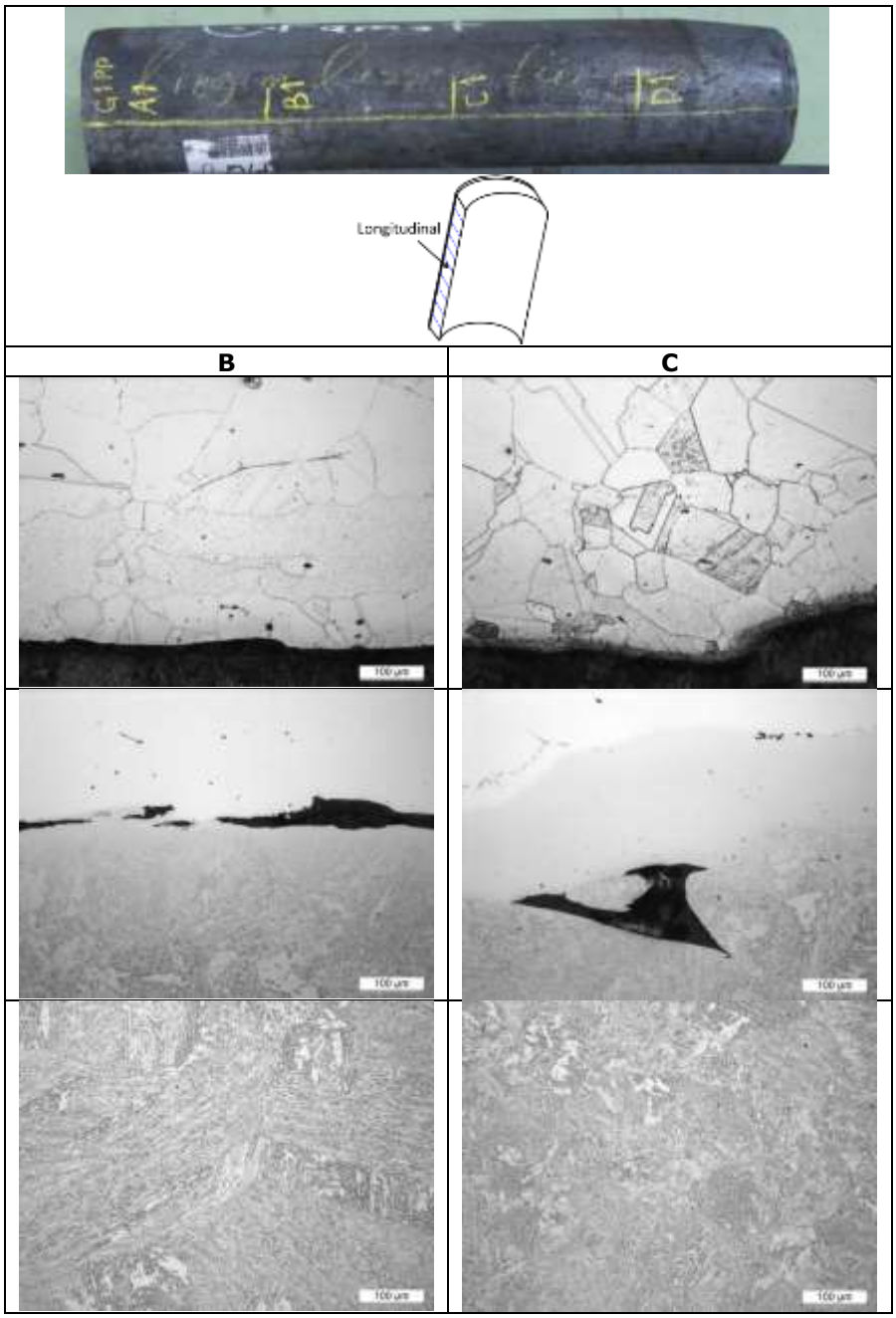

Fig. 53 The shell-body interface and the body microstructure of the piercing-press product, longitudinal cross-section

Hardness in Vickers units was measured with a 1kg pound from the interface. Each measurement was made 1mm apart from the next. The profiles show that the sell material is softer than the body. Also, at some locations the first measurement point is located at the large grain area, where the material is harder. And at the body material the carbon depleted area is somewhat softer (**Fig. 54**). The average hardness of the austenite shell material was HV1 152 ± 12, with a maximum of HV1 203 and a minimum of HV 1 128. The average hardness of the martensitic body material was HV 1 296 ± 20, with a maximum of HV1 338 and a minimum HV1 261.

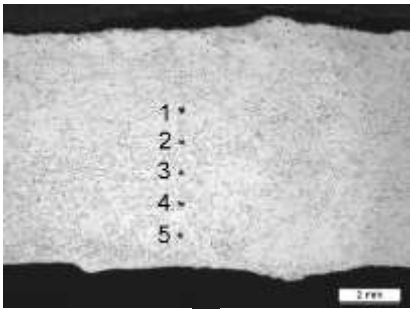

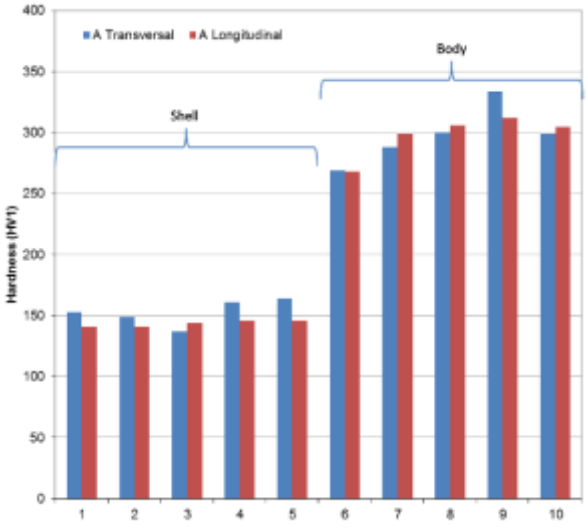

Section A

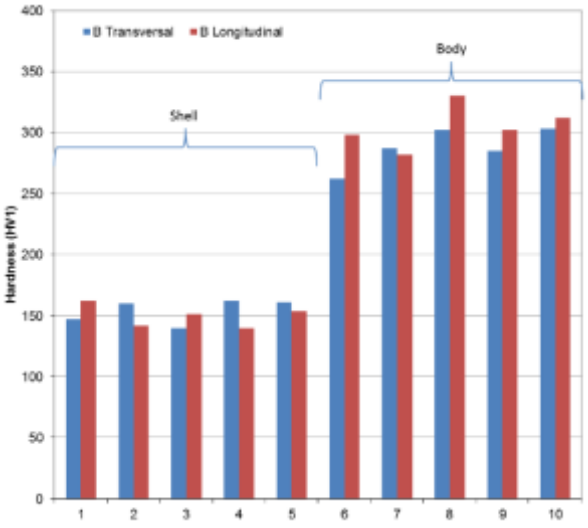

Section B

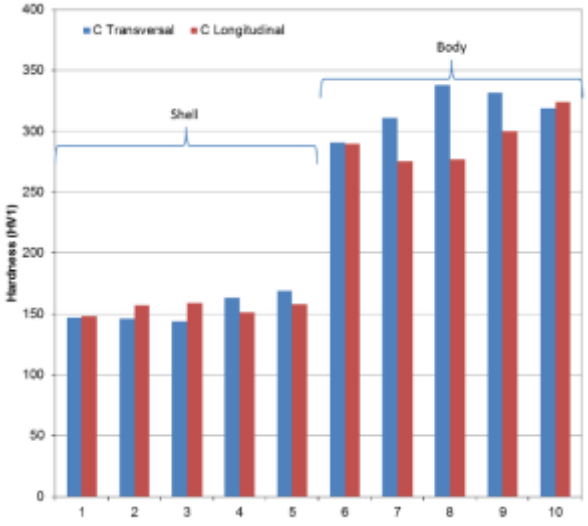

Section C

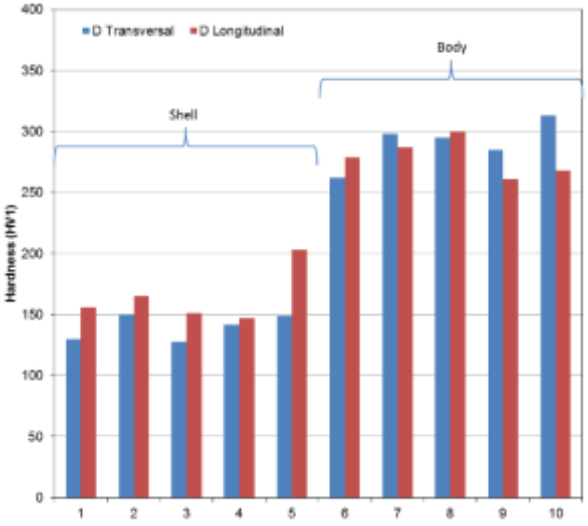

Section D

Fig. 54 Hardness (HV1) profiles of the piercing-press product

Elongator semiproduct

The elongator product was analysed at four different locations (Sections A, B, C and D) with longitudinal and transversal from metallographic cross sections. The austenite layer of the elongator product was thicker at sections A and B ~ 8.5 mm, and thinner at sections C (~7mm) and D (~7.5mm). fairly uniform in thickness. Surface defects (up to 1 mm deep) mainly at section A were observed. At all sections a 2 to 4 mm deep area of a larger grain size was observed (**Fig. 55** and **Fig. 56**).

At the shell-body interface small areas were located with no diffusion layer, the locations were also detected with NDE. At the body a 20-150μm thick carbon depletion area was observed, the thickness of this layer varied a lot throughout the product. A corresponding sensitisation area was observed at the austenite shell side of the interface. The microstructure of the body material was martensitic (**Fig. 57** and **Fig. 58**).

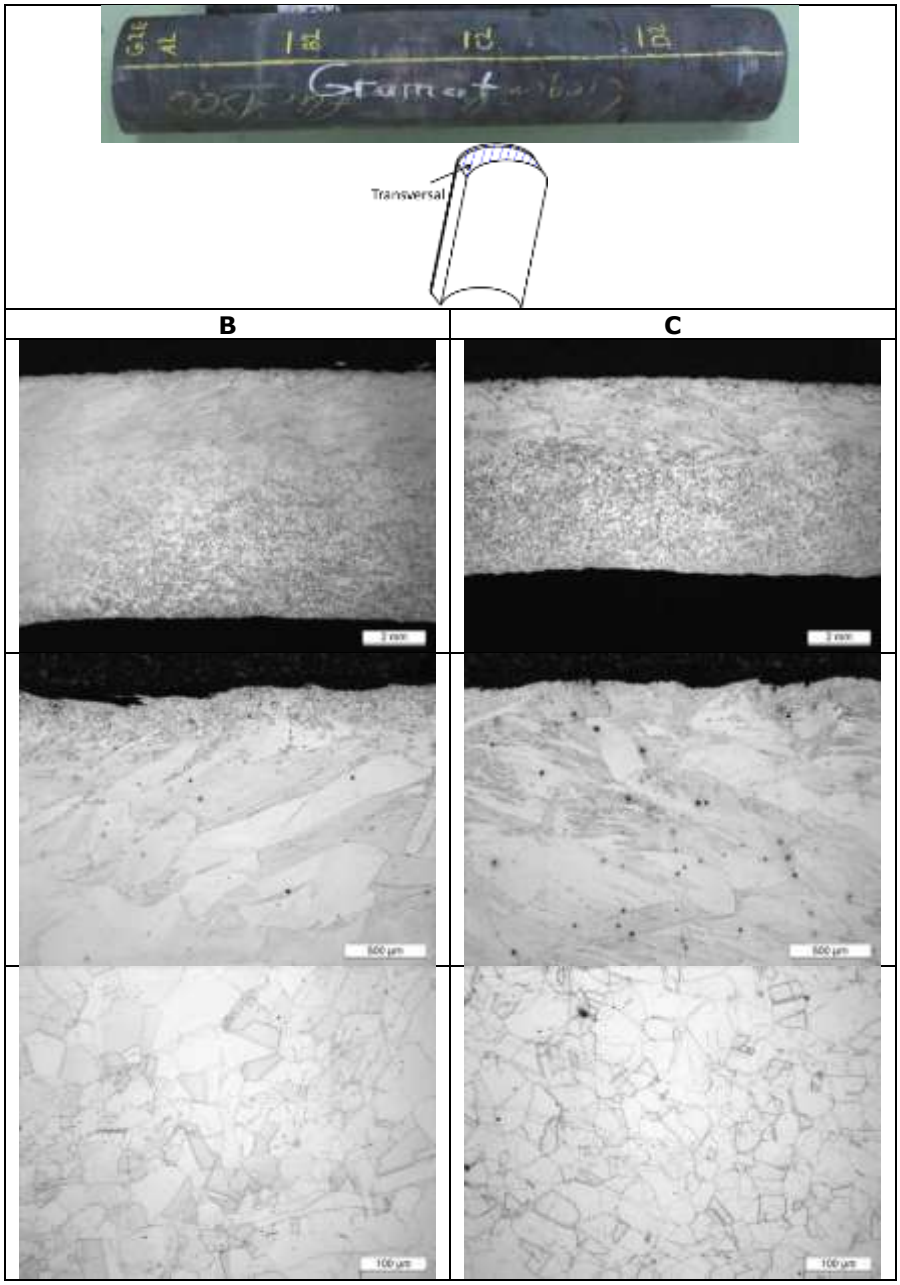

Fig. 55 The austenite surface of the elongator product, transversal cross-section

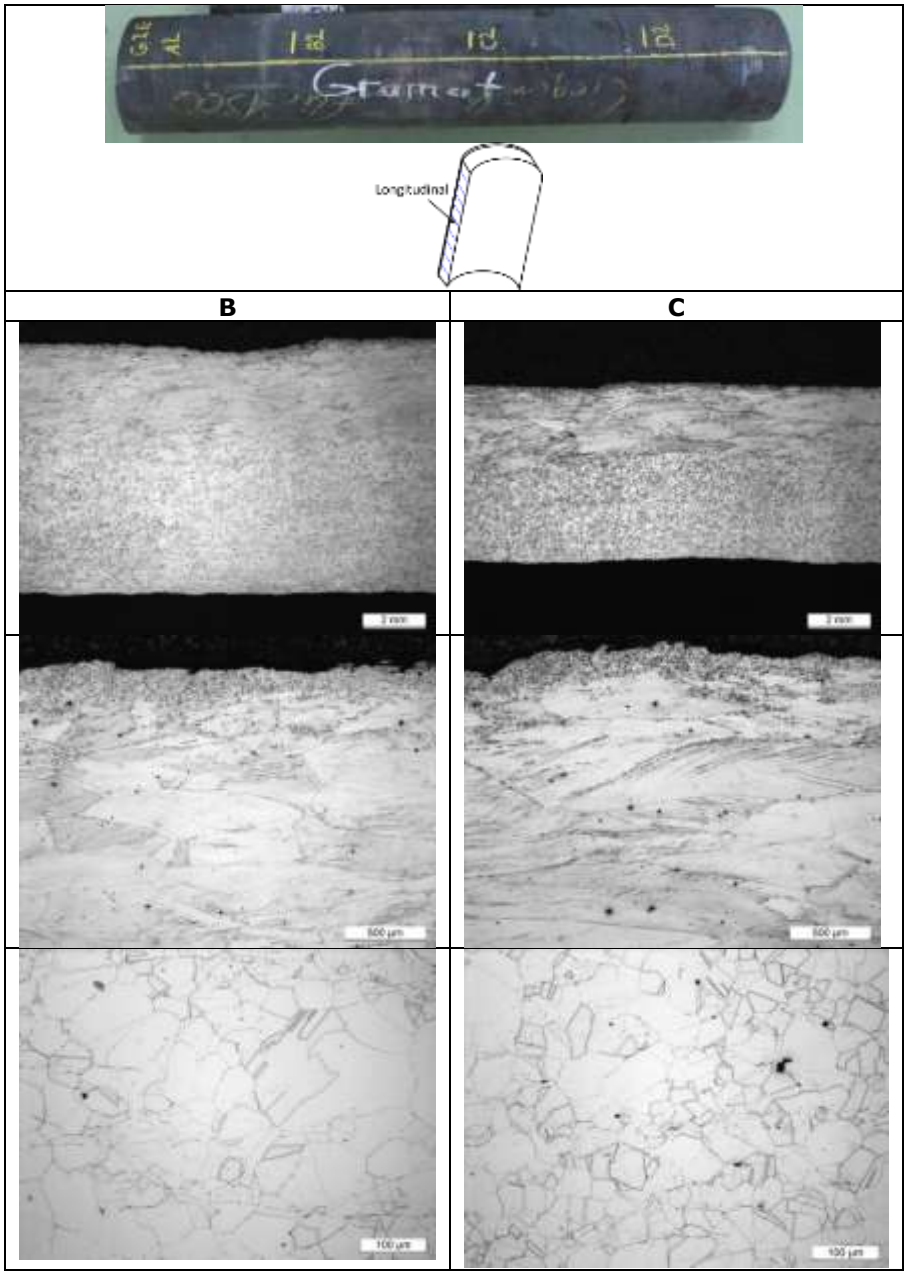

Fig. 56 The austenite surface of the elongator product, longitudinal cross-section

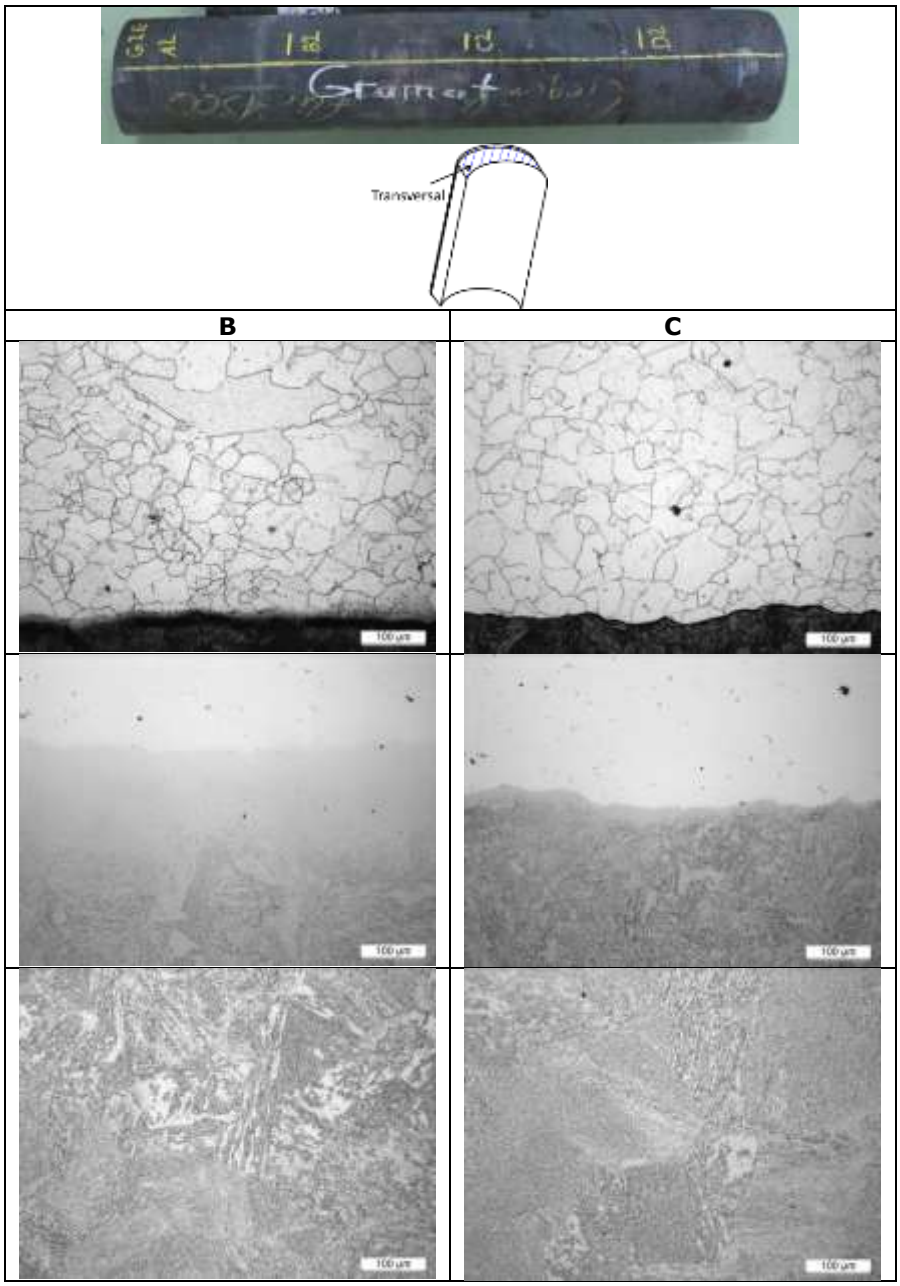

Fig. 57 The shell-body interface and the body microstructure of the elongator product, transversal cross-section

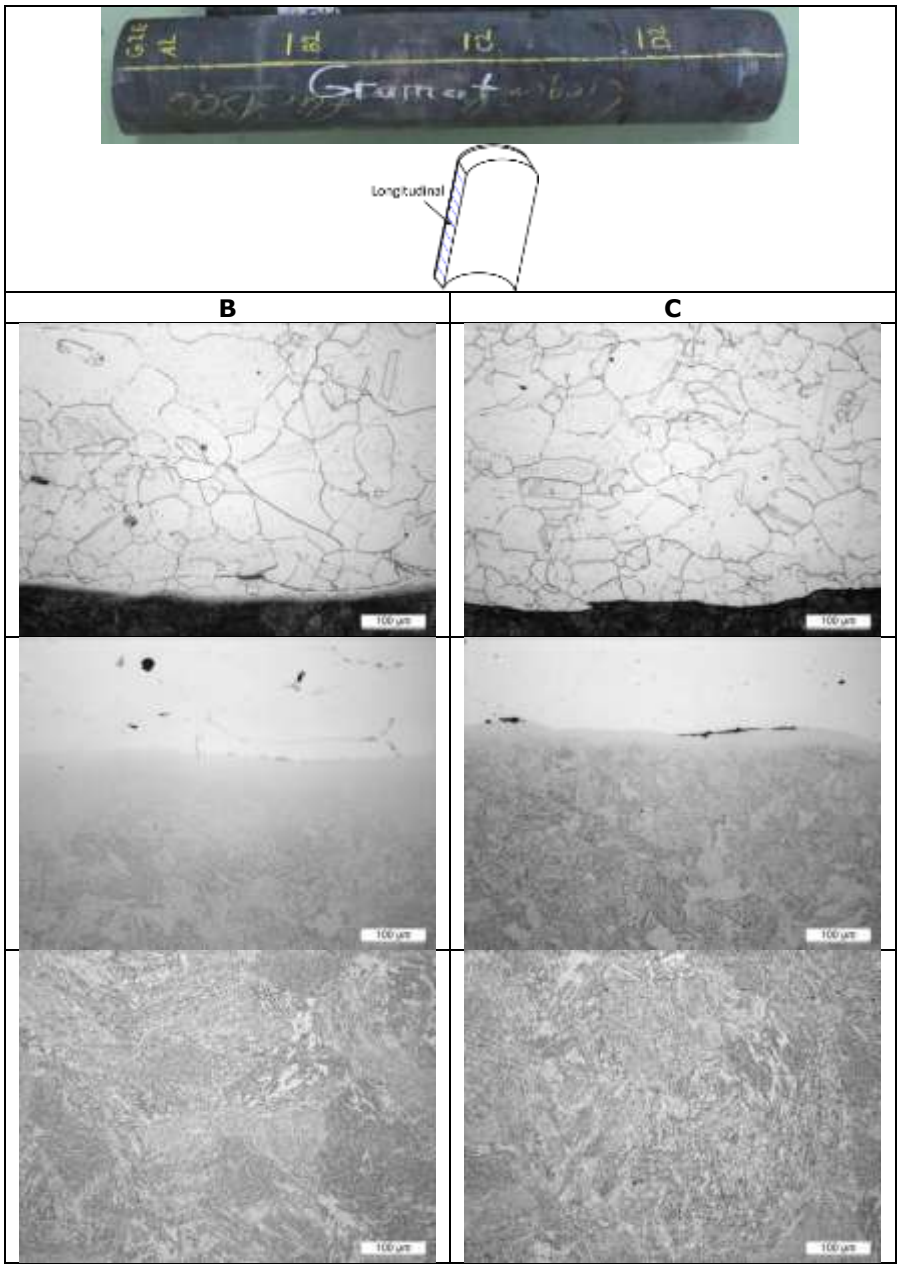

Fig. 58 The shell-body interface and the body microstructure of the elongator product, longitudinal cross-section

Hardness in Vickers units was measured with a 1kg pound from the interface. Each measurement was made 1mm apart from the next. The profiles show that the sell material is softer than the body. Also, at some locations the first measurement point is located at the large grain area, where the material is harder. And at the body material the carbon depleted area is somewhat softer (**Fig. 59**). The average hardness of the austenite shell material was HV1 152 ± 18, with a maximum of HV1 220 and a minimum of HV 1 130. The average hardness of the martensitic body material was HV 1 298 ± 15, with a maximum of HV1 342 and a minimum HV1 257.

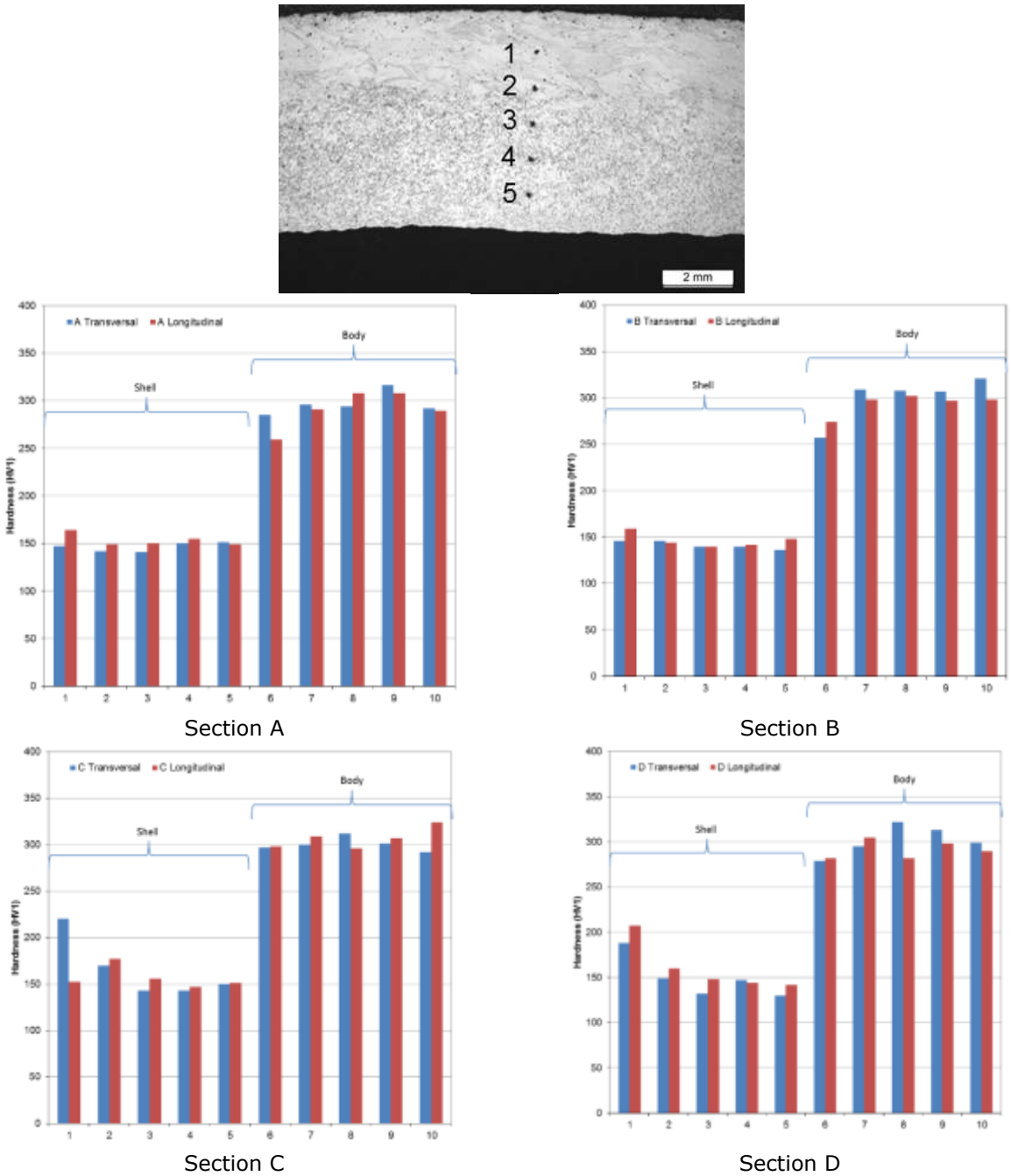

Fig. 59 Hardness (HV1) profiles of the elongator product

The microstructures of the piercing-press product and the elongator product showed a need for improvement of the outer layer of the tube. The larger grained area and the observed surface defects are not beneficial for the end product. The surface defects have been produced at some stage of the manufacturing before the elongation**. It can be clearly seen that the surface defects at the elongation product are aligned with the grains and are therefore initiated before the elongation.** The surface defects on the piercing-press product are mainly at grain boundaries of the large grains, no oxide was observed at the defect surfaces. **This indicates that the surface defects come from the piercing-press process.** An improvement is needed to reduce this layer for the next generation product was applied in terms of temperature optimization in rotary furnace (first principal operation before piercing mill, see chapter devoted to forming).

To summarise: the surface defects originate during the piercing-press process and can be avoided by temperature optimisation.

Also, the larger grained area and the observed surface defects are not beneficial for the product, and this issue has become

TASK 3.4 MECHANICAL PROPERTIES

Relevant mechanical properties of gradient tube and their welds have been tested and modelled.

However, very soon, it was clear that the mechanical properties are not critical for gradient tubes; and therefore, much more effort was focused on other work.

The results show that the mechanical properties of the gradient tube are within the standard requirements for the body material (11CrMo9-10) - see **Tab. 15**).

Tab. 15 Mechanical properties of the gradient tube produced in the large-scale trial at Benteler

Steel	**Note**	**Tensile properties at room temperature**			**Tensile properties at elevated temperature (450°C)**	
		$R_{p0,2}$ min. [MPa]	**R_m [MPa]**	**A_{min} [%]**	**$R_{p0,2}$ [MPa]**	**R_m [MPa]**
		Wall thickness <16 mm		longitudinal		
11CrMo9-10	**1.7383**	355	540-680	20	257	-
X7CrNiNb18-10	**1.4912**	205	510-710	40	127	-
Base metal/ Gradient sample shell X7CrNiNb18-10, body11CrMo9-10	**BM**	491	648	61	443	544

Tab. 16 shows the relevant summary of all the test performed on gradient tubes.

Tab. 16 Summary of results of the gradient tubes testing

Type of testing method	**Frequency of testing**	**Standards**	**Results**
Visual examination	Each tube	-	surface imperfections
Dimensional inspection	Each tube	- Outside Diameter: 38mm +/- 1% or +/- 0,5mm - Wall thickness: 5mm +/-10% - Deviation with all tube lengths max 0,0015 x L (length of the tube), - (deviation with any 1m section of the tube max. 3mm)	acceptable
Thickness measurement (shell)	Each tube	equipment: QuaNix® 7500	from 0,6mm to 1mm (average 0,8mm)
NDT for the detection of longitudinal and transverse imperfections	Each tube	EN ISO 10893-10 to acceptance level U2, sub-category C	The part of selected testing rig was acceptable however the suitable methods (NDT testing) for gradient tubes should be selected.
Manual NDT for detection of diffusion joint	Each tube	EN ISO 17635, EN ISO 11666, EN ISO 17640,	120mm and 160mm section without diffusion joint
Chemical analysis	Cast analysis	Laboratory equipment: ARL 4460, LECO TC 600Laboratory equipment: ARL 4460	acceptable
	Selected cast	C, S – LECO CS 244; STN EN 24935 Mo, Si – PE ICP 5500 System; MS08-LAB-2008, P - SPEKOL 11, STN EN 10184 Mn, Cr, Ni - PE ICP 5500 System; EN ISO 10700, STN EN 10188, STN EN 10136, STN EN 24943	acceptable
Tensile test at room temperature	Benteler gen 1	STN EN ISO 6892-1:2010	$R_{p0,2}$ = 491MPa R_m = 648MPa A_I = 61% KV = 89J acceptable
Tensile test at elevated temperature (450°C)	Benteler gen 1	STN EN ISO 6892-1:2010 STN EN ISO 6892-2:2011	$R_{p0,2}$ = 443MPa acceptable
Flattening test	Benteler gen 1	EN ISO 8492:2014	unacceptable

Additionally, creep tests were performed in order to assess long term creep performance of gradient materials.

When comparing the results of the gradient tube creep tests to the creep to rupture curved of the body material (10CrMo 9-10) and the shell material (347H), it can be seen that the gradient tube material behaves better than expected (see **Tab. 17** and **Fig. 60**). In the initial calculations no load was calculated for the shell part of the gradient tube, whereas based on these results it is clear that the austenite shell material improves the creep properties of the gradient tube.

Tab. 17 Results and conditions of the performed creep tests

		Sample 1	**Sample 3**	**Sample 5**
Working conditions	Temperature [°C]	600	630	660
	Pressure [MPa]	52,5	39,4	28,9
Results	Time of test[1]	2183h/ without fracture	2183h/ without fracture	2183h/ without fracture
	A [%]	0,77	0,77	Test interupted

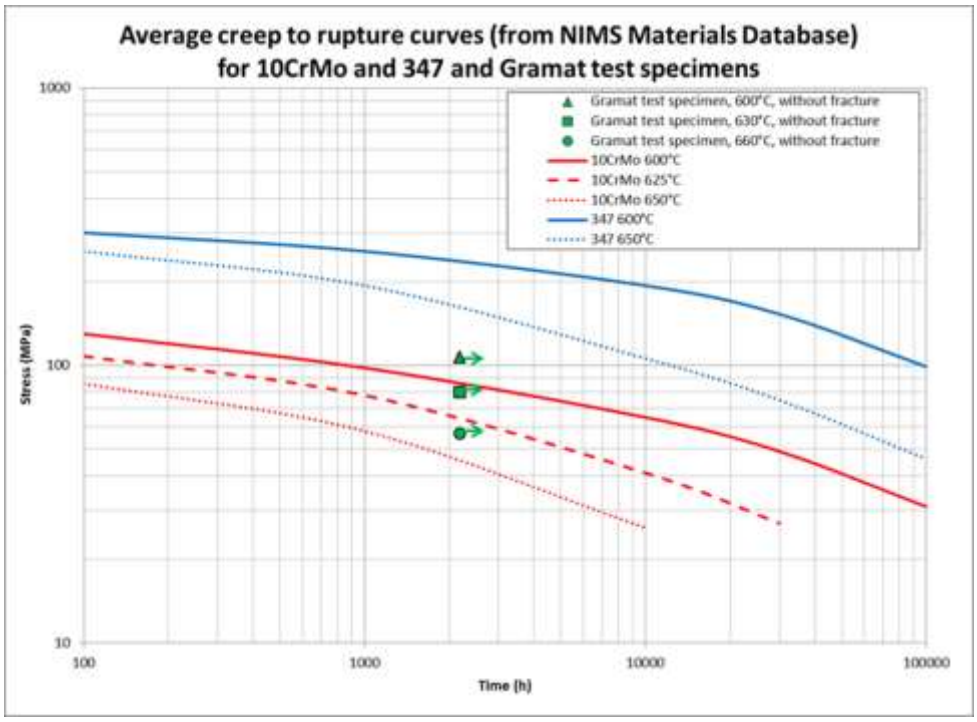

Fig. 60 The creep to rupture curves of 10CrMo9-10 and 347H at different temperatures, as well as the locations of the on-going creep tests for the gradient tubes

The mechanical properties of the gradient tube materials produced at the Benteler large scale trials are in accordance with relevant standards EN 10216-5 and EN 10216-2.

TASK 3.5 LONG-TERM TESTING IN REAL WORKING CONDITIONS

Introduction

After passing all quality tests, the gradient tubes were exposed to real boiler conditions in a recirculation loop at Äänevoima BFB boiler (**see Fig. 61**).

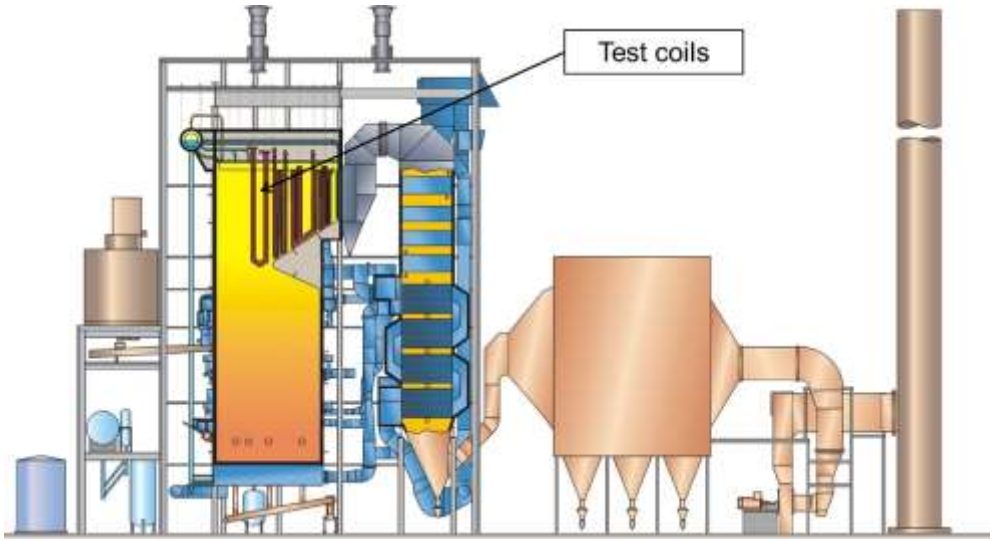

Fig. 61 Test plant, Äänevoima BFB

Results

The steam coil at site has been operating without problems and data acquisition is continuing as planned. Steam temperature, where the gradient tubes are, has been around 480-490 °C which would correspond outer surface temperature 510-530 °C. First gradient tube specimen was collected during May 2016 outage for more detailed analysis (by VTT). Tubes were checked in May 2017 - visually are the base material and the welds in good condition. During the testing, plant has been firing mainly bark, additionally some peat and wood residues. **The shutdown was planned in 2018, however the gradient tubes are still in boiler because their excellent condition (winter 2019) – see the latest available photo from Year 2017 Fig. 62.**

So far, gradient tubes and their welds run app. 23 000 h without any problems.

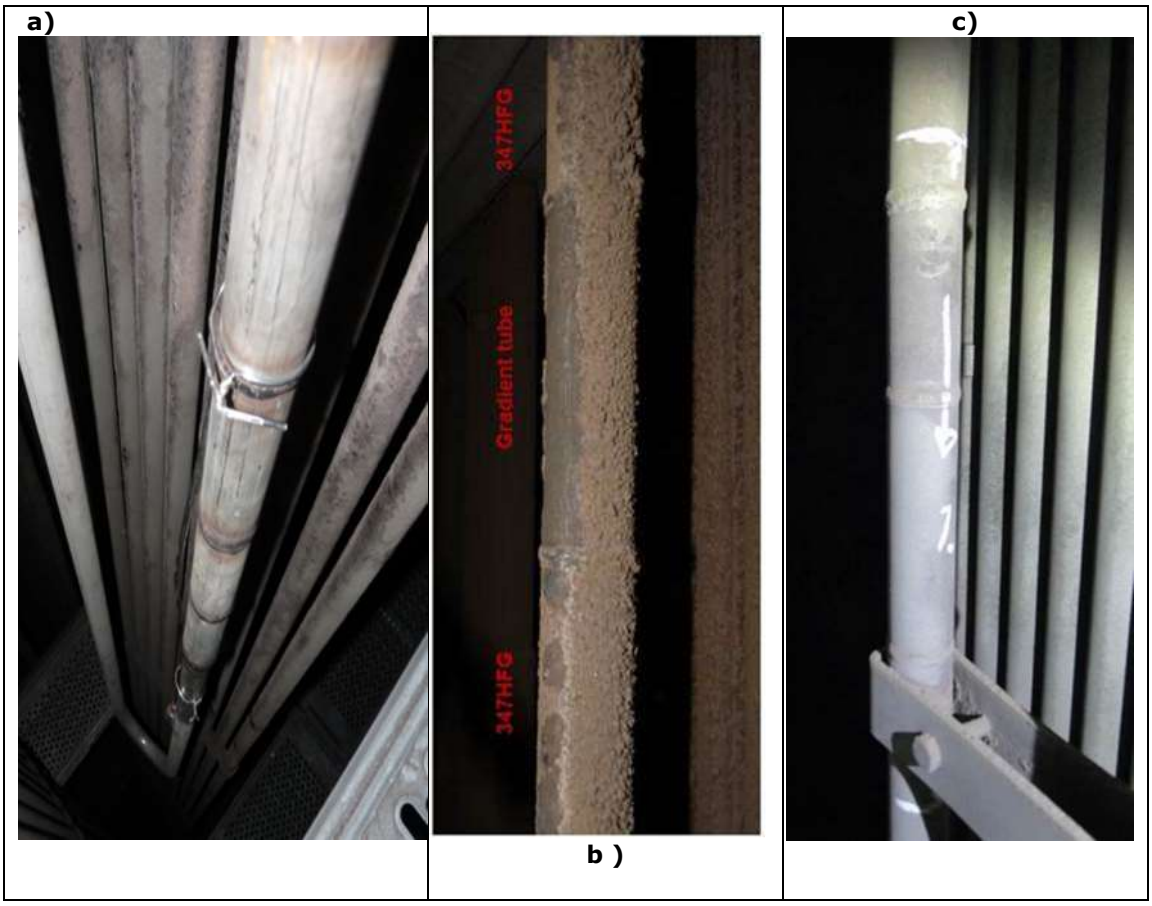

Fig. 62 a) Installed tubes, b) removal, April 2016, c) May 2017 (not removed)

After the exposure the test tube was visually examined, after which metallographic cross section samples were prepared over the weld and tube. The cross-section samples were investigated in more detail with light optical microscopy (LOM), scanning electron microscopy (SEM) and an energy dispersive X-ray analyser (EDX). The hardness of the base materials, and the diffusion zone was measured in Vickers units with a 10kg weight.

In the visual examination, the tube showed a uniform thin oxidation layer all around the tube (figure below). No deposits or signs of accelerated corrosion were observed **Fig. 63**.

Fig. 63 The gradient tube after exposure

The austenite layer after the exposure was approximately 714 ± 90 µm (min. 615 µm, max 850 µm); the overall thickness of the tube was 4970 ± 110 µm. The big variation is most probably due

to the initial variation of the austenite layer). The observed internal oxide was approximately 45 ± 11 µm thick, though possible spallation cannot be excluded -**Fig. 64.**

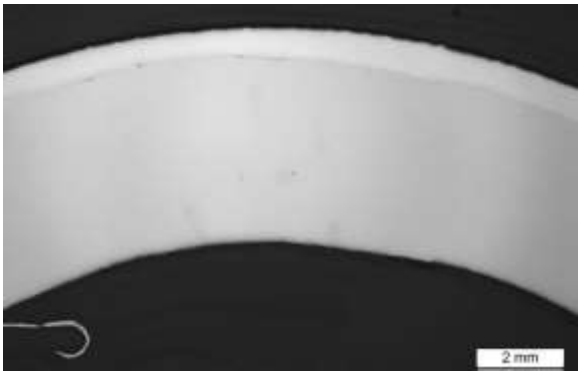

Fig. 64 Cross section of the gradient tube after exposure. Left – general overview. Right – corrosion attack depth – app 20 um per year

The depth of corrosion attack was measured by means of SEM – see **Fig. 65**, the corrosion attack is app 20um.

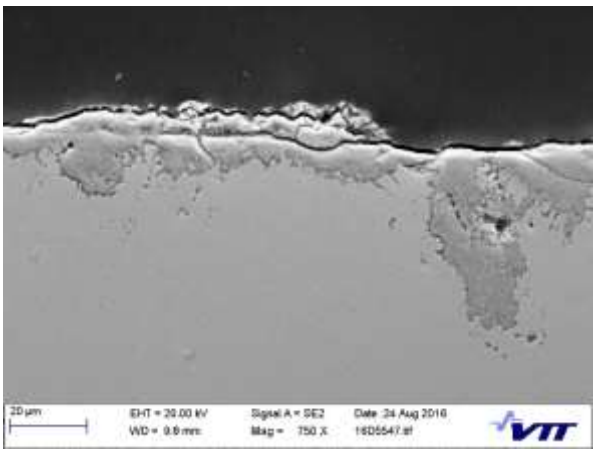

Fig. 65 Cross section of the gradient tube after exposure. Left – general overview. Right – corrosion attack depth – app 20 um per year

Corrosion in HAZ had also progressed similarly as at the tubes; a uniform layer ~50 µm and more rapid corrosion at surface defect sites. Although, the uniform corrosion layer was somewhat thicker at the HAZ than at the tube section, **Fig. 66**.

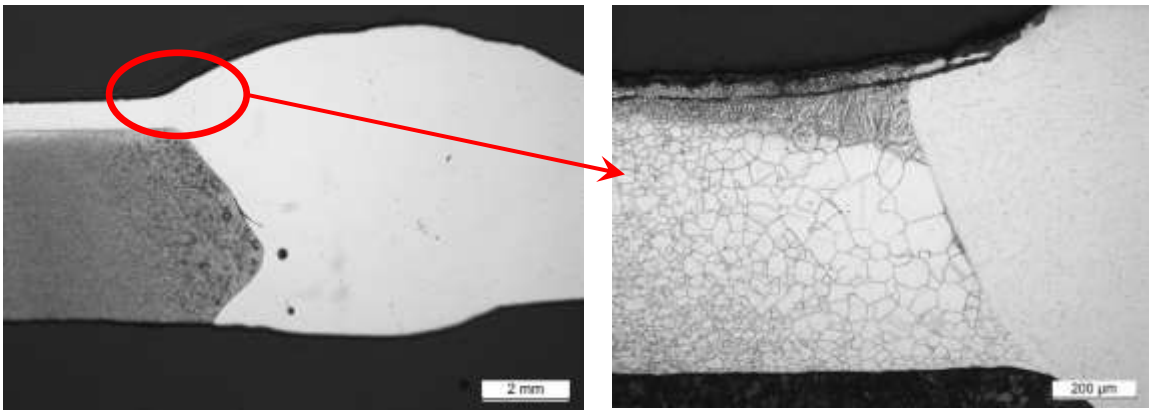

Fig. 66 HAZ at the austenite layer

The gradient tubes were exposed to real boiler conditions in a recirculation loop at Äänevoima BFB boiler. The overall performance of the gradient tube was satisfactory, though some improvements should be made.

The results show that corrosion on the outer surface progresses more rapid though surface defects, as was expected based on the accelerated corrosion tests. The corrosion attack has not progressed to the second zone in the austenite layer (typical austenite structure), at which the corrosion rate is expected to decrease. Sensitisation on the austenite layer at the diffusion zone is at the same thickness as it was in the original tube, though the sensitisation is more intensive showing a hardness peak at the austenite side of the diffusion line.

The most rapid corrosion was seen to progress on the outer surface progressed through surface defects. Somewhat accelerated uniform corrosion, similar to the one observed at the laboratory experiments, was shown at the HAZ area.

In the future, the heat treatment and manufacturing process of the austenite layer should be refined to decrease the less beneficial layers;

sensitisation/decarburisation layer at the diffusion zone and the outer most layer with surface defects. It also would be beneficial to reduce the defects at the austenite-ferrite interface, though the test did not show problems at this area. In addition, the welding parameters should be optimised to decrease the size of the heat affected zone at the austenite layer and decrease welding defects.

Exploitation and impact of the research results

ACTUAL APPLICATIONS;

GRADIENT tubes can be used in any applications where, due to the technological process, media outside the tube are harsher than those inside the tube.

Thus, the first applications in biomass boiler are obvious. On the other hand, boiler tubes are part of very conservative business; and to convince operators to use them would take the time. The pilot installation in testing rig in real biomass boiler is out of importance. Thus, after GRAMAT tube withdrawing from the boiler after app. 25 000 hours (2019 or later), next step will be dissemination of this achievement.

TECHNICAL AND ECONOMIC POTENTIAL FOR THE USE OF THE RESULTS;

The technical potential of gradient tubes is enormous.

The enormous technical potential of gradient tubes is obvious from two factors.

I. Technical capabilities

Utility properties of outer surface, hence surface facing the harsh environment, are equal to high alloyed, hence more expensive material. From this point of view the tubes can be treated as a high alloyed. However, rest of the tube, hence subsurface parts bearing the load, are equal to the low alloyed, hence less expensive material.
Overall price of the gradient tubes as it is discussed in Chapter "Exploitation and impact of results" is therefore cheaper than the price of high alloyed tubes.

In general, materials where the outer surface should withstand much harsher environment that body are in focus recently in many fields. Even the term GRAMAT has gain the popularity along with term surface engineering, functional layers, selective additive manufacturing etc. Approach, chosen and proved within the project, indeed, is capable to produce the gradient tubes in infinite numbers during ordinary production; on ordinary production lines; and with precautions which not exceed the normal production practice. This is a sharp difference to those techniques requiring expensive laboratory devices to produce several cm^2 of functional surface.

Project GRAMAT prove that, generally, concept of surface engineering of materials can be shift toward widespread usage in many fields once accepted by very conservative technical environment.

Project obviously started with the gradient tubes devoted to the **biomass boilers** installations, where lay the most capabilities of consortia. The gradient tubes can be used in both waste heat boilers and waste to energy boilers respectively. The technical potential of gradient tubes in this field is enormous. The boiler makers can utilize the gradient tubes instead of more expensive austenitic ones immediately. To ramp up the gradient tube installation in real biomass boiler by project partner AMF, the 1 mm outer shell of high alloyed material was not considered for stress calculations. This layer was treated as a corrosion protection, not bearing the internal and external load, which is not true as it was proved by for example creep tests which exceeds expectations.
In future – if proper design code followed by legislations is available; and the contribution from high alloyed layer can be considered in stress calculations, the gradient tubes would become even thinner, providing the better heat transfer conditions leading to higher boiler efficiency.

II. Capital investment on production facilities

Instead of any other surface engineering approach, the gradient tubes require minimum investments in general. Some investment is necessary to provide the hardware in casting shops to make the gradient semiproduct. On the other hand, the tube production line requires any intervention but technological parameters. Some marginal investment to update the carousel tube magnetic handling systems ("cold" blocks insertion to the furnace") would be necessary for bigger production.

Other technical potentials of gradient tubes lay in other, less conservative (in terms of temperature and pressure) installations.

The heat exchangers in oil and gas, chemical and petrochemical industries are such a good example. In shell and tubes type heat exchangers, the hotter (usually more aggressive) medium is feed into the shell and flows around the hundreds of exchanger tubes inside which the cooler (usually less aggressive) medium is flowing. Typical examples are syngas cooers. The medium outside the tubes transfer the heat to medium inside the. This process should be fast and effective. In many applications, the heat exchanger tubes are replaced every year, or every production unit planned stopover, just because of corrosion of ferritic tubes. Austenitic ones are too expensive, much less effective in term of heat transfer, not talking about enormous heat expansions of austenite causing the collateral problems in exchanger integrity.

The gradient tubes are the most promising approach, and consortia has already initiated the discussion with the MOL Group (main central European refineries owner). The gradient tubes, available in proper dimensions and chemical combinations will be installed onto heat exchangers without big hesitations, providing the company standards and procedures are preserved.

There are also other installations, where the gradient tubes can be installed without big troubles. One of them is pulp industry in black liquor recovery boilers. The recovery boilers operate at 10 MPa /500°C of steam parameters – which indicate the application of low alloyed creep resistant tubes. However, the conditions in combustion chamber are so harsh that the high alloyed material is able to withstand them. This is why so-called composite tubes are used – those manufactured by coextrusion of two tubes – low alloyed and high alloyed.

The gradient tubes can replace these tubes in all pulp production plants where recovery boilers are used (up to 1000).

PRICE CALCULATION OF FINAL PRODUCT – GRADIENT BOILER TUBE

Introduction

Economy of the gradient tubes production is one of the foremost deliverables from the GRAMAT project. To pick up all the financial aspects, one must understand the life cycle of boiler tubes itself along with all CAPEX costs necessary for the production

The tubes for the biomass preheaters could be made of relatively low-cost ferritic creep resistant steel. In this case, the life cycle of the tube is up to one year very often; and additional costs for dismantling/mantling is tremendous. On the other hand, the tubes can be made of austenitic steel. This brings about very positive effect in increasing in preheaters life. However, the problems arising when thermal conductivity and thermal expansion are considered. In addition, the austenitic material is overestimated in majority of biomass boiler in terms of creep properties; and its only reason for use is to provide the proper fire side corrosion. From the pressure and temperature point of view, ferritic matrix is more than satisfactory. In this chapter, the production price for GRAMAT tubes is calculated as it was learned from the several industrial trials.

The price is compared directly to production cost of ordinary tubes made of austenite/ferrite respectively. Since many numbers are sensitive for both tube makers involved in the project, the indexed prices are used when necessary.

The calculations are made for the gradient tube ϕ 38 and wall thickness 6 mm from which 1 mm (app 20 % of material volume) is made of austenitic steel. Steels **11CrMo910** and **A182F347H** were chosen by GRAMAT partner (AMEC) as a most appropriate combination.

Generally, the price consists of CAPEX costs (if necessary) and production costs including all inputs. It must be split to the two subcategories:

1. Production of gradient ingot (casting shop).

Although the set up for industrial casting did not need the CAPEX costs during the project duration, it is clear from the results obtained that some CAPEX costs would most probably be necessary to get the most reliable ingot production.

1. Production of tube (rolling shop).

One of the biggest achievements of the GRAMAT project are the "ZERO" CAPEX cost for gradient tube production. In other words: ordinary tube production line can produce the gradient tubes. However special set up of process parameters are necessary. Indeed, the special parameters fall within the operational scope of production lines used within GRAMAT (Benteler, Podbrezova).

The schematic information related to production costs is summarized in **Tab. 18**. In general, the gradient seamless tubes can be produced at the same costs as the ordinary tubes. However, some issues were not considered during project proposal stage: common QA and NDT of both gradient semiproduct and final tubes after rolling respectively cannot be just adapted. First online NDT trials of gradient tubes for example (X – RAY) have shown many phantom echoes; finally, the QA process was done manually because consortia did not want to spend so much time on (very expensive) production lines. The solution of this issue is is twofold: a) new NDT device set up would be enough, b) some major hardware/software changes will be necessary. The problems with semiproducts are not so critical, since it is not necessary to perform fast screening.

Tab. 18 Schematic information: gradient tube production related necessary costs compared to production of ordinary seamless tubes

	CAPEX	**Production cost**
Semiproduct	**YES**: expecting on capacity	Not as for ordinary ingot casting, preheating necessary.
Final Tube	**Production:** Marginal investing to carousel furnace feeding system. **Quality Control: YES**	Not bigger than for ordinary seamless tubes.

Price calculation

The price calculation consists of three steps[1]:

1. "liquid steel" price
2. GRADIENT semi product "ingot" price
3. Final tube price

The technical details of the GRADIENT semi product production are written elsewhere in this report. For a short summary, the low alloyed predominantly creep resistant steel is poured onto high alloyed predominantly high temperature corrosion resistant shell. The shell has an oval shape (Benteler) and rectangular shape (Podbrezova) respectively.

The price ratio is very similar for other combinations, so they are not considered in this calculation.

Liquid steel

The price of liquid steel as it was calculated in ZDAS company for materials selected by partners – see **Tab. 19**.

Tab. 19 Price of the liquid metals

Material	**Description**	**€/kg**
11CrMo910	**Internal**	0,83
A182F347H	**External**	2,11

[1] The prices are fixed for 6/2017

GRADIENT Ingot

Please note that all prices are calculated for cylindric ingot. Cylindric ingot is used in Benteler for tubes production. Unfortunately, the production of square ingots, used by Podbrezova as and feedstock, is not possible in desired quality, which is one of the outputs from the WP Metallurgy. The square semiproducts were made by open dye forging for rolling trials in Podbrezova, the results were not satisfactory.

The final ingot with its dimensions is seen in figure **Fig. 67**. The gradient ingot as an input to production line is seen on the left size, final tube is in right size. In the real ratio between ingot and final tube is in scale.

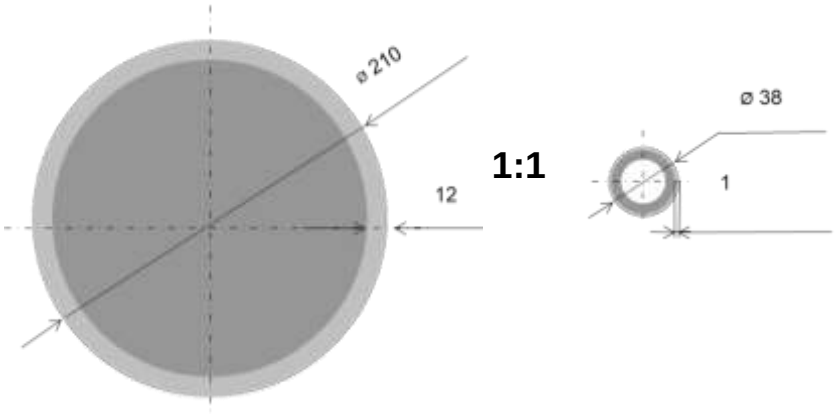

Fig. 67 Gradient ingot (left side) and gradient tube (ride side). The ingot to boiler size ration is real

For further calculation, the volume of austenitic material is estimated from diagram in **Fig. 68**.

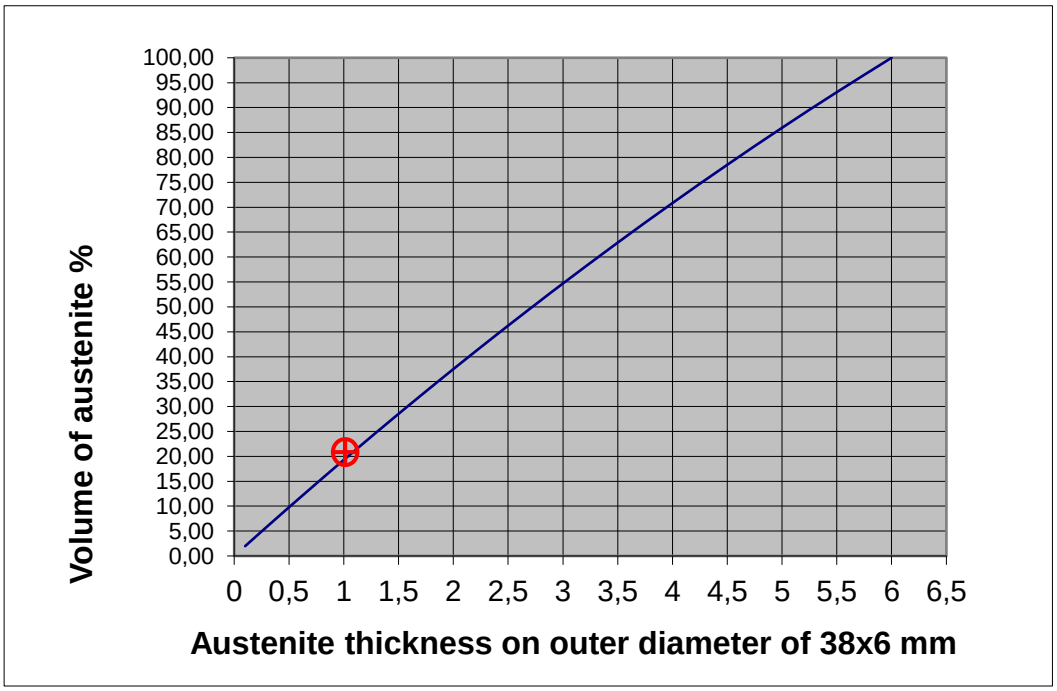

Fig. 68 Austenitic layer thickness versus volume of austenite

The price of materials (low alloyed filling, outer shell in form of thick-walled tube) for gradient ingot manufacturing is seen in table below. The price consists of all expenses necessary for the gradient ingot production. The price of the outer shell (large diameter tube) increased tremendously, from 2.11 €/kg (liquid steel) to almost 18 € (large diameter tube), caused by current market shortage at

the time of tube procurement. In addition, the tube was manufactured by drilling to get the desired wall thickness immediately. The explanation if this lay upon the fact that the consortia main challenge was not to find the best combination of price/quality that time, GRAMAT was focused on technological issues of gradient casting. So, the price of the large diameter tube is much smaller. Recent price varies between 6.5 € /kg and 7 € /kg. The thick-walled tubes can also be longitudinally welded. The optimised kilogram price of the 347H tube is summarized in third line of the **Tab. 20**.

Tab. 20 Ingot price (materials for ingot)

Material	Description	Weight/kg	€/kg
11CrMo910	**Internal material**	**245**	**0,84**
A182F347H	**Large diameter tube**	**59**	**18,00**
A182F347H	**Large diameter tube (actual price).**	**59**	**12,00**

The price of the ingot made in industrial scale is seen in table below. It varies very sharply from 2,03 €/kg (lowest 347 outer shell price per kilogram + 100 % usage) to 8,41 €/kg (highest 347 outer shell price + 70 % usage). 100 % of the ingot usage is an idealistic condition that never happen. However, 70 % of the usage was obtained very often in industrial scale after optimisation of casting process as whole.

Highest price of the ingot is even higher than the lowest price per kg of 347 tube in market (2017). On the other hand, the price of the cheapest ingot is far below the price of the cheapest 347 tube in market. It is obvious that price of the high alloyed shell is crucial for economy of the whole gradient tube approach - **Tab. 21**.

Tab. 21 Ingot price – industrial production (materials + production cost)

347H Price	Ingot usage	kg	€/kg
18 € / kg	**100 % usage (idealistic)**	304,00	4,17
18 € /kg	**70 % usage (realistic)**	213,00	8,41
12 €/ kg	**100 % usage (idealistic)**	304,00	3,01
12 €/ kg	**70 % usage (realistic)**	213,00	6,06

Tube price: ordinary austenitic tube versus GRAMAT tube

The price of the final gradient tube is very sensitive task. One must understand the market competitors will not release the real tube production prices. To prove the project aims were fulfilled undoubtedly, the general principles, at least, can be applied for the final price of the tube.

1. The price of the final product, in general consist of material cost, production cost and profit. The production cost is sensitive task. It was extracted from the open literature that the production cost of seamless tubes made by processes used within the project never exceeds 1 €/kg.

2. The material and production cost for gradient ingot is provided in previous chapter as € per kg.

3. The production cost (in our case rolling and follow up processes) of gradient tube is almost the same as the production cost of ordinary seamless tube. The price index varies from 1 to 1,1 depending on production line.

Based on above mentioned assumptions, the price of the GRAMAT tube has been calculated (**Tab. 22**). As a base, the seamless austenitic tube 347H (38/6) was selected for comparison. Upper and lower price level was set to 12 and 15 €/kg respectively. The price of GRAMAT tube made from overpriced austenitic shell (18 €/kg) is summarized in column 2 for 3 level of ingot usage (portion of ingot that can be used for rolling). 50 % of usage means, that it was possible to use ½ of ingot for final rolling, rest of it was scrap. 70 % was the best results achieved during the GRAMAT project. 80 % is an estimation of the target for the future improvements. When 50 % of the ingots are suitable for further rolling, the price of the GRAMAT tube is bigger than the price of ordinary seamless tube.

If lower price level of seamless tube is taken into consideration, the GRAMAT one is more expensive (see red numbers in columns 3 and 4. When the upper price of ordinary 347H tube is taken into consideration, the result is similar (see red numbers in columns 5 a 6). However, when app. 70 % of gradient ingot is suitable for the rolling, the GRAMAT tube has become cheaper than fully austenitic one. The less economic scenario is however for lower price level of the ordinary tube, but GRAMAT tube I still app. 20 % cheaper. Considering the 15 €/kg as a price for comparison, GRAMAT tube is more than 40 % cheaper. Next step (beyond GRAMAT project) is to tune the casting process in such a way that at least 80 % of gradient ingot will be suitable for following rolling. In this case the savings will be even more attractive.

Tab. 22 Direct comparison of GRAMAT tubes and seamless austenitic tubes in terms of price

Usage of ingot %	Price of the GRAMAT tube	price of the seamless fully austenitic tube 347H			
		12 €/kg		15 €/kg	
		€	%	€	%
50	**17,31**	-5,31	144,23	-2,31	119,23
70	**9,59**	**2,41**	**79,88**	**5,41**	**54,88**
80	**7,58**	4,42	63,19	7,42	38,19

Fig. 69 summarises above stated information in graphical form. As it can be seen, starting from app. 60 % usage of ingot, gradient tubes became cheaper than ordinary ones. Blue triangle in the graph summarise the saving when the worst scenario is adopted: fully austenitic tubes are cheap (12 €/kg); and price of gradient ingot is high due to the very high price of austenitic shell (18 €/kg). All other scenarios give better results. For example, orange line represents the price of the ingot made of cheap austenitic shell (12 €/kg – same price as for ordinary tube). Green trapezoid represents the plausible improvement of gradient ingot casting, an increased usage from current maximum (70 %) to 80 % will open the span between the prices of ordinary tube and those made of gradient ingot.

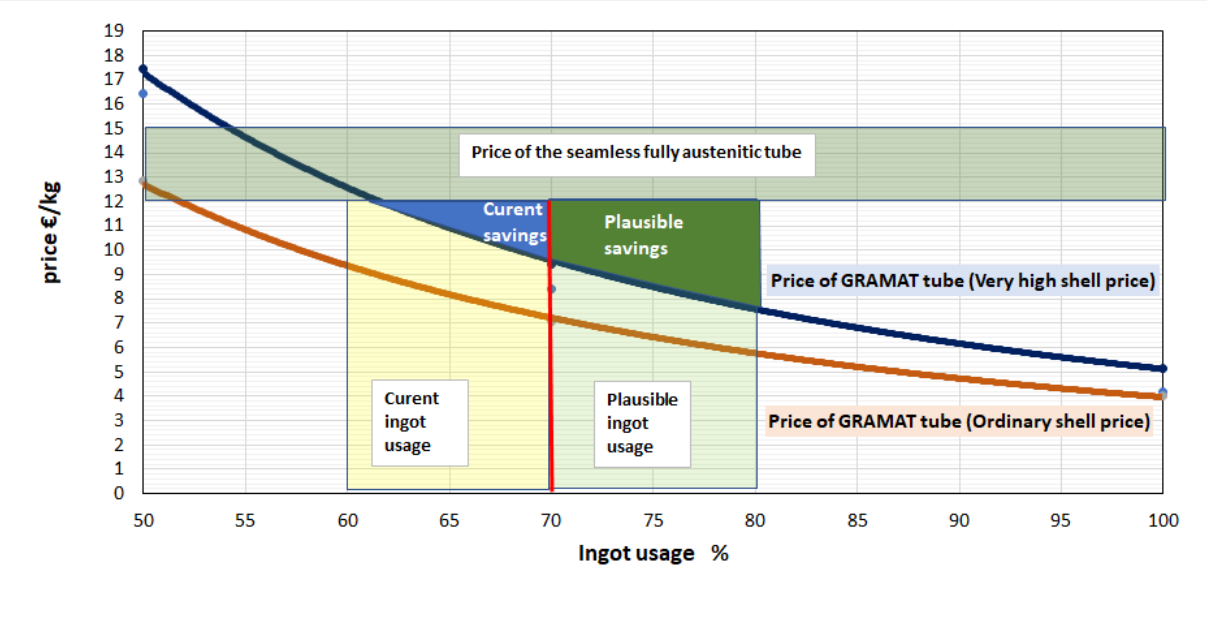

Fig. 69 Schematic price comparison. X axis represents ingot usage. Y axis presents the price of the GRAMAT tube as a function of ingot usage and price of the outer shell of ingot: Orange line = 12 €/kg, blue line = 18 €/kg. Blue and green boxes represent the price advantage of gradient tubes: Blue – current, Green: plausible (beyond GRAMAT project)

In other words, for current final tube diameter and shell to body mass ratio (20:80), if any large diameter outer shall thick walled tube used for semiproduct casting is of the same or even 50 % higher price than ordinary seamless fully austenitic tube; and the ingot usage ratio is more than app. 60 %, the GRAMAT tubes will be always cheaper.

It must be mentioned that the calculations consider the 80 - 90 % of the tubes made are flawless. In fact, it was accomplished in Benteler plant only.

This pattern is generally for other material combinations, for example Nickel Based superalloy or P91 steels. Even if the price of the outer shell is twice as expensive as ordinary seamless tube, the gradient tube could be cheaper. Also, when the thickness of high alloyed layer is smaller than 1 mm (or overall mass of high alloyed steel/alloy is less than 20 %), the gradient tubes are becoming more attractive.

OTHER ASPECTS

Beside the "metallurgical" benefits of gradient tubes, there are also variety of other reasons for GRAMAT tubes:

1. thermal expansion of gradient tubes is lower than the thermal expansion of austenitic steels.

2. at ambient an elevated temperature, gradient tube has a much higher thermal conductivity compared to austenitic steel.

Both these aspects should be considered for implementation in existing boiler, or when new one is designed. Especially the thermal expansion causes several problems during short stopovers, or cold starts.

It should be noted here that the GRAMAT project did not deal with the several other issues, which were omitted by purpose (not to make the project scope even bigger than it was) or simply they occurred during the project implementation. Most important finding relate to the quality control; it was found that current on-line tube monitoring system was confusing many times. The interface high alloyed shell – low alloyed body was the main problem. Most probably some investment to novel/upgraded quality control is necessary.

Indeed, this is a big challenge, which must be solved. However, the GRAMAT project did not intend to solve this problem. In addition, no one was able to predict the behaviour of gradient tubes when ordinary QC devices are employed before they were really tested. Online X -RAY is the common practice for QC in almost all tube making companies. Only those tubes which pass the X-RAY are allowed for further testing as required per grade (chemical testing, mechanical testing, dimensional measurements and others as per specification). It was found that ordinary X – RAY setup gives lot of phantom errors due to interface between body and shell of the gradient tubes. The surface-active probes (EDDY Current and Pulsed Eddy Current) are in consideration as complementary NDT technique. WRI has already made several experiments on rolled products after the push bench (high diameter) and after reduction mills. The results are out of the GRAMAT scope, but they are promising, but laboratory only.

It was found during the creep tests that the austenitic shell reinforces the ferritic body and the creep properties are far beyond those for low alloyed steel only. Since the legislation does not exist, the high alloyed shell will not be taken into the stress analysis for pressure system calculations at first. "Trading" approach is that GRAMAT tube is low alloyed creep resistant tube with improved corrosion properties up to level of austenite. Indeed, the next steps will be realised toward the proper legislation.

Also, other industrial applications of gradient tubes can be highlighted: pulp industry (black liquor transportation), heat exchangers in refineries and chemical plants, civil engineering, automotive and many others. The fitness of GRAMAT tubes for these applications are yet to be evaluated.

Any possible patent filing;

The patent filling is under preparation.

Publications / conference presentations resulting from the project;

1. Sanni Yli-Olli (VTT Technical research centre of Finland Ltd, Espoo, Finland) / Satu Tuurna (VTT Technical Research Centre of Finland LTD, Tampere, Finland) / Peter Brziak (Welding Research Institute – Industrial Institute SR, Bratislava, Slovakia) / Jouni Mahanen (Amec Foster Wheeler Oyj, Varkaus, Finland) / Elisa Isotahdon (VTT Technical Research Centre of Finland Ltd, Tampere, Finland):
   High temperature corrosion of gradient tubes for high temperature application
   EUROCORR 2017 The Annual Congress of the European Federation of Corrosion 20th INTERNATIONAL CORROSION CONGRESS & Process Safety Congress 2017
2. Balážová, M., Brziak, P., Balcar, M., Junker, M., Domovec,: **Investigation of the material properties of gradient tubes for biomass power generation installations** METAL 2015 - 24th International Conference on Metallurgy and Materials, Conference Proceedings, pp. 591-596.
3. Brziak P., Weldability of Gradient Tubes, TMS 2016 Nashville USA.

Note: more presentations are expected when GRAMAT tubes will be removed from boiler (2019 or later – depending on AFW decision during the inspection).

List of figures

List of tables

Getting in touch with the EU

In person

All over the European Union there are hundreds of Europe Direct information centres. You can find the address of the centre nearest you at: https://europa.eu/european-union/contact_en

On the phone or by email

Europe Direct is a service that answers your questions about the European Union. You can contact this service:

– by freephone: 00 800 6 7 8 9 10 11 (certain operators may charge for these calls),
– at the following standard number: +32 22999696 or
– by email via: https://europa.eu/european-union/contact_en

Finding information about the EU

Online

Information about the European Union in all the official languages of the EU is available on the Europa website at: https://europa.eu/european-union/index_en

EU publications

You can download or order free and priced EU publications at: https://publications.europa.eu/en/publications. Multiple copies of free publications may be obtained by contacting Europe Direct or your local information centre (see https://europa.eu/european-union/contact_en).

EU law and related documents

For access to legal information from the EU, including all EU law since 1952 in all the official language versions, go to EUR-Lex at: https://eur-lex.europa.eu

Open data from the EU

The EU Open Data Portal (https://data.europa.eu/euodp/en/home) provides access to datasets from the EU. Data can be downloaded and reused for free, for both commercial and non-commercial purposes.

KI-NA-30-134-EN-N

The main aim of the GRAMAT project was to acquire the critical knowledge necessary to develop new cost-effective manufacturing technology of boiler tubes made from ingots with through thickness gradient chemical composition. The idea is to use these gradient tubes in biomass boilers /waste incinerators where the working pressures/temperatures are suitable for application of low alloyed creep resistant tubes; and, on the other hand, the harsh environment in combustion chamber requires application of high alloyed corrosion resistant grades. To fulfil the project aim, basic knowledge about gradient material behaviour during casting (metallurgy), rolling (forming) and final properties (operation) was collected through numerous simulations and laboratory/ industrial scale experiments respectively.

The square (app. 200x200mm) and oval (app. D150mm) gradient ingots containing app. 12 mm of high alloyed materials were used for D38 gradient tubes production in ordinary production lines. The final wall thickness was 6 mm from which 5 mm (body – creep loading) was made of 10CrMo910 steel; and 1mm (shell – high temperature corrosion protection) was made of 347H steel.

After passing all tests the tubes were installed in biomass boiler, so far, they are fulfilling the expectations.

The main issue in terms of mass production relates to the quality of the gradient ingots. During the project, the maximum usage of the ingots was not higher than 80 %. However, the basic calculations shown that the gradient tubes are to be cheaper comparing with the fully austenitic ones. There is a lot of space for further optimisation of the gradient ingot casting process.

Publications Office
of the European Union